

University of Strathclyde
Department of Naval Architecture and Marine Engineering

**Development of an Intelligent Tool for
Energy Efficient and Low Environment
Impact Shipping**

By

Wei Shao

A thesis presented in fulfilment of the requirements
for the degree of Doctor of Philosophy

March, 2013

This thesis is the result of the author's original research. It has been composed by the author and has not been previously submitted for examination which has led to the award of a degree.

The copyright of this thesis belongs to the author under the terms of the United Kingdom Copyright Acts as qualified by University of Strathclyde Regulation 3.50. Due acknowledgement must always be made of the use of any material contained in, or derived from, this thesis.

To my parents, Changjun Shao & Aizhi Zhang

To my wife, Yue Ma

ABSTRACT

Ship weather routing was first developed for determining the minimum time of a voyage. However, after 90's, driven by the increasing oil price and the environmental considerations, most shipping companies have begun to show more and more interest in minimising fuel consumption in a route, in the meantime, maintaining a certain time schedule which is specified in the chartering contract of a merchant vessel. This topic is the focus of this thesis.

A novel three dimensional dynamic programming method (3DDP) has been developed in this research to determine the optimised ship course and its corresponding engine power for minimum fuel consumption. During the optimisation process, Kwon's method as a new empirical formula is used to calculate ship speed in different weather conditions and an IMO guideline is applied to ensure ship safety during a voyage. In addition to the 3DDP method developed, three multi-objective evolutionary algorithms (MOEAs) are also proposed to treat weather routing as a multi-objective and constrained optimisation problem.

Based on ship hydrodynamic knowledge and optimisation algorithms an Intelligent Tool for Energy Efficient and low environment impact Shipping (ITEES) has been developed. ITEES is established by using the object-oriented software development theory, consisting of several independent functional modules. The OPeNDAP as an advanced communication technique is employed by ITEES for downloading deterministic weather forecast at no cost.

Case studies are given in Chapter 8 of this thesis to evaluate the performance of the 3DDP method in a comparison with other different optimisation algorithms under different weather conditions. A 54,000 DWT container ship is used as the case ship. The case studies have demonstrated that, in medium sea condition, different route optimisation methods offer the similar results that the shortest route with a constant engine power brings the lowest fuel consumption. However, the results of different route optimisation methods vary significantly in rough sea states. Optimised results

are not only just for fuel saving but also, most importantly, for ensuring ship safety during a voyage. Among the optimisation algorithms evaluated by the research, the 3DDP used in ITEES is able to give a better performance for fuel saving than other methods. In addition, it has the characteristics of using straight forward theory and less parameter settings compared with MOEAs that make the ITEES programme easy and convenient for operators to use.

ACKNOWLEDGEMENT

First of all, I would like to express my deep gratitude and appreciation to my supervisor, Professor Peilin Zhou for his valuable suggestion and insightful guidance throughout my years of studies at the University of Strathclyde.

I would also like to thank Professor Liang Zhang for encouraging me to pursue an advanced degree and recommending me for this project.

I also need to thank my colleagues who create such a warm atmosphere in the lab. Thanks are also due to Thelma Will for her administrative support and kindness.

This project is sponsored by Neptune Orient Lines Ltd whose financial support is greatly appreciated. Thanks are also due to Thong Sew Kait of NOL for his advice and direction in real navigation.

I need to further thank all my friends in Glasgow for their care and help. The loves from them makes Glasgow like a second home to me.

I am deeply indebted to my parents who gave me life and brought me up. All the support, loves and encouragement they have provided to me over the years are the greatest gift anyone has never given me.

Last but not least, I thank my wife Yue Ma for her understanding, tolerance and encouragement. Without her I could not have endured the hardest time of my research. I really owe so much to her, I would like to repeat and amplify how I am indebted to her.

CONTENTS

| | |
|--|-----|
| ABSTRACT | I |
| ACKNOWLEDGEMENT | III |
| CONTENTS | IV |
| LIST OF FIGURES | VI |
| LIST OF TABLES | IX |
| INTRODUCTION | 1 |
| 1. 1 Background of this research..... | 1 |
| 1.2 State of the art technology | 3 |
| 1.2.1 Algorithm used for weather routing..... | 3 |
| 1.2.2 Routing service software..... | 10 |
| 1.3 Objects of this research | 13 |
| 1.4 Outline of the thesis | 14 |
| SHIP PERFORMANCE | 16 |
| 2.1 Ship Performance in calm water | 16 |
| 2.1.1 Ship resistance in calm water..... | 16 |
| 2.1.2 Propeller characteristics | 17 |
| 2.1.3 Calculation of engine delivery power and fuel consumption..... | 21 |
| 2.2 Ship speed loss in rough sea..... | 23 |
| 2.3 Calculation of propeller rotation speed..... | 27 |
| 2.4 IMO guidelines for ship safety..... | 28 |
| WEATHER FORECAST | 33 |
| 3.1 WAVEWATCH III model | 33 |
| 3.2 OPeNDAP technique | 34 |
| PROBLEM STATEMENT | 37 |
| 4.1 The system model | 37 |
| 4.1.1 What is minimum fuel route?..... | 37 |
| 4.1.2 Ship control variable | 37 |
| 4.1.3 Ship position vector | 38 |
| 4.1.4 Weather condition | 38 |
| 4.1.5 Constraints condition | 38 |
| 4.1.6 Dynamics of the system | 40 |
| 4.1.7 Fuel consumption | 42 |
| 4.2 Formulation as an optimisation problem | 43 |
| DYNAMIC PROGRAMMING METHOD FOR WEATHER ROUTING..... | 44 |
| 5.1 The introduction of dynamic programming | 44 |
| 5.2 Stage variables in weather routing problems | 45 |
| 5.2.1 Time as a stage variable | 46 |
| 5.2.2 Voyage progress as a stage variable..... | 51 |
| 5.2.3 Choosing the stage variable | 52 |

| | |
|---|-----|
| 5.3 Forward computation procedure | 54 |
| 5.4 Statement of the weather routing problem in dynamic programming | 56 |
| 5.5 Grid system | 57 |
| 5.5.1 Grid points division in geographic projection..... | 57 |
| 5.5.2 Determination of the allowable ship course..... | 62 |
| 5.6 Sub-problem solving | 68 |
| 5.7 Two dimensional dynamic programming (2DDP) for weather routing..... | 72 |
| 5.7.1 Minimum time problem solving | 73 |
| 5.7.2 Minimum fuel problem solving | 74 |
| 5.8 Three dimensional dynamic programming (3DDP) for weather routing..... | 75 |
| 5.8.1 Recursion procedure of forward dynamic programming..... | 76 |
| 5.8.2 Deleting the unmeaning states in every stage to reduce the computing time | 82 |
| EVOLUTIONARY ALGORITHM FOR WEATHER ROUTING..... | 85 |
| 6.1 The introduction of evolutionary algorithms | 85 |
| 6.1.1 Inspiring from Nature Selection..... | 85 |
| 6.1.2 The definition of multi-objective problems | 86 |
| 6.1.3 Pareto Dominance | 87 |
| 6.2 Applications of MOEAs for weather routing..... | 88 |
| 6.2.1 Re-definition of the optimisation problem in weather routing..... | 88 |
| 6.2.2 Parameter setting when using the MOEAs | 92 |
| WEATHER ROUTING SOFTWARE DEVELOPMENT | 93 |
| 7.1 ITEES window information | 93 |
| 7.2 Main modules of ITEES | 96 |
| CASE STUDIES AND DISCUSSION..... | 100 |
| 8.1 Case studies..... | 100 |
| 8.1.1 Case study in medium sea condition..... | 103 |
| 8.1.2 Case study in rough sea condition..... | 111 |
| 8.2 The influence of constraint conditions..... | 125 |
| CONCLUSIONS AND RECOMMENDATIONS FOR FURTHER WORK | 130 |
| 9.1 Conclusions..... | 130 |
| 9.2 Recommendations for further work | 133 |
| Reference..... | 134 |
| PRINCIPAL DIMENSIONS OF THE HULL FORM OF THE CASE SHIP..... | 142 |
| USER MANUAL OF ITEES | 143 |
| PUBLICATIONS..... | 191 |

LIST OF FIGURES

| | |
|--|----|
| Figure 1.1 Minimum time route (dash line) by Bijlsma (Bijlsma, 1975) | 4 |
| Figure 1.2 Modified isochron method (Hagiwara, 1989) | 5 |
| Figure 1.3 Grid system used by De Wit C (1990) | 7 |
| Figure 1.4 Isopone method (Klompstra, 1992) | 8 |
| Figure 1.5 Screenshot form SPOS | 11 |
| Figure 1.6 Ship speed reduction table in SPOS | 11 |
| Figure 1.7 Grid system created by OSI | 12 |
| Figure 2.1 Total resistance in calm water of case ship | 18 |
| Figure 2.2 Propeller pen-water characteristics of case ship | 20 |
| Figure 2.3 K_T / J^2 , $10K_Q$ vs J curves | 22 |
| Figure 2.4 Engine delivered power under different Beaufort number in heading sea condition | 27 |
| Figure 2.5 $10K_Q / J^3$ vs J curve | 28 |
| Figure 2.6 Propeller rotation speed under different Beaufort number in heading sea condition | 28 |
| Figure 2.7 Dangerous zone due to high wave group (IMO, 2007) | 29 |
| Figure 2.8 Risk of surf-riding in following or quartering seas (IMO, 2007) | 30 |
| Figure 2.9 Polar diagram according to IMO guidelines | 32 |
| Figure 5.1 Grid system when time is the stage variable | 47 |
| Figure 5.2 Grid system when voyage progress is the stage variable | 60 |
| Figure 5.3 Cut-out of the region around stage 2 from Figure 5.2 | 61 |
| Figure 5.4 Transitions from stage k to stage $k + 1$ under $q = 2$ | 62 |
| Figure 5.5 Check if a line crosses the land | 65 |
| Figure 5.6 Grid system with obstacle | 67 |
| Figure 5.7 Grid system without obstacle | 68 |
| Figure 5.8 Estimate of fuel consumption between two stages | 72 |
| Figure 5.9 Calculate the trajectory from certain states under different calm water speeds | 78 |
| Figure 5.10 Determine the state | 79 |

| | |
|--|-----|
| Figure 5.11 Pseudo code of the 3DDP method | 80 |
| Figure 5.12 Backward calculation procedure to trace the route (Total number of stages is 10; total number of discrete geographic positions in one stage is 7)..... | 81 |
| Figure 5.13 Critical time points at position $P(i, k)$ | 83 |
| Figure 6.1 Pareto front and curve of minimum fuel consumption vs. en-route time . | 90 |
| Figure 7.1 Interface of ITEES | 94 |
| Figure 7.2 Structure of ITEES | 96 |
| Figure 8.1 Grids system used in the case study | 101 |
| Figure 8.2 (a) Significant wave height at 09:00 28/ 06/ 2011 | 104 |
| Figure 8.2 (b) Significant wave height at 03:00 29/ 06/ 2011 | 104 |
| Figure 8.2 (c) Significant wave height at 21:00 29/ 06/ 2011 | 104 |
| Figure 8.2 (d) Significant wave height at 15:00 30/ 06/ 2011 | 105 |
| Figure 8.2 (e) Significant wave height at 09:00 01/ 07/ 2011 | 105 |
| Figure 8.2 (f) Significant wave height at 03:00 02/ 07/ 2011 | 105 |
| Figure 8.3 Fuel consumption for different ETAs..... | 107 |
| Figure 8.4 Fuel consumption for different ETAs (cut-out of figure 8.3)..... | 107 |
| Figure 8.5 Optimised route under specified arrival time | 109 |
| (EAT = 128 hours, medium sea condition)..... | 109 |
| Figure 8.6 Ship speed over ground of the optimised routes..... | 110 |
| (EAT = 128 hours, medium sea condition)..... | 110 |
| Figure 8.7 Ship engine power of the optimised routes..... | 110 |
| (EAT = 128 hours, medium sea condition)..... | 110 |
| Figure 8.8 Polar diagram according to IMO guidelines at midnight on July, 30th.. | 111 |
| (Shortest route, medium sea condition) | 111 |
| Figure 8.9 Fuel consumption for different ETAs (optimise the grid)..... | 112 |
| Figure 8.10 Fuel consumption for different ETAs (optimise the grid)..... | 113 |
| Figure 8.11 Fuel consumption for different ETAs (optimise the grid)..... | 113 |
| Figure 8.12 Optimised route under specified arrival time | 117 |
| (EAT = 128 hours, medium sea condition)..... | 117 |
| Figure 8.13 Ship speed over ground of the optimised routes..... | 117 |
| (EAT = 128 hours, rough sea condition)..... | 117 |

| | |
|--|-----|
| Figure 8.14 Ship engine powers of the optimised routes | 118 |
| (EAT = 128 hours, rough sea condition) | 118 |
| Figure 8.15 Polar diagram according to IMO guidelines at midnight on July, 30th | 118 |
| (route from 2DDP, rough sea condition) | 118 |
| Figure 8.16 (a) Ship position and significant wave height at 09:00 26/ 01/ 2011 | 119 |
| Figure 8.16 (b) Ship position and significant wave height at 03:00 27/ 01/ 2011 | 119 |
| Figure 8.16 (c) Ship position and significant wave height at 21:00 27/ 01/ 2011 | 119 |
| Figure 8.16 (d) Ship position and significant wave height at 15:00 28/ 01/ 2011 | 120 |
| Figure 8.16 (e) Ship position and significant wave height at 09:00 29/ 01/ 2011 | 120 |
| Figure 8.16 (f) Ship position and significant wave height at 03:00 30/ 01/ 2011 | 120 |
| Figure 8.17 Encounter of rough sea conditions by following the shortest route with constant engine power setting (ship speed in calm water = 21.8 knot) | 121 |
| Figure 8.18 Fuel consumption for different ETAs | 123 |
| (Optimise the engine power based on the shortest route) | 123 |
| Figure 8.19 Fuel consumption for different ETAs | 123 |
| (Optimise the engine power based on the shortest route) | 123 |
| Figure 8.20 Optimised fuel consumptions by the 3DDP method based on the grid system and the shortest route | 125 |
| Figure 8.21 Pareto fronts for different limit setting of the encountered wave height | 127 |
| Figure 8.22 (a) Influence of the application of the IMO guidelines (wave height limit of 8 m) | 128 |
| Figure 8.22 (b) Influence of the application of the IMO guidelines (wave height limit of 7.5 m) | 128 |
| Figure 8.22 (c) Influence of the application of the IMO guidelines (wave height limit of 7 m) | 128 |
| Figure 8.22 (d) Influence of the application of the IMO guidelines (wave height limit of 6.5 m) | 129 |
| Figure 8.22 (f) Influence of the application of the IMO guidelines (wave height limit of 6 m) | 129 |

LIST OF TABLES

| | |
|--|-----|
| Table 2.1 Wake fraction of case ship in loading condition (Samsung, 1996) | 20 |
| Table 2.2 Thrust deduction factor of case ship in loading condition (Samsung, 1996) | 21 |
| Table 2.3 Specific fuel oil consumption of engine in case ship (Samsung, n.d.) | 23 |
| Table 2.4 Speed direction reduction coefficient C_{β} (Kwon, 2008) | 26 |
| Table 2.5 Speed reduction coefficient C_U (Kwon, 2008) | 26 |
| Table 2.6 Ship form coefficient C_{Form} (Kwon, 2008) | 26 |
| Table 2.7 Summary of effects and formulas (Benedict, 2008) | 31 |
| Table 8.1 Fuel saving by the optimisation algorithms compared with the shortest route | 108 |
| Table 8.2 Fuel saving by the optimisation algorithms compared with 2DDP method | 115 |
| Table 8.3 Fuel consumption and distance of the optimised routes (ETA = 128 hours) | 115 |
| Table 8.4 Fuel consumption used by the MOEAs and 3DDP methods | 124 |
| Table 8.5 Fuel and distance saving based on the grid system compared | 125 |
| with the shortest route by the 3DDP method | 125 |

Chapter 1.

INTRODUCTION

1. 1 Background of this research

Shipping transports 90% of world trade (International Chamber of Shipping, 2009). Almost all goods traded worldwide are transported by sea, and it is predicted that trade will triple by the year 2020. This will require bigger, faster and greener ships. But because of the fierce competition and the increase of oil price, profit margins in the shipping market are smaller than before. World shipping consumes currently about 140 million tonnes of fossil fuel annually, which is roughly 6% of world total liquid fuel consumption. As a consequence, shipping activities contribute 14% of global nitrogen oxides emissions and 5% of sulphur emissions. To meet the continuously increasing demand in shipping, fuel saving and emission reduction, ship routing optimisation has already been paid much attention by shipping companies.

Ship routing design can be divided into two levels depending on the purpose of application. The determination of schedule and order in which different ports should be visited by a ship or fleet belong to the tactical level of routing design; the lower level is to determine an optimal route of a ship under specified departure and destination. Weather routing belongs to the latter which is the focus of this thesis.

Ship weather routing is defined as an optimum track of shipping route with an optimum engine speed and power for an ocean voyage based on weather forecasts, sea conditions and individual ship's characteristics. The term optimum means a maximum of ship safety and crew comfort, a minimum of fuel consumption and time

underway, or any desired combination of these factors. The accuracy in determining the optimum route depends on the following three aspects:

- The accuracy of the prediction of ship's hydrodynamic behaviour under different weather conditions.
- The accuracy of weather forecast.
- The capability and practicability of the optimisation algorithm used.

Ship weather routing became a popular subject in the shipping industry after the 1960s. It was first developed for determining shipping courses during a voyage with a minimum of passage time (minimum time route). However, after the 1990s, especially in the economic recession experienced at present, most shipping companies have begun to show more and more interest in reducing fuel consumption, driven by the fuel oil prices, environmental considerations and maintaining a certain time schedule which is specified in the chartering contract of a merchant vessel (minimum fuel consumption route). Using weather routing will not only bring economic benefits to shipping companies as fuel costs are the major cost of ship operation, but also fulfil the global objective of reducing green house gases (CO₂) emissions, at the same time, can maintain the safety of ship, cargo and crew.

Modern ships are equipped with various monitor and control systems for safety and improved performance of machinery systems and ships. However, shipping course, route, engine power and ship speed are set by ship operators. Strategising ship routing design and energy efficient operation of ships are difficult or impossible to be implemented by onboard personnel whose operation practice is mainly based on ship load conditions to set engine power rate, propeller rotating speed to achieve a targeted ship speed. The criteria of setting the ship routing, operation power and speed are often driven by ship speed, i.e. the fast the best within the system's safety margin, which has caused an adverse effect on fuel consumption and emissions. The route design and engine operation setting for a given voyage varies with the experience and knowledge of individual operators often without considering fuel efficiency and emissions. Thus, a routing design system for route optimisation considering weather and sea state is pressingly needed by shipping companies to

reduce the fuel consumption and impact to environment, and to improve the safety of crew, passengers and the ship.

1.2 State of the art technology

1.2.1 Algorithm used for weather routing

Several optimisation methods have been developed for optimising shipping route in an ocean-crossing voyage.

1) Calculus of Variation

Calculus of variations is an analytical method that treats ship routing as a continuous optimisation process. After an arbitrary guess of initial route, the real optimal route is found by refining the gradients of the objective function.

Haltiner, et al (1962) used this method to solve the deterministic minimum time routing problem assuming stationary wave fields without considering any constraints. Bleick, et al (1965) solved the same problem as Haltiner but allowing for time varying wave fields. De Wit (1968). Bijlsma (1975) estimated least time tracks based on Pontryagin's maximum principle as shown in Figure 1.1. In that research, a simple polar velocity diagram was used to calculate the voluntary ship speed reduction without considering the ship hydrodynamics in detail. Some efforts were made by Bijlsma (2001) to extend the minimum time routing to the minimum fuel routing. He also derived the relationship between Pontryagin's maximum principle and dynamic programming (Bijlsma, 2002) for solving weather routing problem, and used the concept of limited manoeuvrability to determine the minimum time/fuel routing (Bijlsma, 2004). Calculus of variations was also used by Perakis et al (1990) to solve the deterministic minimum time routing problem.

This method assumes ship sails at the maximum possible speed. This assumption may not always be optimal especially for optimising the minimum fuel routing.

Much simplification is needed and inaccuracy of the solution may arise in functions when second order differentials are used in the optimisation process. Errors could be expanded to an unacceptable level at the end of the calculation. These disadvantages above make calculus of variations method impractical for ship weather routing software design.

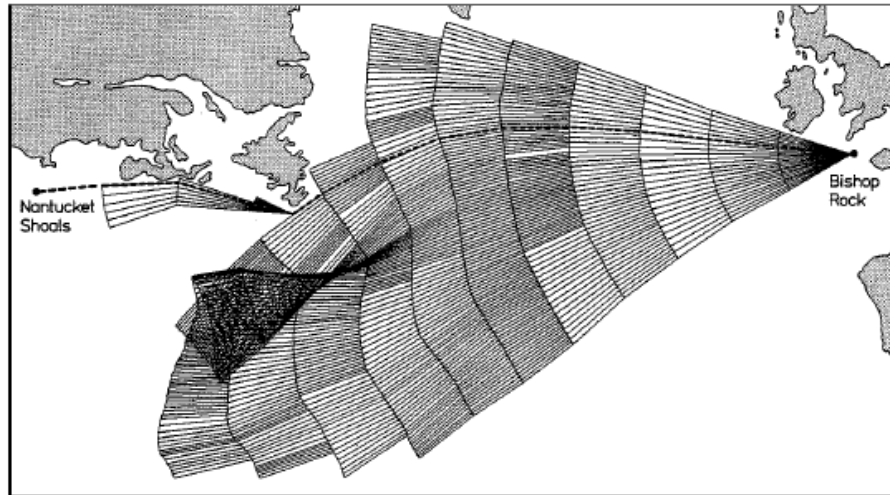


Figure 1.1 Minimum time route (dash line) by Bijlsma (Bijlsma, 1975)

2) Isochrone Method

The isochrone method was first proposed by James (1957) and has been used in many weather routing tools as a manual method to obtain the minimum time route by repeatedly computing isochrones (or time fronts) which are defined as the outer boundaries of attainable regions from the departure point after a certain time. However, this method is unable to give a correct isochrones in a strict sense and is less suitable for programming, especially when the isochrones are in a non-convex shape. Hagiwara and Spaans (1987) and Hagiwara (1989) have developed a modified isochrone method as shown in Figure 1.2 to overcome the shortcoming of the original isochrone method. Since the recursive algorithm used by the modified isochrone method is straightforward and very suitable for computerisation, the modified isochrone method was adopted by the commercial weather routing software SPOS (Ship Performance Optimisation System).

In the research (Hagiwara, 1989), the modified isochrone method is applied to deal with the deterministic minimum fuel / cost routing and stochastic routing as well. The ship's speed, drift angle, rudder angle, heel angle and engine power are calculated by using the equilibrium equations of the forces and moments acting on a ship in a seaway. For stochastic routing, the determined covariance and correlation matrices of the forecasted wind and waves are used. The standard deviations of passage time and fuel consumption are estimated when performing the stochastic routing.

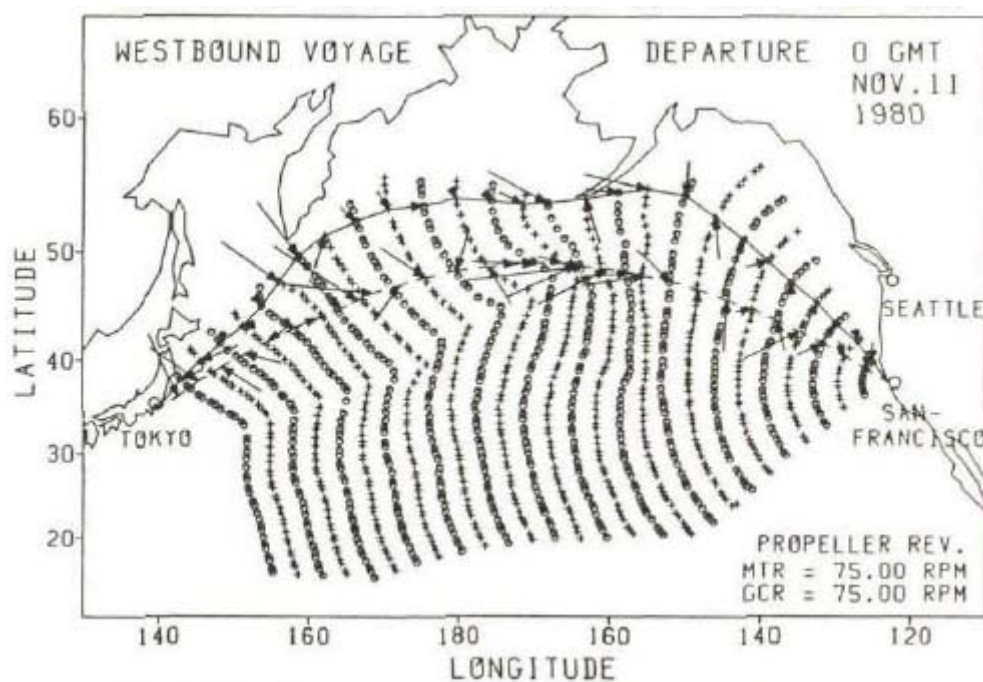


Figure 1.2 Modified isochrone method (Hagiwara, 1989)

A disadvantage of the modified isochrone method is that it assumes the ship sails at a constant propeller rotation speed during the optimisation procedure to get the minimum time route. This assumption may lead to a sub-optimal routing in which the fuel consumption is not optimised. Another problem may exist when calculating the minimum fuel route: this method offers a route with the minimum fuel consumption by keeping the propeller revolution speed as a constant during the simulation first, then applying the modified isochrone method to determine the minimum time of passage. By varying propeller rotation speed this method is able to

find out a propeller rotation speed at which the minimum passage time satisfies the specified arrival time. This minimum time route is then treated as the route of the minimum fuel consumption. Thus, the fuel consumption itself for this route is not minimised.

3) Dynamic Programming

Dynamic programming is developed based on Bellman's principle of optimality (Bellman, 1957). According to this principle dynamic programming can solve the complex weather routing problem by breaking it down into many simpler sub-problems. A term of stage is used in this method to represent divisions of a sequence of various sub-problems of a system. The decision choosing the control variables in routing optimisation is done at every stage. The procedure is to calculate sub-problems stage by stage. Information from the preceding stage is used to determine the control variables of the next stage. The parameters used in describing a stage must be variables which are monotonically increasing with the progress of ship voyage or route optimisation. In ship routing problems, time, and voyage progress are monotonically increasing during a voyage. Both of them can be used to define a stage. Each stage consists of many states which are defined as a specifically measurable condition of the ship, such as time and geographic location.

The dynamic programming is similar to the modified isochrone method. It also uses a recursive formula to solve the ship routing problem expressed as a discrete optimisation problem. Both backward and forward recursive algorithms can be used for the calculation. Chen H. (1978) and Calvert S. (1990) employed voyage progress as the stage variable and used the backward algorithm. Aligne, F. (1998) chose time as the stage variable and used the forward algorithm. The backward and forward recursive algorithms are equivalent mathematically. However, for a weather routing problem, a forward algorithm offers more convenience in programming. In the forward algorithm, the initial departure time is fixed; the arrival time at a location where the optimisation calculation has progressed to can be treated as a flexible parameter. The advantage of the forward algorithm is that it allows a set of route

with a minimum fuel consumption to be obtained corresponding to different arrival times at the current location where the optimisation has been concerned. This is a logical process in line with the ship operation along a voyage course. The newly developed dynamic programming method presented in this paper employs voyage progress as the stage variable together with the use of a forward algorithm.

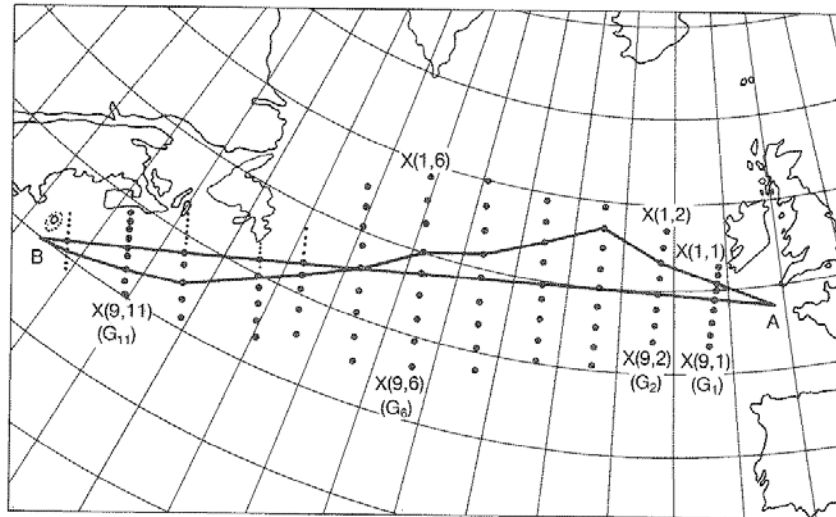


Figure 1.3 Grid system used by De Wit C (1990)

The accuracy of the dynamic programming methods depends on the fineness of a grid system used as shown in Figure 1.3. Compared with the modified isochrone method, an advantage of the dynamic programming method is that it allows the operators to take into account of navigation boundaries by means of an appropriate selection of the grid system (Motte, 1990).

In order to simplify the problem and reduce computing time, several researchers (De Wit, 1990; Calvert, 1991) assume the ship sails at a constant propeller rotation speed, or a constant engine power when the dynamic programming method is used as mentioned in the isochrone method. Under this simplification, a state used in the optimisation procedure is just to consider the ship position in two dimensions (latitude and longitude) without the requirement for time variable since the ship control is restricted by heading only. In this paper, this simplified dynamic programming method is called 2 dimensional dynamic programming method (2DDP).

Several authors (Chen, 1978; Calvert, 1990; Aligne et al. 1998) have already attempted to use the dynamic programming method by treating both engine power and shipping course as the control variables during a voyage. As a result, a state consists of 3 dimensional variables (latitude, longitude and time). This kind of dynamic programming method is named 3 dimensional dynamic programming (3DDP) in this paper. Compared with the 2DDP method, the 3DDP method can provide a better result but obviously use more computing time. In this research, a novel forward 3DDP method is developed and the computing time consumed by this method is totally acceptable by using today's computer technology.

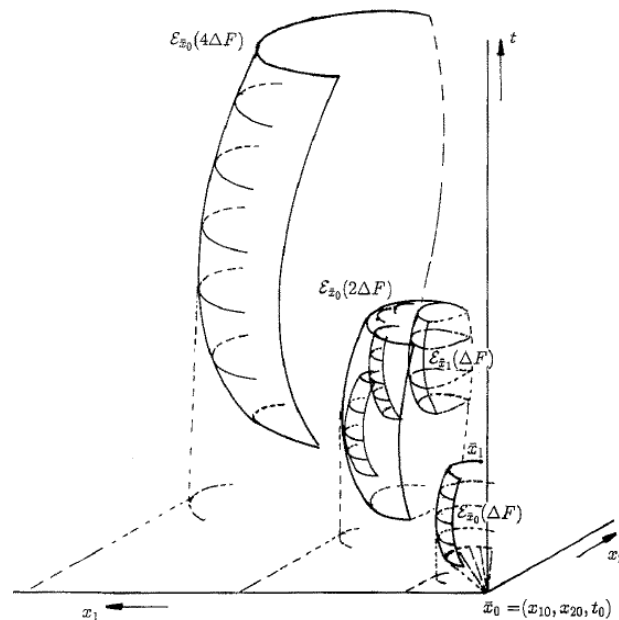


Figure 1.4 Isopone method (Klompstra, 1992)

4) Isopone Method

The isopone method (Klompstra, 1992; Spaans, 1995) is an extension of the modified isochrone method. An isopone is the plane of equal fuel consumption that defines the outer boundary of the attainable regions in a three-dimensional space, i.e. geographical position and time. The first isopone is created by varying the ship course under fixed amount of fuel consumption as shown in Figure 1.4. Each point

on the first isopone thus has the same amount fuel but different arrival times. These discretised points on the first isopone surface are used as the departure points to form the local isopones by repeating this process and the envelope isopone is determined by selecting the points of the local isopones which are closest to the destination in time plane. This envelope isopone are used as the second isopone. This process is computed repeatedly during the optimisation process until there is an isopone cross the time axis at the point of the destination. In author's view, this method can be treated as a kind of particular dynamic programming method which use fuel consumption as the stage variable and adopt the forward recursive algorithm. This method enables the operators to consider a variation of ship engine power in the route optimisation. Theoretically this method can get better results than the modified isochrone method. However the isopone method appears to be more difficult to be understood by the operators onboard ships thus it is not appropriate for software development.

5) Dijkstra's Method

Recently years, some researchers (Padhy, 2008; Panigrahi, 2008) attempt to solve the ship routing problem by using the Dijkstra's method. In this method, positive weights are assigned to the graph edges to represent the transit time in these edges according to weather condition and predefined engine power. It can find the minimum time route in which the sum of the weights is minimal on the directed network. In that study (Padhy, 2008), the minimum time routing over the Indian Ocean is considered under WAM forecasts. A disadvantage of this method is that it is not possible to change engine power deliberately during the route optimisation.

6) Evolutionary Algorithm

Genetic algorithms, as a computational model simulating the biological evolution process of the genetic selection theory of Darwin, is a new global optimisation algorithm and has been widely used in many fields because of its remarkable characteristics of simplicity, stability and practicability. Most importantly, this

method can solve a multi-objective optimisation problem without much difficulty. However, a multi-objective optimisation problem could hardly be solved by other optimisation algorithms.

Harries (2003; 2004), Marie (2009) and Szłapczyńska (2009a, b) have treated weather routing as a two objectives optimisation problem: achieving the minimum of voyage time and minimum fuel consumption simultaneously by using the genetic algorithm. A population of different routes which deviate from a parent route (the great circle mostly) are generated first by this method and the preferable ones are chosen during the optimisation procedure. The Pareto frontier which provides a feasible domain for decision support is finally constructed by this method. Probabilistic ensemble forecasts are applied to account for the stochastic behaviour of weather by Hinnethal (2010). Beside time and fuel consumption, the robustness of a route which is simply defined as the number of ensemble forecasts where the route stays feasible are used as the third objective in that research. It can be assumed that this objective shows an opposing behaviour towards the minimisation of the fuel consumption and travelling time. Therefore, the Pareto frontier becomes a Pareto surface.

The disadvantage of this method is that it uses more parameters during the optimisation process. The operator onboard whose major is not mathematic may have no idea about the meaning of these parameters and how to set these values gives another problem.

1.2.2 Routing service software

Along with the development of the computer and communication technologies, several software tools have already been employed on-board/on-shore for ship's weather routing design based on the optimisation algorithms presented above. Most popular ones are SPOS (Ship Performance Optimisation System) and OSI (Operation Support Information).

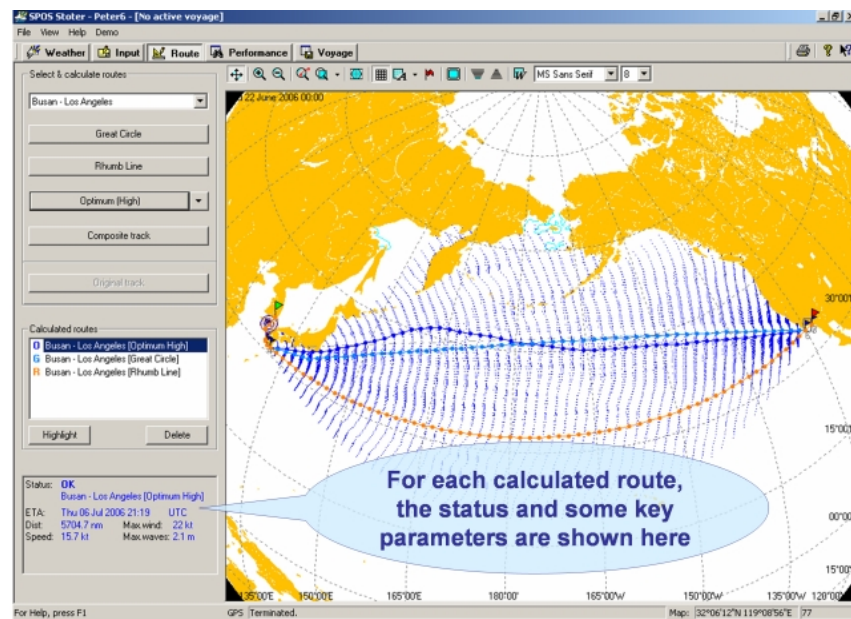


Figure 1.5 Screenshot form SPOS

1) SPOS (Spaans, 2000)

SPOS adopted the isopone method at the beginning of its development. Although the isopone method is mathematically more elegant and offers theoretically more accurate results than that of the modified isochrone method, SPOS had nevertheless abandoned the isopone method and adopted the modified isochrone method in the final products. The main reason for this change over was due to the fact that the isopone method appeared to be more difficult to be understood by the operators onboard, whereas the modified isochrone method is straightforward and easy to understand (Spaans, 2000).

| speed reduction due to WIND | | | | | | speed reduction due to WAVES | | | | | |
|-----------------------------|-------------------------|------|------|------|------|------------------------------|-------------------------|------|------|------|------|
| Wind speed | Wind direction from bow | | | | | Wave height | Wave direction from bow | | | | |
| knots | 000° | 045° | 090° | 135° | 180° | meter | 000° | 045° | 090° | 135° | 180° |
| 0 | 100 | 100 | 100 | 100 | 100 | 0 | 100 | 100 | 100 | 100 | 100 |
| 10 | 100 | 100 | 100 | 100 | 100 | 2 | 98 | 98 | 100 | 100 | 100 |
| 20 | 98 | 99 | 100 | 100 | 101 | 4 | 90 | 90 | 95 | 100 | 100 |
| 30 | 95 | 97 | 98 | 100 | 101 | 6 | 85 | 85 | 90 | 90 | 95 |
| 40 | 85 | 90 | 95 | 100 | 102 | 8 | 65 | 70 | 80 | 85 | 90 |
| 50+ | 80 | 85 | 90 | 95 | 102 | 10+ | 0 | 0 | 0 | 0 | 0 |

Figure 1.6 Ship speed reduction table in SPOS

In SPOS, ship performance data is inputted into the system by the user based on simplified situations, e.g. still water speed and speed loss/gain in percentage due to wind and waves as shown in Figure 1.6. The estimated results can be modified during the ship voyage when true performance data become available.

The disadvantages of SPOS are that the system cannot predict ship safety, motions and engine operation parameters. Furthermore it assumes that the engine power is fixed during a voyage and simply calculates the minimum time route, so its results are just the sub-optimum solutions.

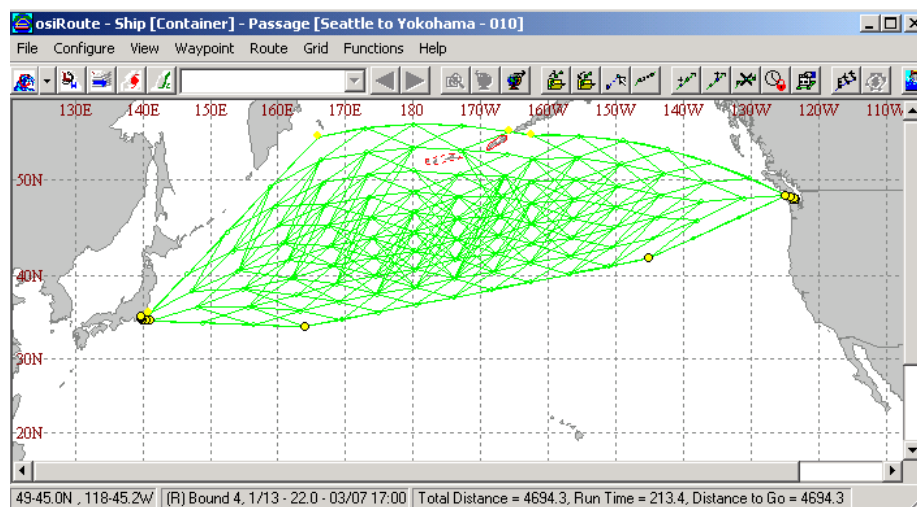


Figure 1.7 Grid system created by OSI

2) OSI (Chen, 1998; Vessel Optimization and Safety System., 2010)

OSI implements a dynamic programming algorithm which can change ship heading and speed at every grid point in both time and position. It is able to predict ship motion, engine conditions and other sea-keeping events based on the weather forecast by using a theoretical approach. The method requires a grid system to be created before optimisation. Response constraints and environment limitations should be set before the optimisation as well. The grid is generated according to the boundaries specified by the user as shown in Figure 1.7. These user-defined boundaries eliminate many route options which would not be practically possible.

It can calculate routes with the minimum voyage time as well as minimum fuel consumption for a range of arrival times for the user to select. OSI is also able to simulate a route in which the vessel speed or propeller rotation speed is specified by the operator and both speed and power can change with the time. The comparison function in OSI can compare the simulated route and optimised route against each other to help the operator to choose the most efficient route.

It can be concluded that with respect to the ability of optimisation algorithm used, OSI is theoretically more advanced than SPOS. However, because of the sake of trade secret, there are no published papers giving the detailed descriptions about the optimisation algorithm used by OSI.

1.3 Objects of this research

The objects of this research are given below.

- To overcome the shortcoming of the optimisation algorithms mentioned in last section, a novel optimisation algorithm need to be developed during this research. This method should be more straightforward with less parameter setting and suitable for weather routing software development. Both ship course and engine power should be used as the control variables during the optimisation process.
- Case studies should be given to illustrate the advantage of the newly developed method in comparison with the traditional weather routing methods.
- An intelligent tool for energy efficient and low environment impact shipping (ITEES) need to be developed in this project. This software emphasises on determining the minimum fuel consumption route by considering the ship engine characteristics, ship hydrodynamic responses in different weather conditions and their impact on fuel consumption. The tool is able to advise ship operators with shipping courses, engine power/speed in advance of and

also during a voyage. Following the instruction offered by the tool, the minimum fuel consumption and maximum ship safety can be ensured. ITEES has a user-friendly graphical user interface (GUI), and requires minimum IT skill and ship hydrodynamic knowledge to operate.

1.4 Outline of the thesis

Outline of the forthcoming Chapters is given below.

- Chapter 2 deals with the analysis of ship performance in different sea conditions. A simpler and easier empirical function is used to estimate the effect of wave and wind on ship performance and the IMO guidelines are employed to ensure the ship safety during the voyage.
- Chapter 3 presents the OpeNDAP technology which can be used to provide a transparent access to the distributed online oceanographic and meteorological datasets.
- Chapter 4 gives the numerical formulations of the ship routing problem.
- The basic concept of the dynamic programming is given in Chapter 5 and it also presents a novel forward three dimensional dynamic programming method (3DDP) which can be used to optimise the route with minimum of fuel consumption during the voyage.
- Chapter 6 presents three kinds of evolutionary algorithms and their applications for weather routing problem.
- The framework and modules of ITEES are presented in Chapter 7.
- Chapter 8 shows two case studies to assess the capability of different optimisation algorithms in different weather conditions. The influences of the

constraint conditions on the optimisation results are also discussed in this Chapter.

- Conclusions of this study and recommendations for further research are given in Chapter 9.

Chapter 2.

SHIP PERFORMANCE

The accuracy of the prediction of ship performance as a necessary condition for weather routing determines the quality of the optimised results. Section 2.1 discusses the ship performance in calm water. Section 2.2 uses a simpler and easier empirical function to estimate the effect of wave and wind on ship performance. The propeller rotation speed under different engine power and ship speed can be estimated by the algorithm described in Section 2.3. Section 2.4 gives IMO guidelines to ensure the ship safety during the voyage. A SAMSUNG 54,000 DWT container ship is used as a case ship in this study. The detailed specifications of the case ship are given in Appendix A.

2.1 Ship Performance in calm water

2.1.1 Ship resistance in calm water

The total resistance R_{total} for a ship can be decomposed into two main components, namely the total resistance in calm water R_T and the total added resistance R_{Tadd} . The total resistance in calm water of a ship is normally regarded as a summation of several components. Principal components affecting calm water resistance are frictional drag R_F , form drag R_f and wave resistance R_W . R_F is affected by the Reynolds number R_e and can be calculated from the frictional resistance of a plate which has the same wetted surface as the ship. Both R_F and R_f are caused by the viscosity of the water. The wave resistance R_W is caused by the energy required for creating and maintaining the ship's bow and stern waves and it can be considered as

an inviscid component of the total resistance in the calm water. In addition of these force above, there exists additional resistances R_{Cadd} that contributes to the calm water resistance. R_{Cadd} can be divided into many components, like resistance of appendages R_{App} , additional pressure resistance of bulbous bow near the water surface R_B , additional pressure resistance of immersed transom stern R_{Tr} , and model-ship correlation resistance R_A . Different methods for calculating the calm water resistance will have different division about R_T .

According to the hypothesis of Froude (1955), R_f and R_W are combined together into what is so called “residuary resistance” R_R (Rawson, 2001) which is assumed to depend only on the Froude number. So the calm water resistance can be given as:

$$R_T = R_R + R_f + R_{Cadd} \quad (2.1)$$

Another component distribution is conducted according to the Holtrop’s method (1978, 1982, 1984) which is a regression analytical method based on the results obtained from model tests and full-scale test data. It assumes the ratio of R_F to R_f is a constant value k which just depends on the form of the ship, so k is called form factor. In the Holtrop’s method the calm water resistance can be described as:

$$R_T = (1+k) R_f + R_W + R_{Cadd} \quad (2.2)$$

In this project, the Holtrop’s method is used for the calculation of total resistance in calm water. Figure 2.1 shows the predicted results of the case ship.

2.1.2 Propeller characteristics

Propellers characteristics are the main impact factors to the engine delivery power and fuel consumption. Extensive model tests have been performed with various types of propeller and the results have been systematically categorized in a series of chart for facilitating general use. Certain dimensionless coefficients that uniquely

characterise the performance of a particular screw propeller have been introduced in relation to the propeller diameter, the rate of revolution, and the water's mass density.

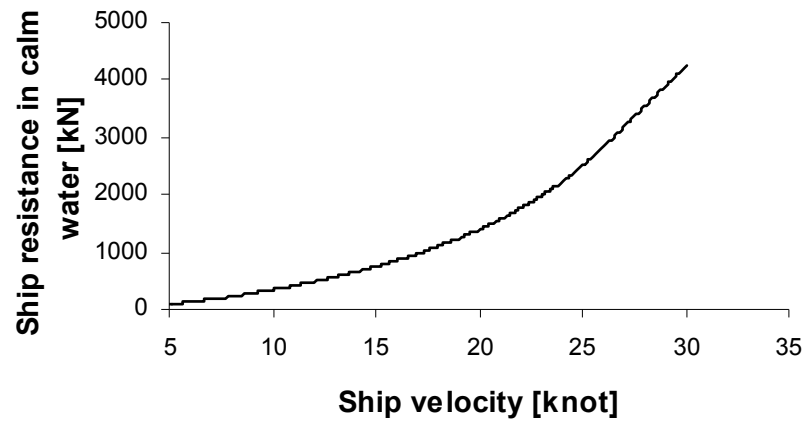


Figure 2.1 Total resistance in calm water of case ship

The most important coefficients are mentioned below.

1) Thrust coefficient K_T

$$K_T = \frac{T}{\rho n^2 D^4} \quad (2.3)$$

Where:

T : Propeller thrust (N).

ρ : Density of water (kg/m^3).

n : Propeller rotation speed (rev/s).

D : Diameter of propeller (m).

2) Torque coefficient K_Q

$$K_Q = \frac{Q}{\rho n^2 D^5} \quad (2.4)$$

Where:

Q : Propeller torque in open water (Nm).

3) Advance ratio J :

$$J = \frac{V_A}{nD} \quad (2.5)$$

Where:

V_A : The propeller's speed of advance (m/s).

4) Open water efficiency η_0

$$\eta_0 = \frac{TV_A}{2\pi nQ} \quad (2.6)$$

From the above, there is

$$\eta_0 = \frac{TV_A}{2\pi nQ} = \frac{K_T}{K_Q} \times \frac{J}{2\pi} \quad (2.7)$$

The open-water characteristics of the propeller of the case ship derived from the model test results are shown in Figure 2.2 (Samsung, 1996).

5) Wake fraction w

When a ship is moving, the water near the propeller has a forward speed tending to follow the ship's motion and forms the wake. Because of the existence of the wake, the propeller is advancing at a lower speed relative to the water than the ship speed relative to the water. The wake behind the ship is highly turbulent and the velocity of

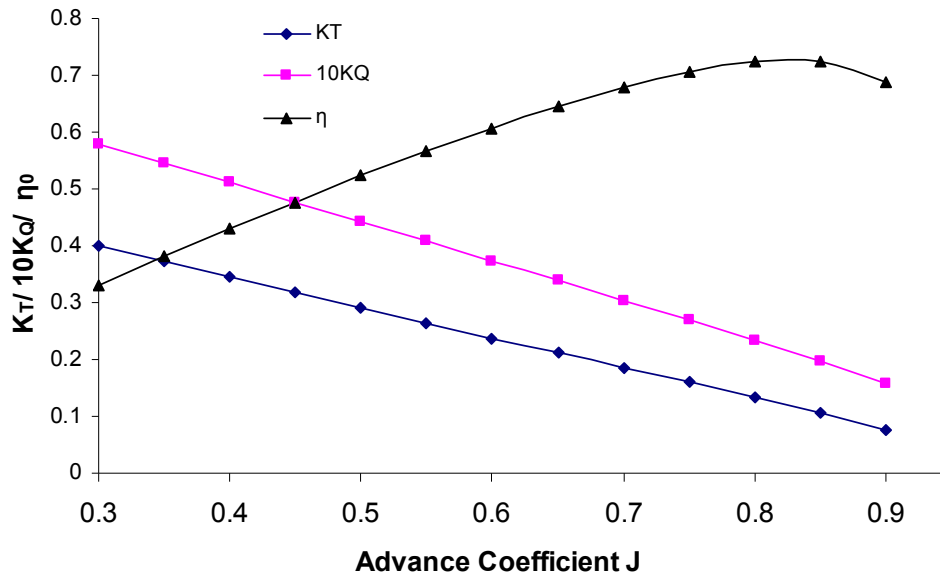


Figure 2.2 Propeller pen-water characteristics of case ship

water differs from point to point around the propeller. To describe the average effect of the wake, the wake fraction is used and defined as:

$$w = \frac{V_{ship} - V_A}{V_{ship}} \quad (2.8)$$

Where, V_{ship} is ship speed.

Table 2.1 Wake fraction of case ship in loading condition (Samsung, 1996)

| | | | | | | | | |
|-------------------|------|------|------|------|------|------|------|------|
| Ship speed (knot) | 20 | 22 | 23 | 24 | 24.5 | 25 | 26 | 27 |
| Wake fraction | 0.23 | 0.24 | 0.24 | 0.24 | 0.24 | 0.24 | 0.24 | 0.24 |

The value of the wake fraction depends largely on the shape of the ship, the position of the propeller and the trim and displacement of the vessel. Table 2.1 gives the wake fraction of the case ship under different ship speed in loading condition. It can see that the influence of ship speed on the wake fraction is not obvious. To simplify the problems, the wake fraction is treated as a constant under certain loading condition in this research.

6) Thrust deduction τ

The action of the propeller behind the ship can also make an effect on the total resistance of the ship. The rotation of the propeller causes the water in front of it to be sucked back towards the propeller and the speed of the water is accelerated. The increased speed of water can cause the pressure decrease near the aft of the ship and increases the frictional resistance; as a consequence an extra resistance occurs. To measure the additional thrust required to overcome the extra resistance due to the existence of the propeller, the thrust deduction factor τ is defined:

$$\tau = \frac{T - R}{T} \quad (2.9)$$

Where:

R : Resistance of ship (N).

The thrust deduction has only a slight change with the ship speed variation as shown in Table 2.2. It is assumed that the thrust deduction remains a constant value under certain loading condition in this research.

Table 2.2 Thrust deduction factor of case ship in loading condition (Samsung, 1996)

| | | | | | | | | |
|-------------------|------|------|------|------|------|------|------|------|
| Ship speed (knot) | 20 | 22 | 23 | 24 | 24.5 | 25 | 26 | 27 |
| thrust deduction | 0.17 | 0.18 | 0.18 | 0.19 | 0.19 | 0.19 | 0.19 | 0.19 |

2.1.3 Calculation of engine delivery power and fuel consumption

When ship resistance and ship speed are known, the engine delivery power can be obtained by using the propeller characteristics. According to Formulas (2.3), (2.4) and (2.5), the ratio K_T / J^2 can be derived as:

$$K_T / J^2 = \frac{T}{\rho V_A^2 D^2} = \frac{R}{\rho (1 - \tau)(1 - w)^2 V_{ship}^2 D^2} \quad (2.10)$$

When K_T / J^2 is known, the advance ratio J can be obtained by using the curve of K_T / J^2 vs J , and then K_Q can be derived by the curve $10K_Q$ vs J as shown in Figure 2.3 Hence, the engine brake power can be determined from

$$P_b = \frac{2\pi n^3 D^5 K_Q}{\eta_{gb} \eta_s \eta_r} \quad (2.11)$$

Where :

η_r : Rotative efficiency.

η_s : The shaft efficiency.

η_{gb} : The gearbox efficiency.

Both η_s and η_{gb} are due to the mechanism transmission and have no relation with the propeller characteristics and ship hydrodynamics. The product of η_s and η_{gb} is called transmission efficiency η_{tm} . In the case ship η_{tm} is 0.98.

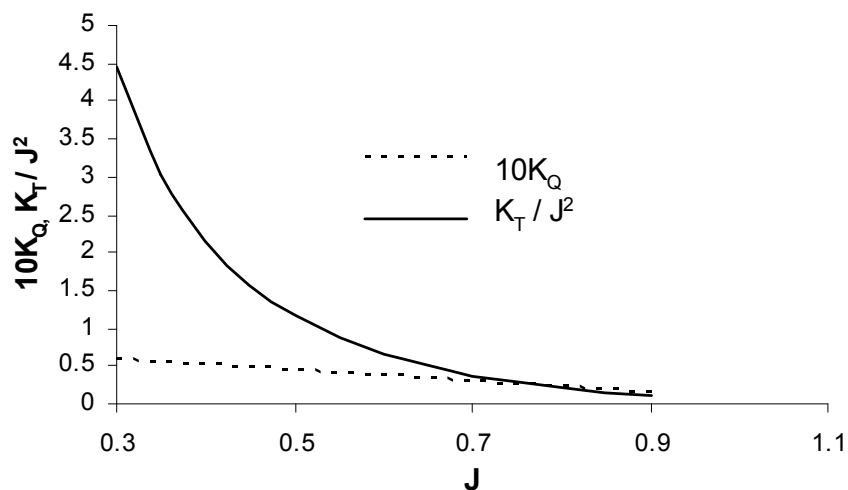


Figure 2.3 K_T / J^2 , $10K_Q$ vs J curves

The engine delivery powers obtained at a set of ship speed in calm water are saved as a database first, to be used by the optimisation algorithm for weather routing.

In the case ship, a Sulzer engine is installed as the propulsion engine. Fuel consumption per hour $spef$ under certain engine brake power can be calculated by the function:

$$spef = sfoc \times P_b \times 3600 \quad (2.12)$$

Where $sfoc$ is specific fuel oil consumption in g/kWh. $sfoc$ varies with engine speed n_e . At a high load of engine, $sfoc$ is roughly a constant value in the operation range as shown in Table 2.3. In this research, $sfoc$ is assumed as a constant value 170g/kWh for the case ship during the voyage. The maximum continuous rating (MCR) of the main engine is 48598 kW. Engine overload is treated as a constraint condition in the routing optimisation. The brake power is not allowed to exceed the MCR value.

Table 2.3 Specific fuel oil consumption of engine in case ship (Samsung, n.d.)

| | | | | |
|----------------|--------|--------|--------|--------|
| Load (%) | 50 | 75 | 90 | 100 |
| $Sfoc$ (g/kWh) | 171.16 | 169.34 | 167.83 | 170.56 |

Reducing the overall fuel consumption of a voyage is the objective of weather routing. To simplify the problem, the fuel consumption of auxiliary engines is not considered. Actually the fuel consumption of auxiliary engines depends on the total travelling time which is treated as a constraint condition in the routing optimisation as well. Thus, fuel consumption of the auxiliary engines can be omitted without influencing the problem solving.

2.2 Ship speed loss in rough sea

In addition to ship resistance in calm water, the total added resistance R_{Tadd} is another main component contributing to the ship's total resistance in seaway. The

total added resistance can be further decomposed into many components, like added resistance due to current, different fluid layers, ice loading, waves, wind and so on. In the present study only the added resistance due to waves and wind is considered since waves and wind are most commonly experienced conditions at sea.

Methods based on strip theory have been widely used for the calculation of added resistance due to wave, but the results for following seas are less accurate since ship motion for following seas is much less linear. The added resistance due to wind should be carried out by wind tunnel experiments for a detailed calculation but the costs are very high.

At this stage, to avoid complicated calculation and make the problem simple, an approximate method established by Kwon (2008) is used to estimate the effect of waves and wind. Clearly, reasonable accuracy of added resistance due to wave and wind is required for all headings and a range of speeds under any wave and wind conditions. This is meaningful for obtaining accurate fuel optimisation results. The effectiveness of this approximate method should be verified in the future which is out of the scope of this research.

As a consequence of the added resistance due to wind and waves, ship's speed is often reduced from the service speed so called involuntary speed reduction. The Kwon's method can predict the involuntary drop of speed in irregular waves and wind with the assumption that the engine of the selected ship is able to provide a constant power output under different weather conditions.

The percentage of speed loss can be expressed as the following (Kwon, 2008):

$$\frac{\Delta V}{V_1} 100\% = C_\beta C_U C_{Form} \quad (2.13)$$

$$\Delta V = V_1 - V_2 \quad (2.14)$$

$$V_1 = F_n \sqrt{L_{PP} g} \quad (2.15)$$

Where:

ΔV : Ship speed difference (m/s).

V_1 : Ship speed in calm water (m/s).

C_β : Speed direction reduction coefficient, depending on weather direction angle and the Beaufort number BN .

C_U : Speed reduction coefficient, varying with ship's block coefficient C_B , loading conditions and the Froude number F_n .

C_{Form} : Hull form coefficient, a function of ship type, the Beaufort number BN and ship displacement ∇ (m^3).

V_2 : Ship speed in the selected weather conditions (m/s).

F_n : Froude number associated with designed ship operation speed V_1 in calm water conditions, L_{pp} is ship length between perpendiculars (m), g is the acceleration of gravity (m/s^2).

Table 2.4, 2.5 and 2.6 show the databases of the speed direction reduction coefficient C_β , the speed reduction coefficient C_U and the hull form coefficient C_{Form} (Kwon, 2008). With the use of the Kwon's method, the prediction of speed loss can be achieved quickly without complex hydrodynamic calculations.

Figure 2.4 shows the engine delivery power of the case ship under different Beaufort number in a heading sea condition. It can be seen that more engine power is needed under a given ship speed in a rough sea condition than in calm water. Consequently, more fuel will be consumed. Under certain sea conditions, the engine power could be beyond the characteristic envelop of the engine power and speed which should be avoided during the voyage.

Table 2.4 Speed direction reduction coefficient C_β (Kwon, 2008)

| Weather direction | Direction angle (with respect to ship's bow) | Speed direction reduction coefficient C_β |
|--|--|--|
| Head sea (irregular waves) and wind | 0° | $2C_\beta = 2$ |
| Bow sea (irregular waves) and wind | 30° to 60° | $2C_\beta = 1.7 - 0.03(BN - 4)^2$ |
| Beam sea (irregular waves) and wind | 60° to 150° | $2C_\beta = 0.9 - 0.06(BN - 6)^2$ |
| Following sea (irregular waves) and wind | 150° to 180° | $2C_\beta = 0.4 - 0.03(BN - 8)^2$ |

Table 2.5 Speed reduction coefficient C_U (Kwon, 2008)

| Block coefficient C_B | Ship loading conditions | Speed reduction coefficient C_U |
|-------------------------|-------------------------|--------------------------------------|
| 0.55 | normal | $1.7 - 1.4Fn - 7.4(Fn)^2$ |
| 0.60 | normal | $2.2 - 2.5Fn - 9.7(Fn)^2$ |
| 0.65 | normal | $2.6 - 3.7Fn - 11.6(Fn)^2$ |
| 0.70 | normal | $3.1 - 5.3Fn - 12.4(Fn)^2$ |
| 0.75 | loaded or normal | $2.4 - 10.6Fn - 9.5(Fn)^2$ |
| 0.80 | loaded or normal | $2.6 - 13.1Fn - 15.1(Fn)^2$ |
| 0.85 | loaded or normal | $3.1 - 18.7Fn + 28.0(Fn)^2$ |
| 0.75 | ballast | $2.6 - 12.5Fn - 13.5(Fn)^2$ |
| 0.80 | ballast | $3.0 - 16.3Fn - 21.6(Fn)^2$ |
| 0.85 | ballast | $3.4 - 20.9Fn + 31.8(Fn)^2$ |

Table 2.6 Ship form coefficient C_{Form} (Kwon, 2008)

| Type of ship | Ship form coefficient C_{Form} |
|---|---------------------------------------|
| All ships (except for containerships) in loaded conditions | $0.5BN + BN^{6.5}/(2.7\Delta^{2/3})$ |
| All ships (except for containerships) in ballast conditions | $0.7BN + BN^{6.5}/(2.7\Delta^{2/3})$ |
| Containerships in normal loading conditions | $0.5BN + BN^{6.5}/(22.0\Delta^{2/3})$ |

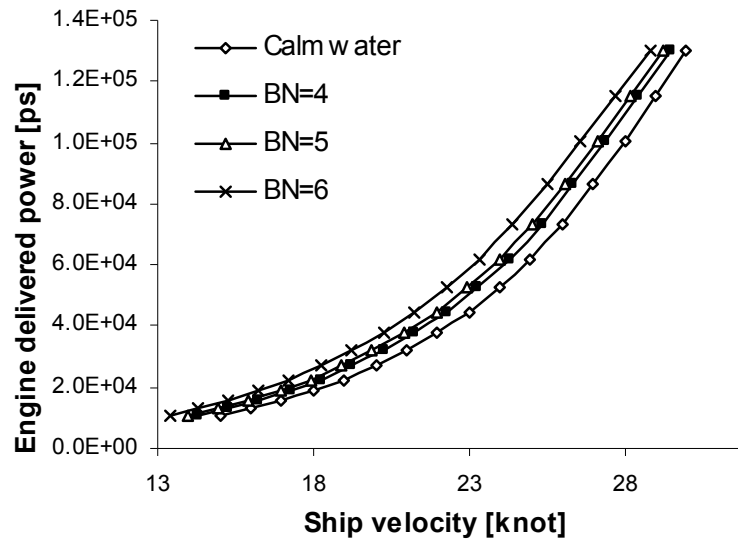


Figure 2.4 Engine delivered power under different Beaufort number in heading sea condition

2.3 Calculation of propeller rotation speed

When the predicted engine delivered power and the ship speed in a rough sea are known, the propeller rotation speed can be determined by using the propeller characteristics.

The ratio $10K_Q / J^3$ can be expressed as:

$$10K_Q / J^3 = \frac{10nQ}{\rho V_A^3 D^2} = \frac{10P_b \eta_{gb} \eta_s \eta_r}{V_{ship}^3 (1-w)^3 (2\pi \rho D^2)} \quad (2.16)$$

$$n = \frac{V_A}{JD} \quad (2.17)$$

The value of $10K_Q / J^3$ can be obtained when the power delivered by the engine P_p and ship speed V are known. The advance ratio J can be calculated from the curve of $10K_Q / J^3$ vs J as shown in Figure 2.5. Figure 2.6 shows the propeller rotation speed under the different Beaufort numbers in heading sea condition.

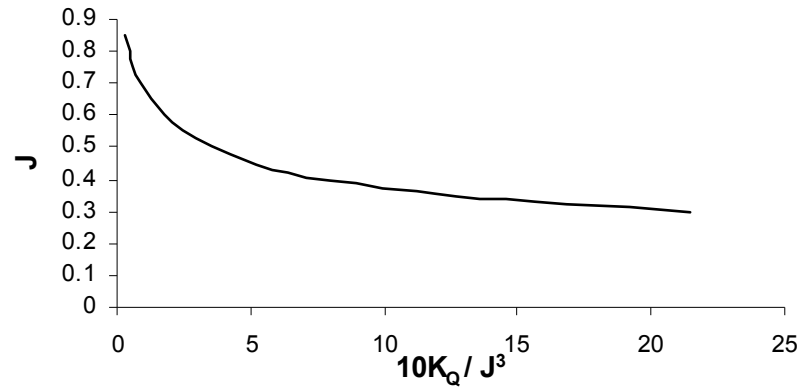
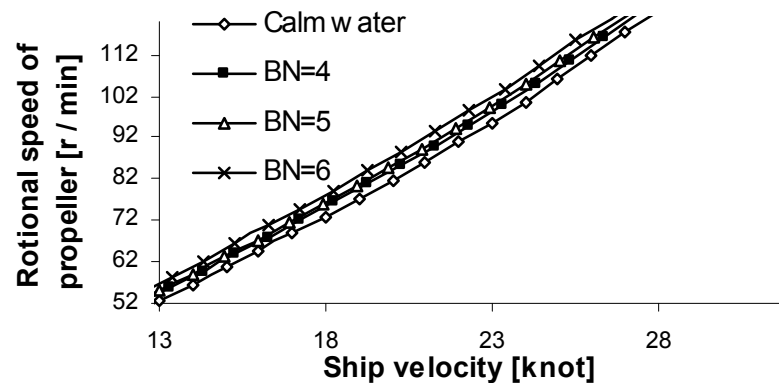
Figure 2.5 $10K_Q / J^3$ vs J curve

Figure 2.6 Propeller rotation speed under different Beaufort number in heading sea condition

2.4 IMO guidelines for ship safety

The sensitivity of a ship undergoing dangerous phenomena depends on the ship own characteristics (stability parameters, hull geometry) and operations in the wave (speed and direction of the ship). In 1995, an IMO “guidance to the master to avoid dangerous situations in following and quartering seas” for ship operation was approved by the MSC (Maritime Safety Committee) to ensure the ship safety under following and quartering seas. In 2007, the “revised guidance to the mater for avoiding dangerous situations in adverse weather and sea conditions” (IMO, 2007)

was released. These guidelines can consider four dangerous phenomena separately or jointly when a ship under certain sea state. The four dangerous phenomena are:

- Synchronous rolling.
- Parametric rolling.
- Riding on a wave crest of high wave groups.
- Surf-riding and broaching-to.

The IMO guidelines provide the advice for ship speed and course setting to avoid such dangerous situations. These guidelines are used in ITEES to ensure the ship safety during a voyage.

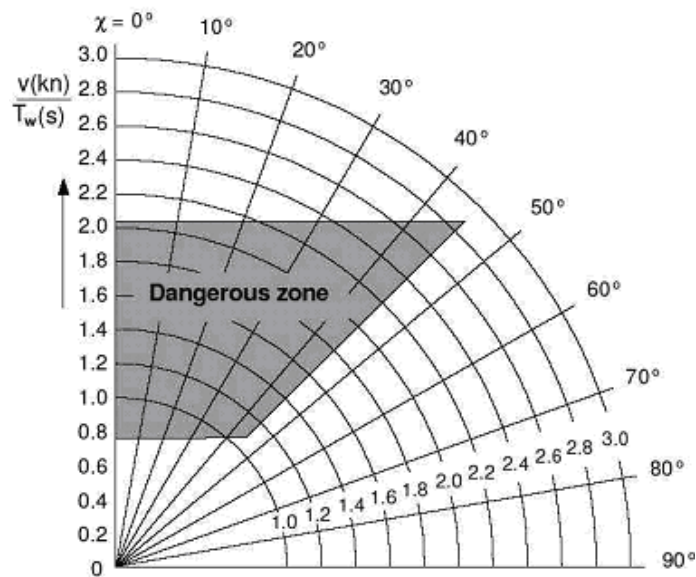


Figure 2.7 Dangerous zone due to high wave group (IMO, 2007)

Two diagrams as shown in Figure 2.7 and 2.8 are given in these guidelines to describe the potential occurrence of these dangerous phenomena and several parameters are needed when use these guidelines as list below:

T_r : Ship natural rolling period. (The natural rolling period of the case ship is 25s).

T_w : wave period.

λ : wave length.

C_w : wave speed.

T_e : wave encounter period.

L : ship length.

Wave height is not mentioned clearly in these guidelines. So wave height will be treated as an additional constraint condition to ensure the ship safety in this research.

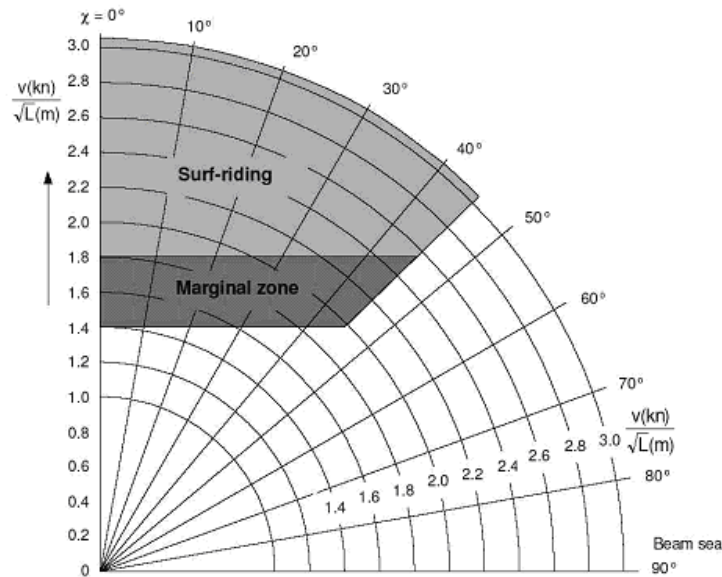


Figure 2.8 Risk of surf-riding in following or quartering seas (IMO, 2007)

The IMO guidelines were already used in the commercial onboard software “ARROW” (Benedict, 2008) to ensure the ship safety during the voyage. For using the IMO guidelines more conveniently, a polar diagram was applied in ARROW for the descriptions of ship operation and the formulas used in the guidelines will be transformed to facilitate the polar diagram drawing as shown in Table 2.7. A similar polar diagram is also applied by ITEES as shown in Figure 2.10 in which the length and the direction of the blue arrow represent the ship speed and heading, respectively. Zones with different colours are employed to represent different hazardous conditions of ship operation corresponding to a given weather condition. If the arrow falls in a colour zone during the route optimisation process, it means the ship safety is at risk. The dangerous zones are drawn in the direction of the wave propagation according to the critical speed formula in Table 2.7 in which negative speed means the following sea condition. By using the polar diagram in ITEES, the assessment of

ship's situation in the wave can be easily done and suitable values of the ships' speed and course to avoid these dangerous situations can be estimated obviously. Additionally the dangerous situation mentioned in the IMO guidelines will be treated as the constrain conditions in the route optimisation by ITEES.

Table 2.7 Summary of effects and formulas (Benedict, 2008)

| Phenomena | Dangerous zoon | Equation to calculate critical speed for polar diagram drawing | |
|---|--|---|---|
| Synchronous rolling | Strip segment over the diagram | $T_e = T_r / 0.8$ $V_{0.8} = \frac{kT_w}{0.514} \left(\frac{T_w}{T_r / 0.8} - 1 \right)$ | $T_e = T_r / 1.1$ $V_{0.8} = \frac{kT_w}{0.514} \left(\frac{T_w}{T_r / 1.1} - 1 \right)$ |
| Parametric rolling | Trapezoidal segment lay in the range of $\pm 30^\circ$ of the direction or reverse direction of the wave | $T_e = T_r / 1.8$ $V_{1.8} = \frac{kT_w}{0.514} \left(\frac{T_w}{T_r / 1.8} - 1 \right)$ | $T_e = T_r / 2.1$ $V_{2.1} = \frac{kT_w}{0.514} \left(\frac{T_w}{T_r / 2.1} - 1 \right)$ |
| Riding on the wave crest of wave groups | Trapezoidal segment lay in the range of $\pm 45^\circ$ of the direction of the wave | $V_{ride_on_wave_0.8} = -0.8T_w$ $V_{ride_on_wave_2.0} = -2.0T_w$ | |
| Surf-riding and broaching-to | Trapezoidal segment lay in the range of $\pm 45^\circ$ of the direction of the wave | $V_{surf_rideing_and_broaching1.4} = -1.4\sqrt{L}$ $V_{surf_rideing_and_broaching1.8} = -1.8\sqrt{L}$ $V_{surf_rideing_and_broaching3.0} = -3.0\sqrt{L}$ | |

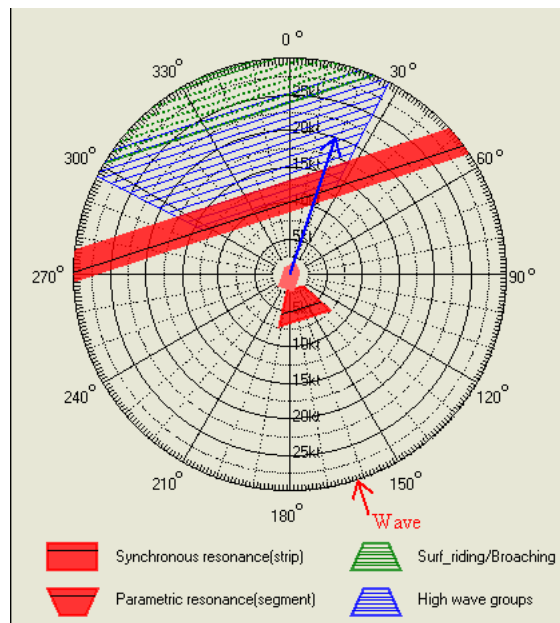


Figure 2.9 Polar diagram according to IMO guidelines

Chapter 3.

WEATHER FORECAST

The weather forecast is an absolutely indispensable factor for weather routing services. The reliability and availability of the weather forecast decide the feasibility of the whole software. However, most weather forecasts offered by the meteorological organisations or other companies can only cover limited sea areas with high price. Furthermore, obtaining cheaper and reliable weather forecast datasets usually becomes a bottleneck of the efficiency of weather routing services. Nevertheless, in this research, the free, highly precise weather forecast offered by the National Oceanic and Atmospheric Administration (NOAA) are used by ITEES and the OpenDAP (Cornillon, 2003; Sgouros, 2004) technology is employed to provide a transparent access to the distributed online weather forecast.

3.1 WAVEWATCH III model

The weather forecast used by ITEES is derived from the WAVEWATCH III (Tolman, 2009) model (sometimes referred to as *wwave3* or NOAA MMAB Operational Wave Model) which is considered to be one of the best models at present for computer generation of ocean surface weather forecasts.

WAVEWATCH III as a third generation wave model is developed at NOAA/NCEP which is an extension of WAVEWATCH (developed at Delft University of Technology) and WAVEWATCH II (developed at NASA). In comparison from its predecessors, some improvements are given in terms of the governing physical equations, the physical parameterizations used in these equations, and the numerical methods used for these equations solving. Furthermore, WAVEWATCH III is

improved from a wave model into a wave modelling framework, so that additional physical and numerical approaches can be easily developed based on it.

The properties of this model are (GMN, n.d.):

- Generates wind forecasts at sea level taking into account wave and current effects.
- Forecasts are only for ocean waters. The model does not generate forecasts for interior bodies of water such as the Mediterranean, Baltic, Black Sea, and Great Lakes.
- Does not forecast winds over land.
- Generates forecasts for significant wave height, mean wave direction, mean wave period, peak wave period, peak wave direction, wind sea direction, and wind sea period.
- Outputs from the model include wind direction (degree), wind speed (m/s), wind U component (m/s), wind V component (m/s), significant wave height (m), mean wave direction (degree), mean wave period (s), peak wave direction (degree), peak wave period (s), wind sea direction (degree) and corresponding wind sea period (s).
- Forecasts are produced in 3 hour intervals for 7 days (168 Hours).
- Model is run 4 times a day.
- Data generated on 1x1.25 degree grids.

3.2 OPeNDAP technique

The weather forecast transmission and service price are the bottlenecks for weather routing services. Nevertheless, the OPeNDAP protocol as a powerful communication technology is proposed which can allow various types of spatiotemporal data to be exchanged through computer networks reciprocally. This protocol has already been used in several fields like remote sensing and earth observation for data communication but this technology has not been widely used for weather routing service. By using OPeNDAP, the “weather forecast download module” of ITEES can obtain the weather forecast transparently and free, and then transmit it to the “route optimisation and simulation module” of ITEES for route optimisation (see Section 7.2).

OPeNDAP, an acronym for “Open-Source Project for a Network Data Access Protocol” was originally called DODS (Distributed Oceanographic Data system) (Sgouros, 2004). The client can use OPeNDAP functions which can send a Uniform Resource Locator (URL) to request data from the OPeNDAP server. In ITEES, the OPeNDAP URL which is used to obtain the weather forecast from the NOAA weather forecast servers is typically like:

http://nomads.ncep.noaa.gov/cgi-bin/filter_wave.pl?file=nww3.t00z.grib.grib2&leftlon=280&rightlon=365&toplat=60&bottomlat=30&dir=%2Fwave.20110610

This URL, contains the constraint expressions “file=nww3.t00z.grib.grib2&leftlon=280&rightlon=365&toplat=60&bottomlat=30&dir=%2Fwave.20110610” appended to the target URL following a question mark which describe the limits conditions for the request data. Only the interested data will be transferred back from the server. So by using this URL, the weather forecast from the date 10/06/2011 with scope longitude from 280 to 365 degree, latitude from 30 to 60 degree are retrieved from the dataset “nww3.t00z.grib.grib2” in the host machine “nomads.ncep.noaa.gov”. Using the OPeNDAP technology can make the weather routing more convenient and reduces the amount of data ITEES needs to process.

The format of the weather forecast retrieved from NOAA sever is GRIB (gridded binary data files) (WMO, 2010). The advantage of the format is that it makes the weather forecast can be downloaded by wireless with a very smaller size. At present, GRIB file cannot be read by ITEES directly. GRIB files will be converted into .shp files (ESRI, 1998) by the “Weather Forecast Download Module” of ITEES at first, and then ITEES reads the .shp file to display the weather forecast.

Chapter 4.

PROBLEM STATEMENT

Ship weather routing was first developed for determining shipping courses during a voyage with a minimum passage time (minimum time route). However, after the 1990s, most shipping companies emphasise on solving the minimum fuel route problem which is the focus of this project. The numerical formulations of the ship routing problem are given in this chapter. Once the essence of the problem is understood and the proper mathematical model is created, this paper will proceed with the task of the development a proper method to optimise the objective function.

4.1 The system model

4.1.1 What is minimum fuel route?

For the minimum fuel route problem, the objective is to find the optimal combination of speed and heading to minimise fuel consumption and subject to the specified departure, destination and voyage time which are included in the chartering contract of a merchant vessel; meanwhile, the ship's safety must be ensured during the whole voyage.

4.1.2 Ship control variable

Ship engine power and ship heading course directly decide the shipping route in the ocean. Instead of engine power, ship speed in calm water is chosen as the possible control since it is convenient to use ship speed in hydrodynamic analysis, determining resistance, ship speed loss, etc, (see Chapter 2). Once the ship speed in

calm water has been determined, the ship's power can be obtained by the one-to-one relationship between engine power and ship speeds described in Section 2.1. In this paper, V_c and ψ are chosen as the control variables to represent ship speed in calm water and shipping course measured from the true north. The control variables are denoted as a control vector \vec{U} , which is defined by $\vec{U} = (V_c, \psi)$.

4.1.3 Ship position vector

The trajectory of the ship sailing in the ocean can be basically described in terms of its position as time progresses. Ship position \vec{X} is specified by longitude φ and latitude θ , $\vec{X} = (\varphi, \theta)$. The departure point is $\vec{X} = X_s(\varphi_s, \theta_s)$ and the destination point is $\vec{X} = \vec{X}_{end}(\varphi_{end}, \theta_{end})$. Ship trajectory is represented by a continuous function of position \vec{X} and time t . The unit of longitude and latitude are degree in this research unless otherwise noted.

4.1.4 Weather condition

Clearly, the motion of the ship is affected by the weather condition at the ship's position. \vec{E} is used to denote weather conditions (speed and direction of wind, significant height, direction and peak frequency of waves and swells), which is a function of position \vec{X} and time t , $\vec{E} = F_E(\vec{X}, t)$.

4.1.5 Constraints condition

During a voyage, ship route constraints \vec{M} must be met to ensure ship and crew safety. The constraints include geographic constraints, control constraints and safety constraints.

1) Geographic constraints: regions of forbidden navigation such as land or dangerous areas such as areas of shallow water, icebergs, sea ice, or military practice, etc..

2) Control constraints include two aspects: ship heading change and engine power control

When optimizing a route, the ship heading is limited on each side relative to the current heading. Chen (1978) states that the maximum degree of the deviation from the current heading is 35 degree. When using the grid system to optimise the route (see Chapter 5 and 6), this constraint is reflected by the number of allowable state trajectories from a positional state to the subsequent stage. The constraint is meaningful since it can reduce much computing time.

Engine power is restricted in the scope of the propulsion plant capabilities. Engine overload is treated as a constraint condition during the voyage. The admissible engine power controls P_b satisfy the inequality $P_{min} < P_b < P_{max}$, where P_{max} correspond to the maximum continuous rating (MCR) of the main engine and P_{min} is minimum power for the ship steering requirement. Since the engine power has a one-to-one relationship with the ship speed in calm water, this constraint can be represented as $V_{min} < V_c < V_{max}$. In calm water and medium sea conditions a higher value of V_{min} can be used to reduce the computing time, and a lower value should be chosen for V_{min} to search the better results in rough sea conditions.

3) Safety constraints

Besides seeking the control policy which will minimise fuel consumption, the optimising program must ensure the ship safety during the whole voyage. The ship's motion is not allowed to exceed a certain value to prevent damage to the hull, cargo, engine, etc. Several researchers use the probability (frequency of occurrence) of severe phenomena such as shipping green water, slamming, propeller racing etc. to assess the severity of the ship's motion. Response amplitude operators (RAOs) are employed to calculate the response spectrum of the ship motion and then obtain the probability of these motions under different weather conditions. Mostly, RAOs are calculated by means of strip theory code based on the assumption of linearity which can give certain inaccuracy especially for following sea conditions. Moreover, the

interpolation of the ship motion database used for route optimisation can add to the burden of the calculation. The more ship motion is considered the more computing time will be used. To make ITEES simple and functional, instead of the complicated calculation of RAOs, the IMO guidance (IMO, 2007) which accommodates all types of merchant ships is used for ship safety consideration. The guideline gives recommendations to prevent capsize and heavy roll motion due to: surf-riding and broaching-to, reduction of intact stability caused by riding on a wave crest of high wave groups, synchronous rolling motion, and parametric rolling motion. A detailed description is given in Section 2.4. Since this guidance lacks a description concerning the restriction of wave height, the maximum wave height, which needs to be specified by the operator, is used as another constraint condition in this project.

4.1.6 Dynamics of the system

The ship speed over the ground V is a function of the ship's control vector \vec{U} and the weather condition \vec{E} .

$$V = f_0 (\vec{U}, \vec{E}) \quad (4.1)$$

Since the weather condition \vec{E} in the ocean can be predicted by specified time and position, so the ship speed can also be represented by

$$V = f (\vec{X}, \vec{U}, t) \quad (4.2)$$

The differentiation of the ship's position with respect to the time $d\vec{X} / dt$ can be given by a two dimensional vector function \vec{F} .

$$d\vec{X} / dt = \vec{F} (\vec{X}, \vec{U}, t) \quad (4.3)$$

The components of the vectors on both sides of the equation (4.3) can be described as follows:

$$d\vec{X} / dt = [d\varphi / dt, d\theta / dt]^T \quad (4.4)$$

$$\vec{F} = \begin{bmatrix} V \times \cos(\psi) / R_m(\theta) \\ V \times \sin(\psi) / R_p(\theta) \end{bmatrix} \quad (4.5)$$

Where:

V : ship speed over ground

ψ : the ship's heading

φ : longitude of the ship's position

θ : latitude of the ship's position

$R_m(\theta)$: radius of curvature in the meridian (Osborne, 2008)

$R_p(\theta)$: radius of curvature in the parallel (Osborne, 2008)

$R_m(\theta)$ and $R_p(\theta)$ can be given by using the world geodetic system 1972 (WGS-72) as follows:

$$R_m(\theta) = a(1 - e^2) / (1 - e^2 \sin^2 \theta)^{3/2} \quad (4.6)$$

$$R_p(\theta) = a \cos \theta / (1 - e^2 \sin^2 \theta)^{1/2} \quad (4.7)$$

Where:

a : radius of equator of the earth (6378.135 km)

e : eccentricity of meridian of the earth (0.08181881)

To simplify the problem, it is assumed that the earth is round and the eccentricity of the meridian e is zero. The error of this simplification is totally accepted for real navigation application (Chen 1978). So the $R_m(\theta)$ and $R_p(\theta)$ can be rewritten as

$$R_m(\theta) = a \quad (4.8)$$

$$R_p(\theta) = a \cos \theta \quad (4.9)$$

The equation 4.3 can be referred to as the dynamic constraint of the optimisation.

4.1.7 Fuel consumption

For the minimum fuel route problem, the fuel consumption of the whole voyage will apparently be used as the objective function since the system is developed for container ship use only where operation mode of electricity gensets and boilers does not change so much during a voyage. Thus, fuel consumption by gensets and boilers are not included in the optimisation of ship operation. The fuel consumption of the main engine becomes the only consideration for minimum fuel route. The main engine power can be treated as a function of the ship control variable \bar{U} , ship position \bar{X} , ship constraints condition \bar{M} and time t , so the fuel consumption per hour q can be calculated by

$$q = sfc \cdot P_b(\bar{X}, \bar{U}, \bar{M}, t) \quad (4.10)$$

Where:

sfc : specific fuel consumption

P_b : main engine power

Since the constraints condition \bar{M} has a direct relation with ship position \bar{X} and control variable \bar{U} , so the fuel consumption per hour q can also be represented by

$$q = sfc \cdot P_b(\bar{X}, \bar{U}, t) \quad (4.11)$$

The fuel consumption of the whole voyage J can be given by this integral as follows:

$$J = \int_{t_s}^{t_{end}} sfc \cdot P_b(\bar{X}, \bar{U}, t) dt \quad (4.12)$$

Or more compactly

$$J = \int_{t_s}^{t_{end}} \alpha'(\bar{X}, \bar{U}, t) dt \quad (4.13)$$

Where:

t_s : departure time

t_{end} : schedule arrive time at the destination

4.2 Formulation as an optimisation problem

The complete formulations of the minimum fuel route problem can be summarised as a standard continuous optimisation problem:

Find the time dependent control variable \bar{U} which can minimise the objective function J given by (4.13)

Subject to:

Dynamic constraint given by (4.3)

Constraints condition as described in section 4.1.5

Initial conditions: ship departure position $\vec{X} = X_s(\varphi_s, \theta_s)$ at time $t = t_s$

Final conditions: ship arrival position $\vec{X} = \vec{X}_{end}(\varphi_{end}, \theta_{end})$ at time $t = t_{end}$

In order to programme the optimisation code by computer it is more convenient to treat a continuous weather routing problem as a discrete optimisation problem. The following chapters will give a detailed description regarding how to solve the minimum fuel route problem.

Chapter 5.

DYNAMIC PROGRAMMING METHOD FOR WEATHER ROUTING

The ship performance, weather characteristics, and the essence of the ship weather routing problem have already been discussed in the previous chapters. This chapter will present a novel three dimensional dynamic programming method (3DDP) which can be used to search for the optimised route with minimal fuel consumption during the voyage. Compared with the traditional two dimensional dynamic programming (2DDP) which only optimise the ship's heading, while the engine power or propeller rotation speed is set as a constant throughout the voyage, this new method considers both the ship power settings and heading controls so this new method could lead to quasi-global optimal routing in comparison with traditional weather routing methods. Section 5.1 gives the basic concepts of dynamic programming. Section 5.2 will discuss the choice of the stage variable. Section 5.3 describes the difference between the forward and backward iteration algorithm. After choosing the proper strategy the weather routing problem, solved by dynamic programming in our research, is summarised in section 5.4. Section 5.5 deals with the construction of a grid system used by the dynamic programming for weather routing. The descriptions of 2DDP and 3DDP methods are given in section 5.6 and 5.7 respectively.

5.1 The introduction of dynamic programming

Dynamic programming, originally developed by Richard Bellman (1957), is a powerful tool utilised to solve optimisation problems and is already widely used in many fields, such as aerospace engineering (Buttazzo, 2009), electrical engineering (Chen, 2011), mechanical engineering (Bullo, 2004), chemical engineering

(Dadebo,1995), economics (Adda, 2003) and so on. The optimisation problems which can be solved by dynamic programming are variously called variation control problems, dynamic optimisation problems or optimisation problems for multistage decision processes. This type of problem is characterised by the fact that each decision transforms the current problem into a new problem, i.e., the control decision taken at the present time affects the behaviour of the system at future times. Hence the dynamic programming can be used to get a sequence of decisions over the entire duration of control, not simply a decision at the present time. Because it is straight forward and can handle the system constraints easily, dynamic programming is very appropriate as the optimisation algorithm for weather routing problem solving.

The main concept of this technique is based on Bellman's principle of optimality which can be stated as follows (Bellman, 1957):

“An optimal policy has the property that whatever the initial state and initial decision are, the remaining decisions must constitute an optimal policy with regard to the state resulting from the first decision.”

The basic strategy behind dynamic programming is quite simple. In general, dynamic programming separates a large complicated problem into many sub problems and solves the sub problems first; then, by recursively using the principle of optimality, the sub problems are combined to reach an overall solution and, finally, the optimal sequence of decisions can be identified. Often, many of these sub problems are really the same. The dynamic programming approach seeks to solve each sub problem only once, thus reducing the number of computations. This is especially useful when the number of repeating sub problems is exponentially large.

5.2 Stage variables in weather routing problems

The criterion used to determine the optimal policy is called the objective function. In our weather routing problem, the objective function is the fuel consumption during

the voyage. In dynamic programming, two variables, stage and state, within the objective function need to be defined first before solving the optimisation problem.

The stage variable is the variable in the objective function representing divisions of a sequence of various sub-problems of a system and determining the order in which events occur in the system. The decision choosing the control vector is done at a stage. The procedure is to calculate the sub-problems stage by stage. Information from the preceding stage is used to determine the control variables of the next stage. The parameters used in describing a stage must be variables which are monotonically increasing over the period in which decisions are being made. In the ship routing problems, time, fuel consumption, and voyage progress are monotonically increasing during a voyage so all these three variables can be used to define a stage. Aligne (1998) uses time as stages; De Wit (1990) and Calvert (1991) take voyage progress as stages; in references (Klompstra, 1992; Spaans, 1995) the isopone method was introduced in which fuel consumption is treated as stages. As many interpolations which can give inconvenience for programming are needed when fuel consumption is treated as stages, the isopone method is not practical for weather routing software development. In this section fuel consumption is out of the scope of the discussion of the choice of the stage variable.

Each stage consists of many states which are defined as a specifically measurable condition of the ship, such as time and geographic location. The different stage variables used can lead to different state variable spaces selected. The state variables must be discrete to form a grid system in the state space before using a dynamic programming method.

5.2.1 Time as a stage variable

Time is a commonly used stage variable in solving many classical optimal control problems. If time is chosen as the stage variable, the states on the stage can be defined by possible locations where the ship could pass. The grid system is shown in Figure 5.1.

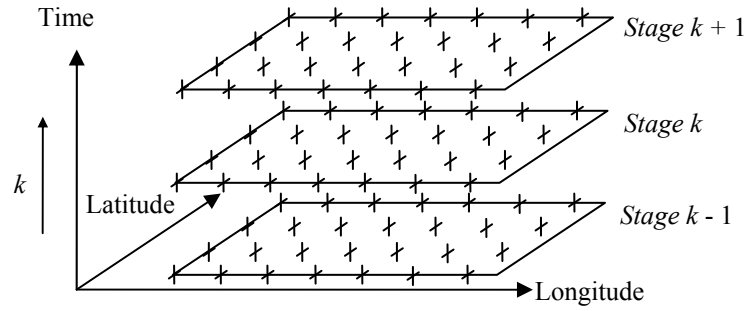


Figure 5.1 Grid system when time is the stage variable

When using dynamic programming, the stage variable t is quantised into uniform increments in order to permit solution by digital computer. Let

$$t = t_s + (k - 1)\Delta t \quad (5.1)$$

Where $k = 1, 2, 3 \dots K$. $K = (t_{end} - t_s) / \Delta t + 1$ which is the total number of the stage and t_{end} and t_s are arrival and departure time respectively.

Hence the dynamic equation of ship position in finite difference form becomes

$$\vec{X}(k + 1) = \vec{F}_d(\vec{X}(k), \vec{U}(k), k) \quad (5.2)$$

In contrast with the objective function (4.11) which has been defined as a continuous function, the objective function is re-written as a discrete form:

$$\begin{aligned} J(\vec{X}_{end}, K) &= \int_0^{t_{end}} \alpha(\vec{X}, \vec{U}, t) dt \\ &= \int_0^{\Delta t} \alpha' dt + \int_{\Delta t}^{2\Delta t} \alpha' dt + \dots \int_{(K-2)\Delta t}^{(K-1)\Delta t} \alpha' dt \\ &= \sum_{k=1}^{K-1} \alpha_k(\vec{X}(k), \vec{U}(k), k) \end{aligned} \quad (5.3)$$

The formula (5.3) can be interpreted as the total fuel consumption of the voyage is a summation of the fuel consumption between each time interval of the stage. The objective, now, becomes how to find the optimum solution which can minimise the formula (5.3). The recursive computation procedure based on Bellman's principle of optimality can be used for problem solving:

The minimum cost function at stage k can be defined in a reverse form as

$$J^* (\bar{X}(k), k) = \underset{\substack{U(j) \\ j=k, k+1, \dots, K-1}}{\text{Min}} \sum_{i=k}^{K-1} \alpha_i(\bar{X}(i), \bar{U}(i), i) \quad (5.4).$$

Where $k = K, K - 1, \dots, 3, 2, 1$. The term $\alpha_i(\bar{X}(i), \bar{U}(i), i)$ which represents the fuel consumption from stage i to stage $i + 1$.

Equation (5.4) means that the cost function at stage k is a summation of the fuel consumption from stage k via stage $k + 1, k + 2$ to stage K . It assumes that the control variables, ship delivery engine and ship course, for the trajectory from stage to stage are constant values unless the voluntary ship speed reduction is needed to ensure the ship safety during the rough sea condition. The control variables are only changed at each stage.

Formula (5.4) can be rewritten as follows:

$$J^* (\bar{X}(k), k) = \underset{\substack{U(j) \\ j=k, k+1, \dots, K-1}}{\text{Min}} (\alpha_k(\bar{X}(k), \bar{U}(k), k) + \sum_{i=k+1}^{K-1} \alpha_i(\bar{X}(i), \bar{U}(i), i)) \quad (5.5)$$

In formula (5.5) the cost function at stage k can be treated as a minimisation of two parts of fuel consumption: fuel consumption from stage k to stage $k + 1$, and the fuel consumption from stage $k + 1, k + 2, \dots, K$.

Rewriting formula (5.5) as

$$J^* (\bar{X}(k), k) = \underset{U(K)}{\text{Min}} \left(\underset{\substack{U(j) \\ j=k+1, k+2, \dots, K-1}}{\text{Min}} (\alpha_k(\bar{X}(k), \bar{U}(k), k) + \sum_{i=k+1}^{K-1} \alpha_i(\bar{X}(i), \bar{U}(i), i)) \right) \quad (5.6)$$

the first term in the brackets which represents the fuel consumption from stage k to stage $k + 1$ is clearly subject to the control variable $\bar{U}(k)$ and is independent of any other control variables from stage $k + 1$ to stage K . So, formula (5.6) can be written as

$$J^* (\bar{X}(k), k) = \underset{U(K)}{\text{Min}} \alpha_k(\bar{X}(k), \bar{U}(k), k) + \left(\underset{\substack{U(j) \\ j=k+1, k+2, \dots, K-1}}{\text{Min}} \sum_{i=k+1}^{K-1} \alpha_i(\bar{X}(i), \bar{U}(i), i) \right) \quad (5.7)$$

The second term in formula (5.7) has the same form with (5.4). It is the minimum cost function at stage $k + 1$ which depends on $\bar{X}(k + 1)$ determined by $\bar{X}(k)$, $\bar{U}(k)$ through the dynamic equation of ship position (5.2). Therefore, the minimum cost function at stage k can be rewritten as a recursive function:

$$J^* (\bar{X}(k), k) = \underset{U(K)}{\text{Min}} \alpha_k(\bar{X}(k), \bar{U}(k), k) + J^* (\bar{X}(k + 1), k + 1) \quad (5.8)$$

Formula (5.8) can be explained according to the Bellman's principle of optimality. The minimum cost function at stage k can be solved based on the minimum cost function at stage $k + 1$.

As a recursive algorithm, a boundary condition which is corresponding to terminal cost function at the destination must be prescribed at stage K . It can be clearly seen that

$$J^* (\bar{X}(K), K) = 0 \quad (5.9)$$

The minimum cost function at any state defined by the grid point in the state space can be calculated by using equation (5.8) and (5.9) in a backward recursion stage to stage from the last stage $k = K$ to the first stage $k = 1$. Once the minimum cost function is obtained, the corresponding optimised control at this state and the state index of the last stage the ship will arrive under this control need to be saved for tracing the optimum route by a forward procedure at the end of the calculation.

It should be pointed out that the above derivation for the calculation of the optimised route is based on the backward recursive computation procedure which is a powerful technique and commonly used in most of optimisation problems. However, the property of the weather routing problem makes such a strategy unsuitable. Instead of the backward method, a forward computer procedure can give much more advantage and a detailed description will be introduced in section 5.3.

It might also be noted that the dynamic equation (5.2) cannot be directly used in most time. Usually, two normal means are employed to deal with the dynamics property of the problem:

1) The inverse function of equation (5.2) can be written as

$$\vec{U}(k) = \vec{F}_d^{-1}(\vec{X}(k), \vec{X}(k+1), k) \quad (5.10)$$

Use this inverse function to calculate the control variable $\vec{U}(k)$ which can make the ship transfer exactly from state $\vec{X}(k)$ at stage k to state $\vec{X}(k+1)$ at stage $k+1$. The interpolating method which will certainly increase the calculation and computing time is needed to solve this function and it will become difficult especially for rough sea condition in which the voluntary ship speed reduction is required to ensure the ship safety. Even if the control variable $\vec{U}(k)$ is obtained other interpolation is also needed to obtain the ship performance under this control based on the ship's hydrodynamic database. It also increases the computational burden.

2) The discrete control variable $\vec{U}(k)$ can be used in equation (5.2), but in most time the $\vec{X}(k+1)$ obtained from this equation will possibly not coincide exactly with the grid points in the state space. In that case, the value of the minimum cost function $J^*(\vec{X}(k+1), k+1)$ in equation (5.8) should also be interpolated among the known values of the grid point on stage $k+1$.

The large number of the interpolations in these two means become the shortcoming of the dynamic programming.

5.2.2 Voyage progress as a stage variable

Voyage progress can be defined as a measure of the progress of the vessel from departure. If voyage progress is chosen as the stage variable, the states should be defined by time and possible geographical positions. The grid system can be designed as Figure 5.2 (in section 5.5.1). A detail description of the grid system is given in section 5.5.

The objective function remains the same as mentioned in the last section but the equation (5.3) is written in an alternative form which is an integral with respect of the distance of the voyage.

$$\begin{aligned}
 J(\vec{X}_{end}, K) &= \int_0^{t_{end}} \alpha(\vec{X}, \vec{U}, t) dt \\
 &= \int_0^{t_{end}} \alpha(\vec{X}, \vec{U}, t) \frac{dt}{dl} dl \\
 &= \int_0^L \alpha(\vec{X}, \vec{U}, t) \frac{1}{V_{ship}} dl \\
 &= \int_0^{L_1} \alpha' dt + \int_{L_1}^{L_2} \alpha' dt + \dots \int_{L_{(K-2)}}^L \alpha' dt \\
 &= \sum_{k=1}^{K-1} \alpha_k(\vec{X}(k), \vec{U}(k), k)
 \end{aligned} \tag{5.11}$$

Where L is the total distance of the voyage and the voyage is divided according to the stage as drawn in Figure 5.2.

Similar with the explanation of the equation (5.3), the formula (5.11) can be interpreted as the total fuel consumption of the voyage is a summation of the fuel consumption between each distance segment of the voyage.

The dynamic equation and the recursive procedure to calculate the minimum cost function have the same form as discussed in the last section. The 3DDP method adopts the voyage progress as the stage variable. As mentioned in the last section, the tradition means to deal with the dynamics of the problem needs a lot of interpolation which can increase the computation. To overcome this disadvantage, a “floating state” technique is used in the 3DDP method which will be addressed in section 5.4.

5.2.3 Choosing the stage variable

Clearly, the different choice of stage strategies does have some distinct different computing efficiency and results in considering the respective feasible state space.

Time has often been used as the stage variable in many optimisation problems especially for a system in which the control is changed with time. At first sight, time used as the stage variable seemed very reasonable for the weather routing problem and this strategy was already adopted by Aligne (1998). But in the author’s opinion, time as a stage variable has several disadvantages.

First, consider the inverse function which is used to determine the control variables as mentioned in 5.2.1. The ship’s heading from stage to stage is expressed explicitly by the grid system shown in figure 5.1. If the ship’s engine power is used as another control variable, interpolations must be used to solve the inverse function. Interpolations seem to be avoided if the ship’s speed over ground is the control variable. But, if the weather condition is so severe during two stages, the ship’s speed must be slowed down to ensure ship safety at some time. In this situation, the trouble of interpolation is also caused unless the time interval is so small that the weather condition during this time interval can be treated as a constant value without much

difference. Nevertheless, the minor time interval will add to the computation burden because of the increment of the total number of stages.

If discrete control variables (ship's heading and engine power) are used in the dynamic equation, the ship state of the next stage obtained from the dynamic equation (5.2) cannot exactly coincide with the grid system. As a result, the minimum cost function which is explicitly related to time when time as the stage variable cannot be expressed as a function of the grid point in the state space (ship's position). It creates serious difficulties for the interpolation of the minimum cost function which needs to consider two dimensions i.e. longitude and latitude between the discrete operated grid points. As a result a finer grid system is also required to ensure the precise interpolation which increases the computation when optimising the ship routing.

When considering the voyage progress as the stage variable, the great circle between departure and destination is usually used as a reference to create the grid system and the state becomes the geographic location perpendicular away from the great circle together with time. The grid system is shown in Figure 5.2. The ship's heading from one stage to another is specified by the pre-defined grid system, so that the ship's engine power or ship speed in calm water becomes the only defined control variable between two stages since the heading is expressed explicitly by the grid. It requires the ship to be perfectly controllable during the navigation between the grids points. This restriction is not a big problem for the modern ship with powerful control devices (Chen, 1978). In the other side, this restriction implies that the ship can only go ahead in the severe the sea condition but can reduce speed to insure the ship's safety

The advantage of the voyage progress as the stage variable is that the ship position at every stage is restricted by the geographic position of grid points and the minimum cost function only depends on the time variable. The interpolation which only needs to be executed in the time domain makes the calculation procedure simpler than the interpolation in two dimensions (longitude and latitude) when time is used as the

stage variable. In the 3DDP method, the interpolation can be further avoided by using a “float state” technique so that the calculation procedure is simplified and the computing time can be reduced.

Since the voyage progress shows the advantages than when time is used as the stage all discussion below is based on the voyage progress as the stage.

5.3 Forward computation procedure

In the last two sections, the minimum cost function at stage $k - 1$ is derived from the value of the last stage k , so the direction of problem solving is from the last stage K to the first stage. This kind of strategy is called “backward dynamic programming” which can be described as a path is optimal if, and only if, for any intermediate stages, the choice of the following path is optimum for this stage. Backward dynamic programming is a powerful technique commonly used for solving an optimised problem by dynamic programming. However, the properties of the weather routing problem make such a solution strategy unsuitable.

When using the backward strategy, the ship arrival time at the destination which determines the states of the last stage must be known to finish the recursive calculation. It really poses certain obstacle for minimum time problems. For the minimum fuel problem, which our research focuses on, the minimum fuel solution under a different departure time but the same arrival time can be obtained when using the backward strategy. In most time, the optimised route needs to be recalculated once the weather forecast is updated during the voyage, the departure time at the current location where the optimisation has been concerned is certainly known and the arrival time at the destination is an unknown value. It can be clearly seen that the backward recursive procedure is not proper for weather routing problems.

Instead of using the backward procedure, a forward algorithm offers more convenience in programming. As a contrast with the backward version, the forward

algorithm can be interpreted as that: a path is optimal if, and only if, for any intermediate stages, the choice of the past path is optimum for this stage. In the forward algorithm, the initial departure time is fixed; the arrival time at a location where the optimisation calculation has progressed to can be treated as a flexible parameter. This allows a set of route with a minimum fuel consumption to be obtained corresponding to different arrival times at the current location where the optimisation has been concerned. This is a logical process in line with the ship operation along a voyage course.

The equations used in the forward dynamic programming simply require a re-arrangement of these functions used in the backward strategy. The minimum cost function at stage k can be defined in a forward form as

$$J^* (\vec{X}(k), k) = \underset{\substack{U^{(j)} \\ j=2,3,\dots,k}}{\text{Min}} \sum_{i=2}^k \alpha_i(\vec{X}(i), \vec{U}(i), i) \quad (5.12).$$

Where $k = K, K - 1, \dots, 3, 2, 1$. The term $\alpha_i(\vec{X}(i), \vec{U}(i), i)$ represents the fuel consumption from stage $i - 1$ to stage i .

Equation (5.12) means that the cost function at stage k is a summation of the fuel consumption from the stage 1 via stage 2, 3 to stage k . and it assumes that the control variables, ship delivery engine and ship course, for the trajectory from stage to stage are constant values unless the voluntary ship speed reduction is needed to ensure the ship safety during rough sea conditions. The control variables are only changed at each stage.

With the similar derivation process as the backward strategy, the minimum cost function under forward direction can be rewritten as the following recursive equation:

$$J^* (\vec{X}(k), k) = \underset{U^{(K)}}{\text{Min}} \alpha_k(\vec{X}(k), \vec{U}(k), k) + J^* (\vec{X}(k-1), k-1) \quad (5.13)$$

Formula (5.13) can be explained as a contrast with the backward strategy that the minimum cost function at stage k can be solved based on the minimum cost function at stage $k - 1$ and the boundary condition can be given as

$$J^* (\vec{X}(1), 1) = 0 \quad (5.14)$$

The forward strategy is used in this research for weather routing problems.

5.4 Statement of the weather routing problem in dynamic programming

After choosing the proper strategy in the previous section, the weather routing problem solved by dynamic programming in our research can be summarised as follows:

Stage variable: k , which indexes the measure of the progress of the vessel from departure (voyage progress). The division of the stage variable uses the great circle form departure to destination as a reference.

State variable: $\vec{X}(k) = (\vec{P}, t)$, where \vec{P} denotes the discrete ship positions in the predefined grid system on a latitude \times longitude plane. Unlike traditional dynamic programming, the time variable t of states in the 3DDP is not fixed. It will be determined as the optimisation procedure is progressed (See 5.8.1).

Control variable: $\vec{U} = (V_c, \psi)$, where V_c is ship speed in calm water (corresponding to engine power). It should be a set discrete value when using the 3DDP method. The ship's heading ψ is pre-defined on the grid system, hence V_c becomes the only control variable.

Constraints: \bar{M} , which includes geographic constraints, control constraints and safety constraints. The geographic constraints and the control constraints can be considered when designing the grid system. Grids, which cross islands/rocks, can be deleted when designing the grid system. Safety constraints according to the IMO guidelines described in Chapter 2 and the specified maximum wave height become the explicit constraint condition when using the dynamic programming.

Objective Function: minimise the total fuel consumption during the voyage.

$$J^* (\bar{X}(K), K) = \underset{j=2,3,\dots,K}{\text{Min}}_{U(j)} \sum_{i=2}^K \alpha_i (\bar{X}(i), \bar{U}(i), i) \quad (5.15)$$

5.5 Grid system

Dynamic programming uses a grid system to specify the space layout of stages and states used in the algorithm calculation. The grid system can have a strong influence on the optimised result. Different grids will result in different optimal routes even by the same dynamic programming method. A new creation method of the grid system is presented in this section. This new method is based on few parameter settings and makes the grid construction understandable and easy to tune. This kind of grid system can be used for ocean voyages and coastal navigation.

5.5.1 Grid points division in geographic projection

The grid system used by the 3DDP method is of three dimensions, i.e. time and geographical location (longitude and latitude), to represent the states. Unlike the traditional dynamic programming, the time variable of a state in the 3DDP is not fixed. It will be determined during the optimisation procedure, but the geographical distribution of the grid points should be defined before the optimisation calculation.

When designing the grid system, it is assumed that the earth is spherical, ignoring ellipsoidal effects, which is accurate enough for the weather routing problem. A great circle, which is the intersection of a sphere with a plane passing through the centre of the sphere, represents the shortest route between two points on the surface of the earth. Clearly the great circle is the optimum route under calm water from the departure to the destination, so it is chosen as a reference route which forms the central line for the construction of the grid system used in the 3DDP route optimisation.

Before addressing the process of the grid system construction, three useful formulas are presented:

(1) Given the departure location $\vec{X}_1(\varphi_1, \theta_1)$ and the destination location $\vec{X}_2(\varphi_2, \theta_2)$, the distance of the great circle between these two points on the earth can be calculated by

$$D = \arccos(\sin(\theta_1) \cdot \sin(\theta_2) + \cos(\theta_1) \cos(\theta_2) \cdot \cos(\varphi_2 - \varphi_1)) \cdot 60 \quad (5.16)$$

Where the unit of the return value of acos is degree and the unit of the distance is sea mile. If using km as the unit this formula can be written as:

$$D = \arccos(\sin(\theta_1) \cdot \sin(\theta_2) + \cos(\theta_1) \cos(\theta_2) \cdot \cos(\varphi_2 - \varphi_1)) / 180 \cdot \pi \cdot R \quad (5.17)$$

where R is the mean radius of the earth which is 6371 km. To make the process convenient, in this research all distance parameters adopt sea mile “nm” as the unit corresponding to the speed unit “knot” unless otherwise noted.

(2) Given the departure location $\vec{X}_1(\varphi_1, \theta_1)$ and the destination location $\vec{X}_2(\varphi_2, \theta_2)$, the initial course along the great circle at departure position is computed by

$$C = \arctan(\sin(\varphi_2 - \varphi_1) \cdot \cos(\theta_2), \cos(\theta_1) \cdot \sin(\theta_2) - \sin(\theta_1) \cdot \cos(\theta_2) \cdot \cos(\varphi_2 - \varphi_1)) \quad (5.18)$$

Since arctan returns values in the range -180 to 180 degree, the result of the last formula needs to be normalised in the compass bearing range 0 to 360 degree. Please note that if a ship sails along the great circle, the course will vary during the voyage.

(3) Given the departure location $\vec{X}_1(\varphi_1, \theta_1)$, the distance D of the great circle between departure and destination and the initial course C along this great circle, the destination location $\vec{X}_2(\varphi_2, \theta_2)$, can be given by

$$\begin{aligned} \theta_2 &= \arcsin(\sin(\theta_1) \cdot \cos(D/60) + \cos(\theta_1) \cdot \sin(D/60) \cdot \cos(C)) \\ \varphi_2 &= \varphi_1 + \arctan(\sin(C) \cdot \sin(D/60) \cdot \cos(\theta_1), \cos(D/60) - \sin(\theta_1) \cdot \sin(\theta_2)) \end{aligned} \quad (5.19)$$

By using these three formulas, the geographical locations of the grid points can be determined.

The distance D of the referenced great circle (RGC) between ship departure position $\vec{X}_s(\varphi_s, \theta_s)$ and the destination position $\vec{X}_{end}(\varphi_{end}, \theta_{end})$ can be calculated by Formula 5.16. The initial course C at departure position is computed by Formula 5.18.

The RGC is divided equally by a series of grid points on it to measure the stage. The departure and the destination point represent the first and last stage respectively. The total number stages is K , so every segment length between two stages on the great circle is $\Delta X = D / (K-1)$. The total number of stages is determined according to the total distance of route and the availability of computing capacity.

After calculating the initial course C and the length X , these two values are placed with the departure position $\vec{X}_s(\varphi_s, \theta_s)$ into the Formula 5.19. The grid point P_2 with position (φ_2, θ_2) to measure the second stage on the great circle can be determined. The initial course C_2 at point P_2 along RGC can be given by using Formula (5.18) when using P_2 as the departure position in this equation.

After obtaining the grid point P_2 , the lateral positional grid points, away from RGC at the second stage, can be created. All these lateral positions are located with a predefined unit spacing ΔY on another great circle which crosses the point P_2 and have 90 degree intersection at P_2 with RGC as shown in Figure 5.2 in which a grid system with 16 stages is given. Figure 5.3 is a cut-out of the region around stage 2 from Figure 5.2. The scope of coverage for a stage can be defined as a certain proportion of the RGC. The farthest grid on a stage from the RGC is the possible locations where the ship may pass to avoid bad weather or sea conditions. Assume the total number of the grid points on one stage in geographic projection is N , the length of RGC is L_{RGC} and the proportion between the breadth of one stage and L_{RGC} is ζ , then $\Delta Y = L_{RGC} \times \zeta / (N - 1)$. Note that N should be an odd number since the amount of the grid points in geographic projection on both sides of the RGC is the same.

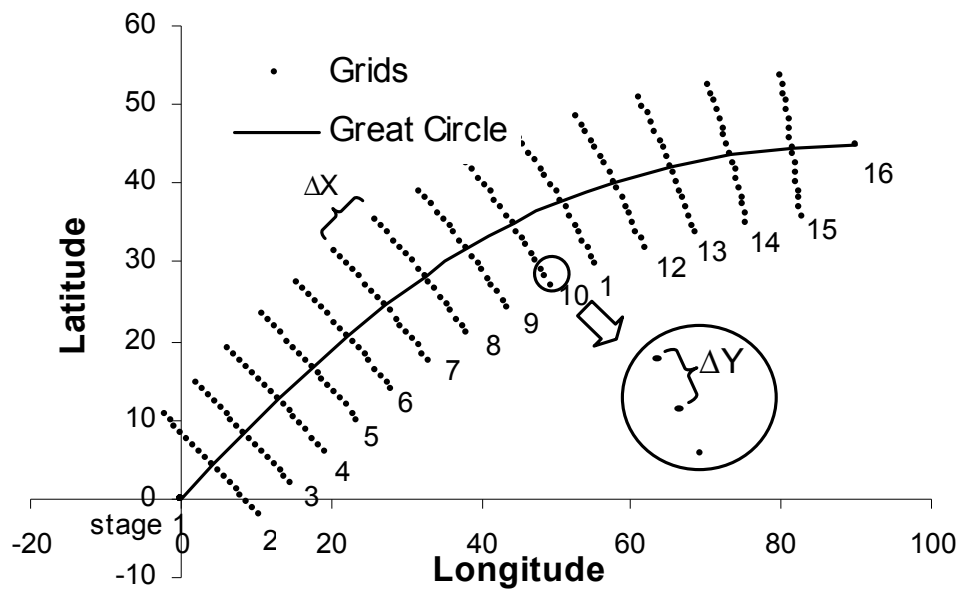


Figure 5.2 Grid system when voyage progress is the stage variable

The initial course C_{2L} at point P_2 along the further great circle on the port side of RGC should be C_2 plus 90 degrees. By substituting ΔY and C_{2L} for relevant parameters in Formula 5.19 and treating point P_2 as the departure position in this formula, the position $\vec{X}_{p_{21}}(\varphi_{21}, \theta_{21})$ of the first lateral grid point P_{21} on the portside

of point P_2 can be determined. The initial course C'_{21L} from point P_{21} to point P_2 can be calculated by function 5.18 so the initial course C_{21L} from point P_{21} to the next lateral grid point P_{22} on the port side is C'_{21L} plus 180 degree. As mentioned above, this value needs to be normalised in the range 0 to 360 degree. By substituting ΔY and C_{21L} for relevant parameters in Formula 5.17 and treating point P_{21} as the departure position in this formula, the position $(\varphi_{22}, \theta_{22})$ of the grid point P_{22} can be determined.

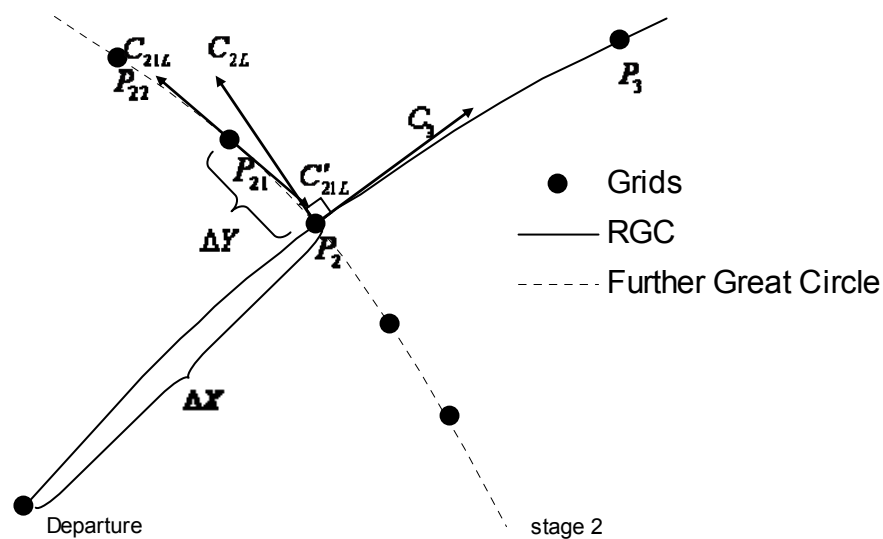


Figure 5.3 Cut-out of the region around stage 2 from Figure 5.2.

As with calculating the geographic position of P_{22} , the geographic position of remaining lateral grid points on the portside of RGC at stage 2 can be determined one by one. The geographical location of grid points on the starboard side of RGC at stage 2 can be calculated in the same way.

By repeating the processes above, all the geographical distribution of grid points from stage 2 to stage $K-1$ are defined. The geographic position of the grid points are saved in array $P(i, k)$, where $i = 1, 2, \dots, N$, $k = 1, 2, \dots, K$. Here, k represents the stage number and i is used to specify the index of a grid point position in an incremental

order from the port side to the starboard side on stage k . So, the position of departure and destination correspond to $P((1 + N)/2, 1)$ and $P((1 + N)/2, K)$. Other values of P on stage 1 and stage K are set as NULL.

5.5.2 Determination of the allowable ship course

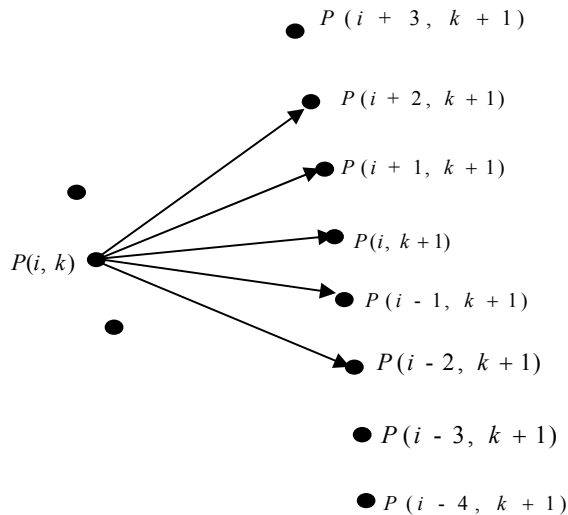


Figure 5.4 Transitions from stage k to stage $k + 1$ under $q = 2$

The ship is restricted in transit from one stage to the next according to the predefined geographic position of the grid points. As mentioned in Chapter 4, the larger course deviations are not feasible and would not be expected to form parts of an optimum route, so that the number of available trajectories from one stage to the next is restricted. For example, at point $P(i, k)$, the ship can transit to $P(i \pm q, k + 1)$, as in Figure 5.4, where q is a pre-set value to represent the number of such transitions allowed. Large q ensures the optimised route can be obtained but too many non-optimised routes may be evaluated which cause waste of the computing time. Small q can reduce certain unnecessary calculations but may miss the optimised solutions and sometimes obtain a zigzag route.

Trajectories connected between two stages are rhumb lines. A rhumb line is a curve on the earth surface and intersects all meridians of longitude at the same angle, i.e. without changing the direction as measured relative to true north. In short distance

navigation rhumb line is appealing since it is easier to follow a constant compass course than continually adjusting the heading as the ship follows a great circle, though rhumb lines are normally longer than great circles.

Given the start position $\vec{X}_1(\varphi_1, \theta_1)$ and the destination position $\vec{X}_2(\varphi_2, \theta_2)$, the distance of the rhumb line between these two points and the constant course along this rhumb line can be given as

$$D = ((\theta_2 - \theta_1)^2 + q'^2 \cdot (\varphi_2 - \varphi_1)^2)^{1/2} \cdot 60 \quad (5.20)$$

$$C = \arctan((\varphi_2 - \varphi_1), \Delta\eta) \quad (5.21)$$

Where:

D : the distance of the rhumb line (nm).

C : the course of the rhumb line (degree)

η : $\Delta\eta = \ln(\tan(\theta_2 / 2 + 180 / 4) / \tan(\theta_1 / 2 + 180 / 4))$, \ln is natural log.

q' : if the star and destination positions have the same latitude, then $q' = \cos(\theta_1)$ otherwise, $q' = (\theta_1 - \theta_2) / \Delta\eta$.

Note that if C and $(\varphi_2 - \varphi_1) / \pi \cdot 180$ are in the range -180 to 180 degree, these values need to be normalised in the compass bearing range 0 to 360 degree.

Given a start point and a distance D along a rhumb line with constant heading C , the following formula will calculate the position of destination point.

$$\begin{aligned} \theta_2 &= \theta_1 + D/60 \cdot \cos(C) \\ \varphi_2 &= (\varphi_1 + D/60 \cdot \sin(C)/q + 180) \% 360 - 180 \end{aligned} \quad (5.22)$$

where % is modulo.

To satisfy the geographic constraints, the grid points and the trajectories connected between two stages which cross islands/rocks should be ignored when optimising the route.

In ITEES software, a vector graphic is used to display the world map. A set of polygons with several vertices defined by longitude and latitude are used to represent the land on this map. However, the coastlines are very complicated and usually consist of hundreds of vertices to ensure the resolution. On the other hand there is no sufficiently convenient and fast algorithm which can check if a line crosses a polygon (Szłapczyńska, 2007). To make ITEES functional and practical, the raster graphic is used instead of vector map for checking if a line intersects with land. A high resolution raster graphic is created based on the vector map. This raster graphic covers the whole vector map but it is set as invisible in ITEES. So, in ITEES software, a vector graphic is used to display the world map, route lines or grid system, but uses an invisible raster map to check if a line crosses land. A similar method is also adopted by research Szłapczyńska (2007).

The raster graphic consists of many cells which correspond to a Boolean value “true” or “false” depending on whether or not land covers the entire cell. According to the position of a point, the corresponding cell which the point gets into on the raster graphic can be found easily. The rhumb line connecting two points are divided by several equal intermediate points with unit spacing ΔD (nm) which is one sea mile adopted by ITEES and equal to the resolution of the raster graphic. The positions of the intermediate points can be calculated one by one by using formula (5.22). The process of checking if a rhumb line between position $\vec{X}(\varphi_{start}, \theta_{start})$ and $\vec{X}(\varphi_{end}, \theta_{end})$ crosses land is given as the following flow chart and a similar process is also adopted by Szłapczyńska (2007).

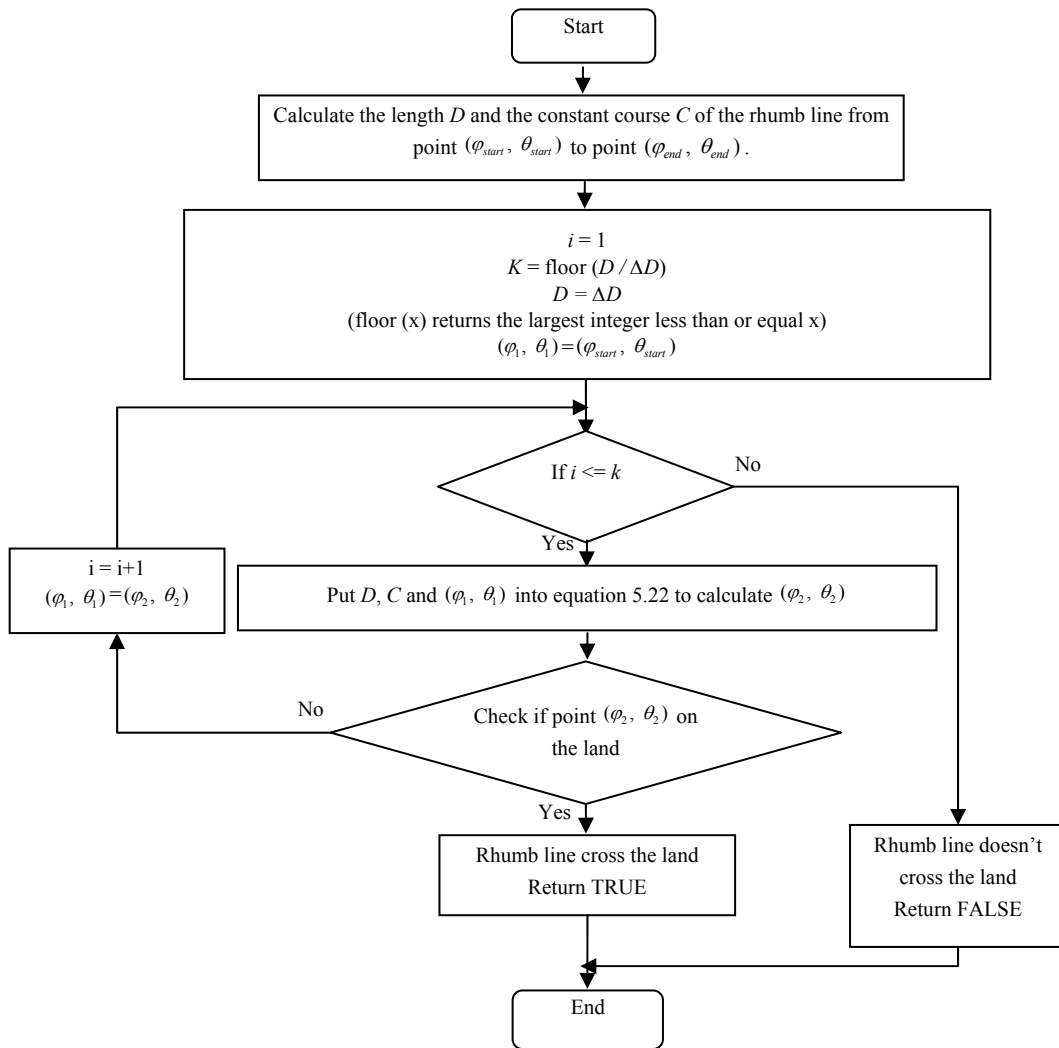


Figure 5.5 Check if a line crosses the land

All the trajectories connected between the grid points on the geographic plan need to be inspected to ensure that the control constraints and the geographic constraints are not violated. On the other hand, only the trajectories which can be achieved by previous trajectories are considered. The inspection is dealt with first so several unavailable trajectories on the grids system can be deleted before optimisation to save computing time. Before introducing this inspection procedure, the parameters used in this procedure are defined first:

- K : Total number of stages.
- N : Total number of grid points on a stage in geographic project.

- $P(i, k)$: The geographic position of the grid points as mentioned in section 5.5.1. $i = 1, 2 \dots N, k = 1, 2 \dots K$.
- Available_grid_point (i, k) : It is Boolean value correspond to point $P(i, k)$ and the value “FALSE” or “TRUE” indicate whether or not this point cross the land.
- Achieved_grid_point (i, k) : It is Boolean value correspond to point $P(i, k)$ and the value “TRUE” or “FALSE” indicate whether or not this point can be achieved by a trajectory form a point on the previous stage.
- Available_trajectories (i, k, j) : It is Boolean value correspond to the rhumb line from $P(i, k)$ to $P(j, k+1)$ and the value “TRUE” or “FALSE” indicate whether or not this rhumb line can be used for optimised the route.
- q : An integer value reflect the control constraints and indicate the ship can transit from $P(i, k)$ to $P(i \pm q, k + 1)$. Here $P(i \pm q, k + 1)$ means $P(i - q, k + 1), P(i - q + 1, k + 1) \dots P(i + q, k + 1)$.
- Flag_iteration: A Boolean value. “TRUE” or “FALSE” indicate weather or not stop the iteration.

The procedure of connecting the available trajectories according to a given grid system are as follow.

Step 1: Assign the array Available_grid_point by checking if the point crosses land. Note that except for the value corresponding to departure and destination, all other values of Available_grid_point on stage 1 and stage K are set as “FALSE”.

Step 2: Set $k = 1$, Flag_iteration = “TRUE”, all the values in array Available_trajectories as “FALSE” and all the values in array Achieved_grid_point as “FALSE” except for Achieved_grid_point $((1 + N)/2, 1)$ which correspond to the departure point.

Step 3: Iterate step 4 below for each geographic position i on stage k . If Achieved_grid_point (i, k) is “FALSE” there are no available trajectories

from a point of the previous stage to point $P(i, j)$, set Available_grid_point (i, k) as “FALSE”. If Available_grid_point (i, k) is “FALSE”, the calculation of this position is give up and go to the calculation of the next position on stage k .

Step 4: check if the rhumb lines from $P(i, k)$ to $P(i \pm q, k + 1)$ cross the land by using the algorithm as shown in figure 5.5 and assign the Available_trajectories $(i, k, i \pm q)$ according to the check results. If point $P(j, k + 1)$ among points $P(i \pm q, k + 1)$ can be achieved by a trajectory from $P(i, k)$, then set Achieved_grid_point $(j, k+1)$ as “TRUE”. If there are no available trajectories form $P(i, k)$ to $P(i \pm q, k + 1)$, then set Available_grid_point $(i, k) =$ “FALSE” and Flag_iteration = “FALSE”.

Step 5: Let $k = k+1$, go to step 3 until $k = K - 1$.

Step 6: If Flag_iteration = “FALSE” go to step 2. Otherwise, stop the calculation.

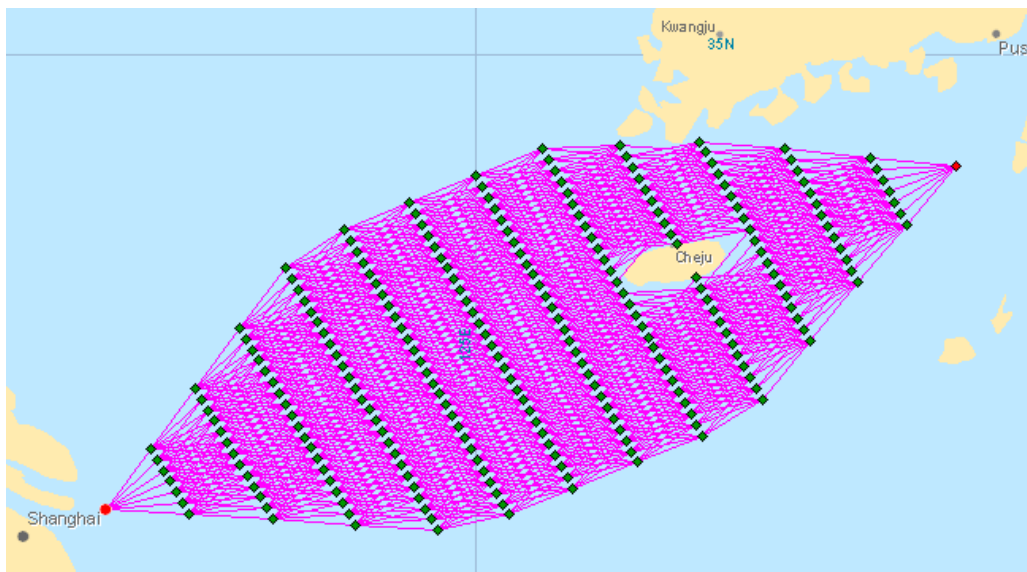


Figure 5.6 Grid system with obstacle

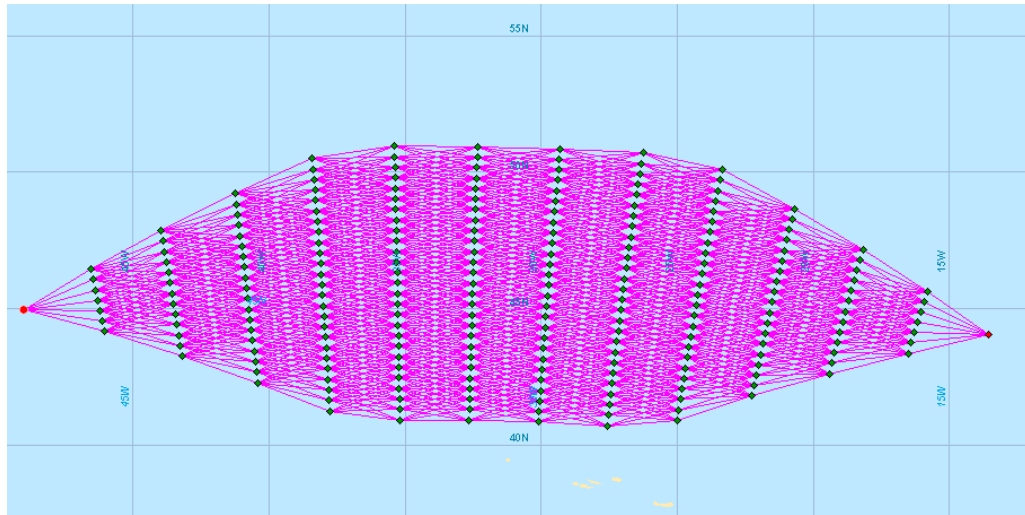


Figure 5.7 Grid system without obstacle

After obtaining the value of Available_grid_point and Available_trajectories by using the algorithm described above, all the available trajectories can be drawn on the grid system in geographic projection.

In conclusion, the input parameters to create a grid system by using all algorithms mentioned above are:

- Departure position.
- Destination position.
- The proportion between the breadth of one stage and the length of RGC.
- The total number of stages.
- The total number of states on one stage in geographic position.
- The integer indicates how many headings the ship can choose from one stage to the next.

Figure 5.6 (without obstacle) and figure 5.7 (with obstacle) show the grid system with 14 stages, 27 states on one stage in geographic project, nine heading choices on one grid and the breadth of one stage as 20% of the length of RGC.

5.6 Sub-problem solving

By using Bellman's principle of optimality, the complex weather routing problem can be broken down into a sequence of simpler sub-problems. Reviewing Formula 5.13, the procedure of predicting fuel consumption α_k between two stages can be considered as the sub-problem solving in the weather routing optimisation. The predicted optimum fuel consumption during an entire voyage is obtained by adding up all fuel consumed between two stages along the entire route.

In the execution of the 3DDP, the engine delivery power is taken as a constant value between two stages during the optimisation process except for situations when ship has to slow down (voluntary speed reduction) in certain weather conditions to ensure the ship safety. Since it is convenient to use ship speed in calm water instead of engine delivered power as the control variable as mentioned in Section 4.1.2, fuel consumption can be obtained indirectly once ship speed is known. The selected calm water ship speed between two stages is not allowed to be larger than the value corresponding to the maximum continuous rating (MCR) of the main engine.

Most of the time, the weather condition along the trajectory between two stages is changed with time and position. For obtaining the fuel consumption α_k in Formula 5.13, α_k should be split into several components in which the weather condition can be treated as a constant value. As a result ship performances such as speed or engine power within one interval remain constant. The division process can be done according to time and distance (position) (Calvert, 1991).

If time interval δt is used, the ship trajectory between two stages becomes a summation of n segments with equal time intervals δt plus the remaining track δx . Note that $\delta x < V_{ship} \cdot \delta t$ where V_{ship} is the ship speed over ground at time $n \cdot \delta t$ count from $\vec{X}(k)$. So, α_k can be written as

$$\alpha_k = \left(\sum_{i=1}^n \alpha'_k(i \cdot \delta t, \vec{U}(k), k) + \alpha''_k(\delta x, \vec{U}(k), k) \right) \quad (5.21)$$

Where α'_k and α''_k are the fuel consumption in equal time intervals and remaining track respectively.

If distance interval is considered, the ship trajectory between two stages consists of several segments with equal distance interval δx plus the remaining track $V_{ship} \cdot \delta t$ where $\delta x > V_{ship} \cdot \delta t$. Formula (5.21) can be re-expressed as

$$\alpha_k = \left(\sum_{i=1}^n \alpha'_k(i \cdot \delta x, \vec{U}(k), k) + \alpha''_k(\delta t, \vec{U}(k), k) \right) \quad (5.22)$$

Where α'_k and α''_k are the fuel consumption in equal distance interval and remaining track respectively.

Two methods will result in different optimised routes due to interpolation of the weather conditions at different positions and times along the route. In this research, the method with equal time intervals is adopted. The time interval in Formula 5.21 should match with the time step of the weather forecast. By adjusting the first time interval in 5.21, the departure time of every segment except the first can coordinate with the weather forecast and the interpolation of the weather data can only be done in the position domain. This treatment can give some convenience for the interpolation and reduces the calculation amount.

According to Formula 5.21, the procedure of determining the fuel consumption for a given ship speed in calm water between two stages is as the following:

- Step 1: Setting the calm water ship speed.
- Step 2: If the calm water ship speed is smaller than the minimum allowed value, skip out the calculation for the given heading. That means the navigation for this given heading is not available under this calm water ship speed or engine delivery power.

- Step 3: Calculation of ship speed. Ship speed loss is calculated based on the Kwon's method.
- Step 4: If ship operations violate the set constraints, ship speed in calm water will be reduced by Δu , then go back to step 2.
- Step 5: Calculation of propeller rotation speed. The propeller rotation speed is determined by the method described in section 2.3.
- Step 6: Calculation of ship position and fuel consumption for the next time interval Δt . The fuel consumption can be calculated from the ship hydrodynamic database.
- Step 7: Execute Step 1 to 6 repetitively with the fixed time interval Δt between two stages until the ship (simulation step) arrives at the next stage or the final destination.

The time interval Δt for calculation is normally chosen at the frequency of reception of weather forecasting which is usually every three or six hours. Figure 5.8 shows the procedure described above.

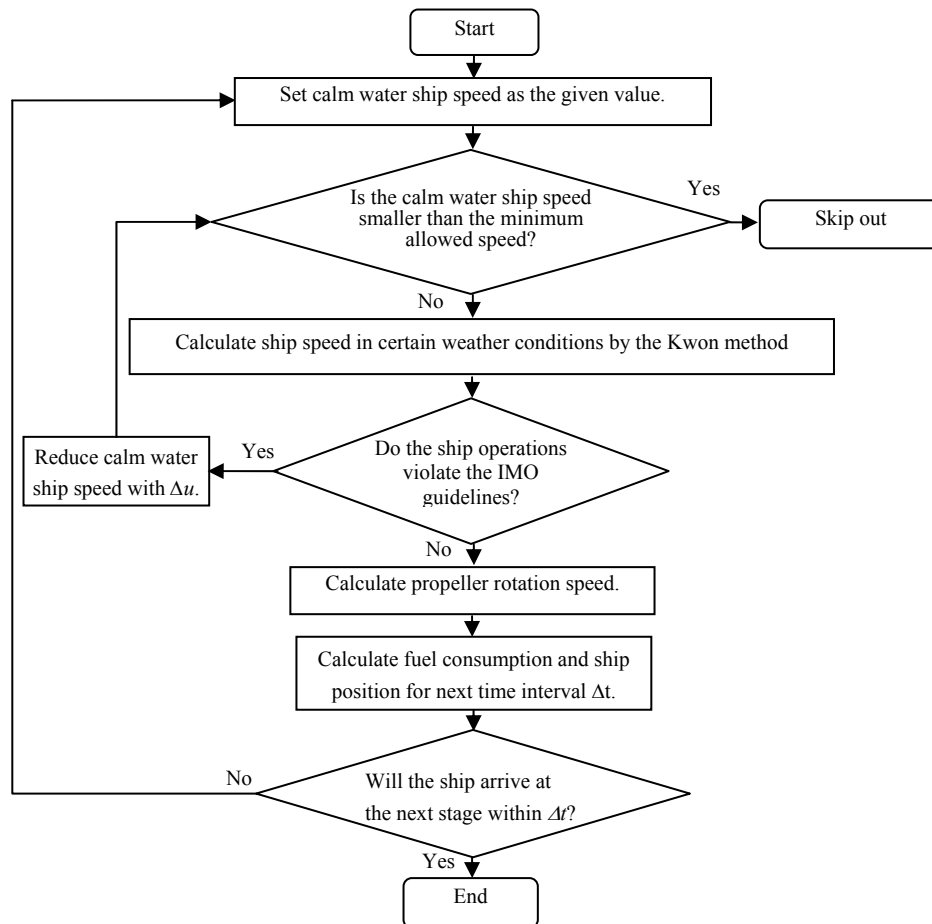


Figure 5.8 Estimate of fuel consumption between two stages

5.7 Two dimensional dynamic programming (2DDP) for weather routing

The 2DDP method was first presented by De Wit (1990). It chooses voyage progress as the stage variable and assumes a ship sails at a constant propeller rotation speed or a constant engine for the purposes of simplifying problems and reducing computing time. Under this simplification, there is a one-to-one relationship between the ship position and time. Thus, time variable is not needed to specify states in this method and the states used in the optimisation procedure just consider the ship position which is two dimensional (latitude and longitude). In this paper, it is assumed that

the ship speed in calm water (engine power) is used as the control variable when introducing the 2DDP method.

5.7.1 Minimum time problem solving

In addition to the notation mentioned in section 5.5.2, two new notations are used in 2DDP method:

- $T(i, k)$: is used to present the time consumption from the departure to position $P(i, k)$.
- $\text{Achieved_point}(i, k)$: It is boolean value correspond to point $P(i, k)$ and the value "TRUE" or "FALSE" indicate whether or not this point can be achieved by a trajectory form a point on the previous stage.

The recursion procedure of solving the minimum time problem by the 2DDP can be described as follows:

- Step 1: Create the grid system according to the departure and destination by the method as mentioned in Section 5.5.2.
- Step 2: Initialise all element in array $T(i, k)$ as infinite and all element in array $\text{Achieved_point}(i, k)$ as "FALSE" except for $T((1 + N) / 2, 1)$ and $\text{Achieved_point}((1 + N) / 2, 1)$ which are corresponding to the departure point. Set $T((1 + N) / 2, 1) = 0$ and $\text{Achieved_point}((1 + N) / 2) = \text{"TRUE."}$ Assign the ship speed in calm water V_c (the engine power) as the preset value.
- Step 3: Set stage variable $k = 1$.
- Step 4: Iterate steps 5 to 6 below for each position $P^* = P(i, k)$ on stage k , where: $i = 1, 2, 3, \dots, N$. If $\text{Achieved_point}(i, k)$ is "FLASE" which means the position P^* is unattainable due to constraints, the

calculation of P^* is given up and go to the calculation of the next point.

Step 5: Iterate step 6 below for each heading from point P^* to point $P(j, k+1)$ on stage $k+1$ where: $j = 1, 2, 3, \dots, N$. If Available_trajectories(i, k, j) (get from step 1) is "FALSE" which means the rhumb line from P^* to point $P(j, k+1)$ is forbidden for the ship navigation, skip out the calculation for this heading and go to the next heading calculation.

Step 6: Calculate the time consumption ΔT from P^* to point $P(j, k+1)$ by using the method described in Section 5.6. If $\Delta T + T(i, k) < T(j, k+1)$ then replace the old value of $T(j, k+1)$ as $\Delta T + T(i, k)$. The departure point P^* on stage k , from which the ship (simulation step) arrives at the point $P(j, k+1)$ on stage $k+1$ and the corresponding control variables are saved for tracing the optimum route by a backward procedure at the end of the calculation.

Step 7: Let $k = k + 1$, go to step 3 until $k = K$.

Once the destination point $P((1+N)/2, K)$ on the final stage K has been obtained, a backward calculation procedure will be used to identify a route with the minimum time consumption under the specified calm water ship speed.

5.7.2 Minimum fuel problem solving

When dealing with the minimum fuel problem, the departure and arrival time are prefixed. By varying the preset calm water ship speed, it is possible to find the correct value of the minimum passage time by using the method above to satisfy the specified arrival time. This minimum time route is then treated as the route of minimum fuel consumption.

De Wit treats propeller rotation speed as the control variable and uses an iteration process to find the correct value of the propeller rotation speed for minimum fuel problem solving. When the calm water ship speed is treated as the control variable, this process can be re-written as follows:

- Step 1: Given a set calm water ship speed, computer the minimum time route by using the method in 5.7.1.
- Step 2: Under this minimum time route, computer the calm water ship speed which will satisfy the arrival time constraint by using Newton iteration method.
- Step 3: Use this new calm water ship speed, re-compute the minimum time route then go to step 2 until there is no further improvement of the calculated value of the calm water ship speed.

5.8 Three dimensional dynamic programming (3DDP) for weather routing

To overcome the disadvantage of the 2DDP method, several authors (Chen, 1978; Calvert, 1990; Aligne, 1998) have already attempted to solve the weather routing problem by treating both engine power and shipping course as the control variables during a voyage. Aligne (1998) chose time as the stage variable and used the forward algorithm; Calvert (1990) and Chen (1978) employed voyage progress as the stage variable and used the backward algorithm. The 3DDP method presented in this paper employs voyage progress as the stage variable together with the use of the forward algorithm. As a result, a state consists of three dimensional variables (latitude, longitude and time).

Notations used in the programming are defined as follows.

- K : Total number of stages.

- N : Total number of states' projection on a latitude \times longitude plane on stage k , where: $k = 1, 2, 3 \dots K$.
- $P(i, k)$: Position of states' projection on a latitude \times longitude plane on stage k , where: $i = 1, 2, 3 \dots, N$. The space between $P(i, k)$ and $P(i + 1, k)$ is Δy . $P((1 + N) / 2, 1)$ is the departure position; $P((1 + N) / 2, K)$ is the destination position.
- J : Total number of intervals on time axis for a stage.
- $\Delta \bar{t}$: Time interval between two adjacent grids on time axis for a stage.
- $X(i, j, k)$: State on stage k , where: $i = 1, 2, 3 \dots, N, j = 0, 1, 2 \dots, J - 1, k = 1, 2, 3 \dots, K$. The geographical position of the state $X(i, j, k)$ is defined by $P(i, k)$ on stage k , the time variable of a state is $t_{i, j, k}, \bar{t}_j \cong t_{i, j, k} \cong \bar{t}_{j+1}, \bar{t}_j = \Delta \bar{t} \times j, \bar{t}_{j+1} = \Delta \bar{t} \times (j + 1)$. Between point $(P(i, k), \bar{t}_j)$ and $(P(i, k), \bar{t}_{j+1})$, there is only one state that correspond to minimum fuel consumption. A state $X(i, j, k)$ on stage k has a floating status during the iteration until a point with minimum fuel consumption is found. This is then chosen as state $X(i, j, k)$ before proceeding with the following calculation.
- $X((1 + N) / 2, 0, 1)$: Initial state. Time variable $t_{1, 0, 1}$ of the initial state is 0.
- $X((1+N)/2, j, K)$: States on the final stage $K, j = 0, 1, 2 \dots, J - 1$, the positions of these states on a latitude \times longitude plane is $P((1 + N) / 2, K)$.
- $F_{opt}(i, j, k)$: The minimum fuel consumption from the initial state to the state $X(i, j, k)$.
- $u(m)$: Discrete calm water ship speed, where: $m = 1, 2, 3 \dots, M. u(m + 1) - u(m) = \Delta u, M$ is the total number of discrete speeds between two stages.

5.8.1 Recursion procedure of forward dynamic programming

The recursion procedure of forward dynamic programming can be described as follows:

- Step 1: Create the grid system according to the departure and destination by the method as mentioned in section 5.5.2.

- Step 2: Set stage variable $k = 1$. Set $F_{opt}((1 + N) / 2, 0, k)$ which is corresponding to the initial state as zero and all other elements in array $F_{opt}(i, j, k)$ are set to infinite.
- Step 3: Iterate steps 4 to 8 below for each state $X^* = X(i, j, k)$ on stage k , where: $i = 1, 2, 3, \dots, N, j = 0, 1, 2, \dots, J - 1$. Parameters with the symbol * are used as interim parameters on stage k when performing iterations. If a state $X^* = X(i, j, k)$ is unattainable due to constraints, the calculation of the state is abandoned and go to the calculation of the next state.
- Step 4: Iterate step 5 below for each heading H^* from point P^* to point $P(i', k + 1)$ on stage $k + 1$ where: $i' = 1, 2, 3, \dots, N(i' + 1)$. If Available_trajectories(i, k, i') (get form step 1) is "FALSE" which means the rhumb line from P^* to point $P(i', k + 1)$ is forbidden for the ship navigation, abandon the calculation for this chosen heading and go to the next heading calculation.
- Step 5: Iterate steps 5 to 7 for each $u^* = u(m)$, where: $m = 1, 2, 3, \dots, M$.
- Step 6: Calculate the fuel consumption $\Delta f_{m, i'}$ and the voyage time $\Delta t_{m, i'}$ between state X^* of stage k and a state of stage $k + 1$ by using the method described in 5.6, If a ship speed u^* violates the set constraints, skip out the calculation of the chosen speed and go to the calculation for the next speed. $t_{m, i'}$ is denoted as the arrival time (simulation progression) at position $P(i', k + 1)$ from the initial state, $t_{m, i'} = t_{i, j, k} + \Delta t_{m, i'}$, as shown in Figure. 5.9. Position $X' = (P(i', k + 1), t_{m, i'})$ represent a new possible state at stage $k + 1$, The total fuel consumption from the departure to X' is f' , $f' = F_{opt}(i, j, k) + \Delta f_{m, i'}$. Parameters attached with symbol ' are used as interim parameters on stage $k + 1$ when performing iterations.

Step 7: Calculate j' which satisfies $\bar{t}_{j'} \cong t_{m, i'} \cong \bar{t}_{j'+1}$. If $f' < F_{opt}(i', j', k+1)$, then replace the old $X(i', j', k+1)$ and $F_{opt}(i', j', k+1)$ by X' and f' respectively to form new $X(i', j', k+1)$ and $F_{opt}(i', j', k+1)$ as shown in Figure. 5.10. It can be seen that, only one possible state which has the minimal fuel consumption between the time interval $\bar{t}_{j'}$ to $\bar{t}_{j'+1}$ at the position $P(i', k+1)$ of stage $k+1$ will be treated as the state $X(i', j', k+1)$. The time variable of the state $X(i', j', k+1)$ is not fixed. The benefit of using non-fixed time for possible (floating) states is that it eliminates the need for interpolation which is usually used in dynamic programming problems. Thus, it can save computing time. When the weather in $\Delta\bar{t}$ time does not change too much using the floating technique will not influence the accuracy of the optimised results. The departure state X^* on stage k , from which the ship (simulation step) arrives at the state $X(i', j', k+1)$ on stage $k+1$ and the corresponding control variables are saved for tracing the optimum route by a backward procedure at the end of the calculation.

Step 8: Let $k = k + 1$, go to step 2 until $k = K$.

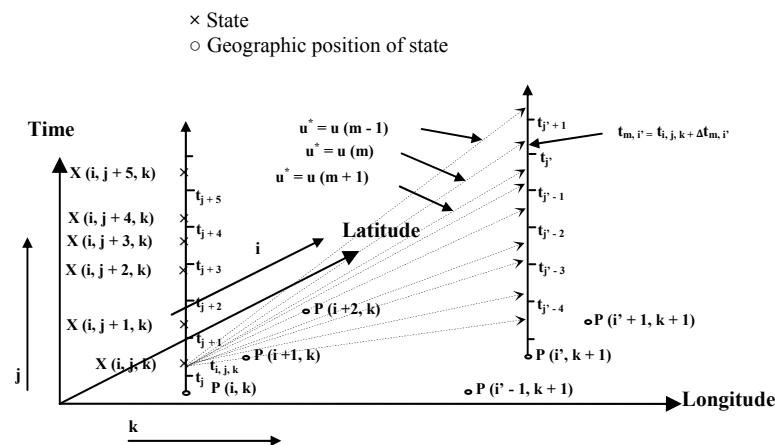


Figure 5.9 Calculate the trajectory from certain states under different calm water speeds

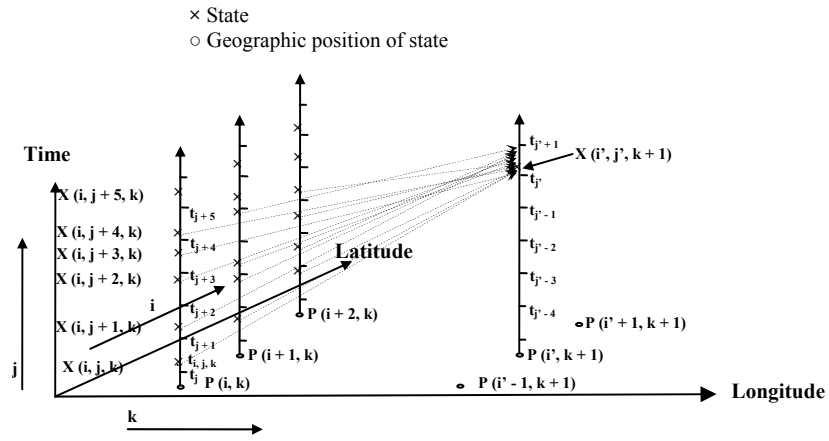


Figure 5.10 Determine the state

The pseudo code of the procedure above is shown in Figure 5.11.

```

k = 1.
 $F_{opt}(1, 0, 1) = 0$ 
 $F_{opt}(i \geq 1, j \geq 0, k \geq 2) = \infty$ 
Do
  For i = 1 to N (k)
    For j = 0 to J
       $X^* = X(i, j, k)$ 
      If  $X^*$  is unattainable Then
        Continue For
      End If
      For i' = 1 to N (k + 1)
        Calculate the ship's heading  $H^*$  from the position  $P(i, k)$  of state  $X^*$ 
        to the next stage position  $P(i', k + 1)$ 
        If  $H^*$  violates the heading constraints or geographic feasibility Then
          Continue For
        End If
        For: m = 1 To M
           $u^* = u(m)$ 
          Choosing  $u^*$  and  $H^*$  as the control variables, calculate the fuel consumption  $\Delta f_{m,i'}$  and the
          during-routing time  $\Delta t_{m,i}$  between state  $X^*$  at stage k and geographic position  $P(i', k + 1)$ 
          at stage k + 1 by using the method described in section 3.3
          If  $u^*$  violates the control constraints or safety constraints Then
            Continue For
          End If
           $t_{m,i'} = t_{i,j,k} + \Delta t_{m,i}$ 
           $f^* = F_{opt}(i, j, k) + \Delta f_{m,i'}$ 
           $X' = (P(i', k + 1), t_{m,i'})$ 
          Calculate j' which satisfy  $t_{j'} \leq t_{m,i'} \leq t_{j'+1}$ 
          If  $f^* < F_{opt}(i', j', k + 1)$  then
             $X(i', j', k + 1) = X'$ 
             $F_{opt}(i', j', k + 1) = f^*$ 
          End If
        Next
      Next
    Next
  Next
  k = k + 1
Loop Until k = K.

```

Figure 5.11 Pseudo code of the 3DDP method

Once the state on the final stage *K* has been obtained, a backward calculation procedure will be used to identify a route with the optimised fuel consumption. This route is the optimised route resulting from the 3DDP.

For example, once the state $X((1 + N) / 2, j, K)$ with the time variable *t* on stage *K* has been obtained, the backward calculation procedure identifying the optimised fuel

consumption route at the specified arrival time t and the corresponding control variables during the voyage is as follows:

Find the state at stage $K - 1$ from which the ship arrived at $X((1 + N)/2, j, K)$ and the ship's control variables from this state at stage $K - 1$ to $X((1 + N)/2, j, K)$. The state at stage $K - 1$ and the defined control variables is represented by $X^*(K - 1)$ and $U(K - 1)$ respectively. Then find the state at stage $K - 2$ from which the ship arrived at $X^*(K - 1)$ and the ship's control variables from this state at stage $K - 2$ to $X^*(K - 1)$, use $X^*(K - 2)$ and $U(K - 2)$ represent them respectively.

Repeating the above tracing procedure to the initial state $X((1 + N) / 2, 1, 1)$ as shown in Figure 5.12, the minimum fuel consumption route $X((1 + N) / 2, 1, 1), X^*(2), X^*(3), X^*(4) \dots, X((1 + N) / 2, j, K)$ and the optimum ship control variables $U(1), U(2), U(3) \dots, U(K - 1)$ are obtained.

It must be made clear that the optimised route calculated by this algorithm is not the real global optimal route. The degree of the approximation to the real global optimal route depends on the fineness of the grids system, the accuracy of the ship hydrodynamic calculation, the accuracy of weather forecast and the discretisation of the ship's speed.

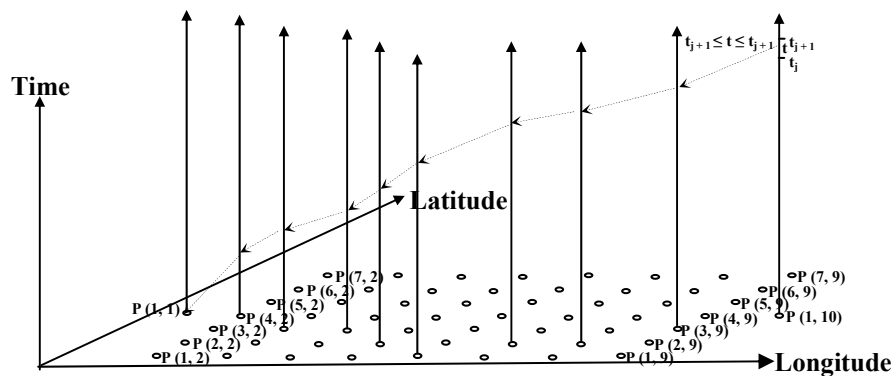


Figure 5.12 Backward calculation procedure to trace the route (Total number of stages is 10; total number of discrete geographic positions in one stage is 7)

5.8.2 Deleting the unmeaning states in every stage to reduce the computing time

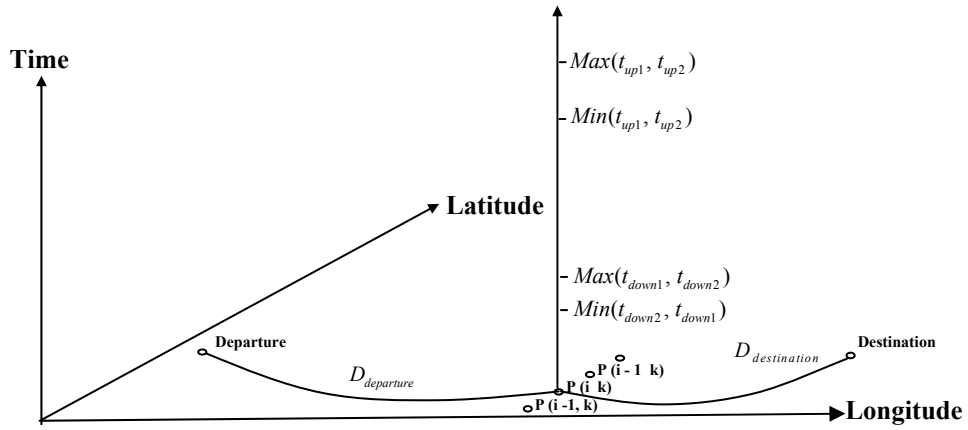
Since the forward strategy is adopted in the optimisation processes described in 5.8.1, the attainable states in every stage can be confirmed stage by stage as the recursive procedure going on. The difference between the available times spaces in every stage is increasing along with each stage away from the departure and obtaining an open ended time envelope at the final stage. As a result a set of routes with minimum fuel consumption under the same pre-set departure time but different arrival times can be obtained from the states on the last stage. The solution with minimum time is the minimum time route. But most times, the operator hopes to obtain an optimised route with minimum fuel consumption whilst also maintaining a certain time schedule or certain time scope which is specified on the merchant contract. So, during the optimised solutions, only the routes with the arrival times around the time schedule are our concern and others are meaningless for the problem consideration.

Several critical points at the position $P(i, k)$ in the time dimension can be defined as shown in Figure 5.13.

$$(1). t_{down1} = D_{departure} / V_{max}$$

Where $D_{departure}$ is the great circle from departure to point $P(i, k)$; V_{max} is the maximum value of the calm water ship speed. So, even under maximum engine power, the states on position $P(i, k)$ with a time variable smaller than t_{down1} cannot be obtained during route optimisation since the maximum ship speed during the voyage will smaller than V_{max} for most of the time, so using V_{max} to calculate t_{down1} is conservative.

$$(2). t_{up1} = 1.5D_{departure} / V_{min}$$


 Figure 5.13 Critical time points at position $P(i, k)$

Here, it is assumed that the longest route distance from departure to point $P(i, k)$ is 1.5 times of $D_{departure} \cdot V_{min}$ the minimum value of the calm water ship speed. So, even under minimum engine power, the states on position $P(i, k)$ with the time variable which is greater than t_{up1} cannot be obtained during route optimisation. Actually, the minimum ship speed during the voyage should be smaller than V_{min} for most of the time, but 1.5 times of $D_{departure}$ is large enough to overcome the use of bigger V_{min} instead of the minimum ship speed over the voyage.

$$(3). t_{down2} = t_{end} - t_r / 2 - 1.5D_{destination} / V_{min}$$

Where t_{end} is the specified arrival time; t_r is the interesting time range around the specified arrival time so $t_{end} - t_r / 2$ and $t_{end} + t_r / 2$ are the lower and upper boundaries of the considered time scope; $D_{destination}$ and $1.5D_{destination}$ are the distance and 1.5 times distance of the great circle from point $P(i, k)$ to destination respectively. So even by using minimum engine power, the ship cannot reach its destination with an arrival time larger than $t_{end} - t_r / 2$ from point $P(i, k)$ at the departure time t_{down2} .

$$(4). t_{up2} = t_{end} + t_r / 2 - D_{destination} / V_{max}$$

It can be explained that even by using the maximum engine power, the ship cannot reach its destination with an arrival time smaller than $t_{end} + t_r / 2$ from point $P(i, k)$ at the departure time t_{up2} .

According to the four critical time points, the available time space at point $P(i, k)$ on stage k can be expressed as:

$$\begin{aligned} t_{down} &= \text{Max}(t_{down1}, t_{down2}) \\ t_{up} &= \text{Min}(t_{up1}, t_{up2}) \end{aligned} \quad (5.23)$$

So, if the time variables of the states are out of the scope defined by Formula 5.23, these states will be neglected during the optimisation process. A similar algorithm is also adopted by Calvert (1990)

Chapter 6.

EVOLUTIONARY ALGORITHM FOR WEATHER ROUTING

To illustrate the advantage of the novel forward 3DDP method, 3 kinds of evolutionary algorithms (EAs) which can solve the weather routing as a multi-objective optimisation problem are used for the comparison in this research. Section 6.1 gives a brief description about the evolution algorithms. Section 6.2 deals with the application of multi-objective evolutionary algorithms (MOEAs) for weather routing.

6.1 The introduction of evolutionary algorithms

6.1.1 Inspiring from Nature Selection

The EAs refer to the Natural Selection, which were first described by Darwin (1859): *“Owing to this struggle for life, variations, however slight and from whatever cause proceeding, if they be in any degree profitable to the individuals of a species, in their infinitely complex relations to other organic beings and to their physical conditions of life, will tend to the preservation of such individuals, and will generally be inherited by the offspring. The offspring, also, will thus have a better chance of surviving, for, of the many individuals of any species which are periodically born, but a small number can survive. I have called this principle, by which each slight variation, if useful, is preserved, by the term Natural Selection.”*

The principle of Nature Selection constructs the core ideas of the EAs. According to above statement of Darwin, the optimisation process of EAs can be summarised in

the following components during the solution evolution as the process in the biological evolution of the nature world (Eiben and Smith, 2003):

- The definition of individuals
- Initialisation
- The fitness function
- Population
- Selection mechanism
- Recombination
- Mutation
- Replacement

Many steps above in the evolution process are stochastic. In the selection process, the fitter individuals which have better “gene” can pass to their “offspring” have a higher chance to be selected for the reproduction than less fit ones. Nevertheless, the weak individuals still have a chance for recombination or are selected for mutation. The mutation process is stochastic which can avoid being stuck in a local optimum and ensure the global optimum value can be found. Evolutionary algorithms consist of many optimisation techniques like genetic algorithm (GA) and particle swarm optimisation (PSO) which only differ in the implementation details of the steps mentioned above. Nevertheless, the common ideas behind all these techniques are the same.

To solve a certain optimisation problem, EAs only require the relation between the objective function and the input parameters. This advantage makes EAs can be easily used to deal with the complex problems. Most important, the EAs can solve multi-objective optimisation problems.

6.1.2 The definition of multi-objective problems

In the real world, most problems involve several conflict objectives which can occur simultaneously such as the fuel consumption and the en-route time in weather routing problem. Multi-objective optimisation (or multi-objective programming) also

known as multi-criteria or multi attribute (Osyczka, 1985; Deb K, 2001; Coello 2007) are able to find a set of solutions which can balance the conflicting objectives subject to certain constraints.

For a minimisation problem which has m conflict objective components to be optimised, the multi-objective problem in mathematical terms can be written as:

$$\text{Min}_{\vec{x}} [f_1(\vec{x}), f_2(\vec{x}) \dots, f_m(\vec{x})]^T \quad (6.1)$$

Subject to:

$$\begin{aligned} g(\vec{x}) &\leq 0; \\ & \quad i=1,2,\dots,N \\ h(\vec{x}) &= 0; \\ & \quad i=1,2,\dots,N \\ \vec{x} &\in X \end{aligned} \quad (6.2)$$

Where $[f_1(\vec{x}), f_2(\vec{x}) \dots, f_m(\vec{x})]$ is the objective vector F with m objective components; $\vec{x} = [x_1, x_2 \dots, x_n]$ is the decision vector including n decision variables, f_i is the i -th objective function, g_i and h_i are the i -th inequality and equality constraints respectively.

6.1.3 Pareto Dominance

Pareto dominance which was first proposed by Pareto (1896) can be used to estimate the better one between any two candidate solutions in multi-objective optimisation. For a minimisation problem Pareto domination can be defined as:

For two objective vectors F_a and F_b , F_a is said to dominate F_b iff

$$\begin{aligned} f_{a,i}(\vec{x}) &\leq f_{b,i}(\vec{x}) \quad \forall i \in \{1,2,\dots,m\} \\ \text{And} & \end{aligned} \quad (6.3)$$

$$f_{a,j}(\vec{x}) \prec f_{b,j}(\vec{x}) \exists j \in \{1, 2, \dots, m\}$$

If there is no solution P_i in solution space ψ can dominate any member P_j in solution set Ω , then Ω is defined as the Pareto front. The Pareto front is usually a curve when there are two conflict objectives and a surface when there are three conflict objectives.

In the past decade, a number of MOEAs have been developed. In this paper, three MOEAs, NSGA-II (Deb K, 2002), SPEA (Zitzler, 1999), MOPSO-CD (Raquel, 2005) are presented and employed for weather routing problems.

6.2 Applications of MOEAs for weather routing

6.2.1 Re-definition of the optimisation problem in weather routing

Before using the MOEAs to solve the weather routing problem, there are clearly five things that should be understood first: initialisation, control (decision) variables, objectives, evaluation function, and constraints.

1) Initialisation

Since weather routing is a very complicated problem, most often, the random generation cannot offer the available solutions. The initial population of the MOEAs should be generated based on the random selection of results obtained by the 2DDP method. Otherwise the MOEAs are very hard to converge to real Pareto front and, even no solutions can be obtained by MOEAs in rough sea condition especially for MOSPO_CD which should use a non-dominated solution archive to update the search direction during the optimisation process.

2) Control (decision) variables

A same grid system as used by the 2DDP and 3DDP method should be specified first before being applied to the MOEAs. The advantage of using the grid system is that the geographic constraint (unavailable routes like cross the land) can be deleted before the optimisation procedure, so some computing time can be saved. The routes are chosen according to this grid system and a route can be specified by the indexes of the geographic position of state on a stage which can be used as the control variables for MOEAs to determine the ship route. Use I_{si} to denote these indexes, here, $i = 1, 2, \dots, K$, K is the total number of the stages of the grids system.

As mentioned in Chapter 4, ship engine and shipping heading of course directly decide the ship route in the ocean. Ship engines have a one-to-one relationship with ship speed in calm water. Since it is convenient to use ship speed in hydrodynamic analysis, determining resistance, ship speed loss, etc, the ship speed in calm water is used as a reference to create the ship hydrodynamic database according to certain formats as shown in Appendix B. The database is created with certain intervals of ship speed in calm water and should be done before applying the MOEAs for weather routing. If treating the ship speed in calm water during a voyage as a discrete variable with the value as it is in the database, then the indexes of the database are the equivalent to the ship speed in calm water and can be used as the control variables for MOEAs to determine the engine power. During a voyage, ship speed in calm water (the engine power) will be changed at every stage (calculation process), so the total number of index variables pointing to the hydrodynamic database should be one less than the total number of stages K . Here use I_{vi} to denote the index variables of the database, $i = 1, 2, \dots, K-1$. For example, if the total stage number is 16, 29 (14 indexes of the geographic position and 15 calm water ship speed settings) control variables will be used for MOEAs.

3) Objectives

The objectives should be 1) the en-route time and 2) the fuel consumption of the whole voyage. When employing MOEAs for weather routing, these two objectives should be two conflicting values. In the Pareto front, the fuel consumption of the

whole voyage should decrease with the increase of the en-route time and a single objective cannot be further improved without deteriorating any objective. However, in certain weather conditions, the two objectives may not be contradictory with each other. The relation curve of the minimum fuel consumption (under certain en-route time) vs. the values of the en-route time is not usually concave as shown in Figure 6.1. In this situation which is of no frequent occurrence, the MOEAs are not competent at all but it can be solved by the 3DDP without any difficulty.

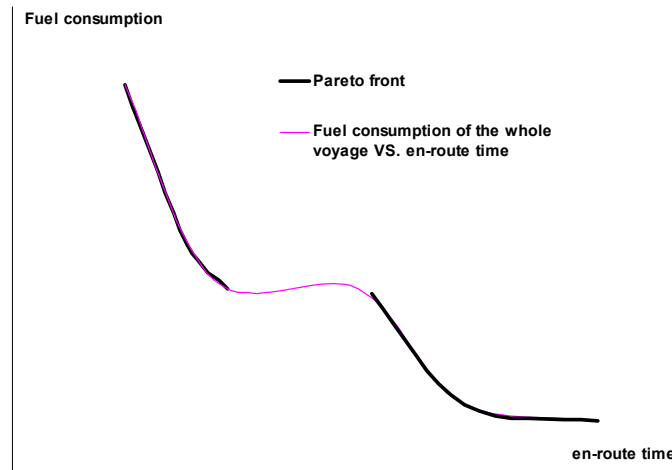


Figure 6.1 Pareto front and curve of minimum fuel consumption vs. en-route time

4) Evaluation function:

Evaluation function reflects the relationship between the control variables and the objectives. Once the values of control variables are assigned, the fuel consumption and the en-route time of the whole voyage can be obtained by adding up all these values between two stages by using the method described in Section 5.6.

5) Constraints:

Since a grid system is already created, the geographic constraints will be satisfied automatically. *Isi* should meet the condition:

$$1 \leq I_s \leq N \quad (6.4)$$

Where N is the total number of grid points on a stage in geographic project.

The control variables I_s should meet the condition:

$$I_{s_{\min}} \leq I_s \leq I_{s_{\max}} \quad (6.5)$$

In Formula 6.5, $I_{s_{\min}}$ and $I_{s_{\max}}$ are integers which correspond to the minimum and maximum ship speeds in calm water which are specified by the operator respectively. It should be noted that the specified maximum ship speed in calm water should be smaller than the value corresponding to the maximum continuous rating (MCR) of the main engine.

When using the 2DDP or 3DDP for weather routing, the solution which violates the safety constraints will be deleted directly during the optimisation process. But when using the MOEAs for weather routing, the strategy is changed. Once the ship is in a dangerous situation in which even voluntary ship speed reduction (see Section 5.6) cannot ensure the ship safety, the ship speed in calm water is set as a small value for maintaining steerage of the ship and the time period in this situation will be saved in the memory. As soon as the ship passes the bad weather, the ship speed will be re-set to the pre-specified value. A solution in which the ship just undergoes a short time period of severe weather putting the ship in a dangerous situation can also have certain outstanding characteristics such as less fuel consumption or en-route time. To ensure the good characters of this solution are preserved for the next iteration, this study uses the time period of undergoing severe weather conditions during the voyage as the constraint value of the solution for Pareto dominance operation during the optimisation process. Once the en-route time goes beyond the scope of the weather forecast, this constraint value will be set as infinite.

The constraint strategy of MOEAs does not consider the ship's heading constraint as mentioned in section 4.1.5. However, since the solutions violating this constraint

condition are usually the weak solution and will be deleted during the evolution process, the non-dominated solutions of the Pareto front can satisfy this constraint automatically.

6.2.2 Parameter setting when using the MOEAs

When use the NSGA II and SPEA method, the real-coded method is adopted by using the simulated binary crossover (SBX) operator and polynomial mutation (Deb K, 1995). Polynomial mutation is also used for MOPSO-CD. The parameters setting of these three optimisation algorithms are shown in table 6.1.

Table 6.1 Parameters setting for NSGA II, SPEA and MOPSO-CD

| | η_c | η_m | p_c | p_m | external archive number | population size | generation |
|----------|----------|----------|-------|-------|-------------------------|-----------------|------------|
| NSGA II | ✓ | ✓ | ✓ | ✓ | × | ✓ | ✓ |
| MOPSO_CD | × | × | × | ✓ | ✓ | ✓ | ✓ |
| SPEA | ✓ | ✓ | ✓ | ✓ | ✓ | ✓ | ✓ |

η_c : Crossover distribution indexes η_m : mutation distribution indexes

p_c : Crossover probability p_m : mutation probability

In the comparison with the parameters used by the 3DDP method, much more parameters setting is needed by the genetic algorithm. These extra parameters used definitely give some inconvenience to the operator, and how to set these parameters gives another problem. The impact and sensitive study of these parameters used by the genetic algorithm are out of the scope of this paper and will be treated in further studies. The other disadvantage of the genetic algorithm is that this method is a kind of stochastic method and cannot ensure the same results can be achieved in every run.

Chapter 7.

WEATHER ROUTING SOFTWARE DEVELOPMENT

According to the knowledge presented above, an intelligent tool for energy efficient and low environment impact shipping (ITEES) is developed during this research. Visual Basic .NET (VB.NET), an objective-oriented computer programming language based on the .NET Framework, is used for the software development.

This software emphasises on solving the minimum fuel route by considering the weather condition, ship engine characteristics, ship hydrodynamic responses in different weather conditions and their impact on fuel consumptions. It can advise ship operators with shipping courses, engine power/speed in advance of and also during a voyage. Following the instruction offered by the system enables ship's fuel consumption to be minimal, increases the ship safety and reduces the CO₂ emissions.

The interface information of ITEES is given in Section 7.1 and the main modules of ITEES are introduced in Section 7.2.

7.1 ITEES window information

ITEES has a user friendly graphical user interface (GUI) which requires minimum IT skill and ship hydrodynamic knowledge. After ITEES is activated, the user interface will be shown as in Figure 7.1:

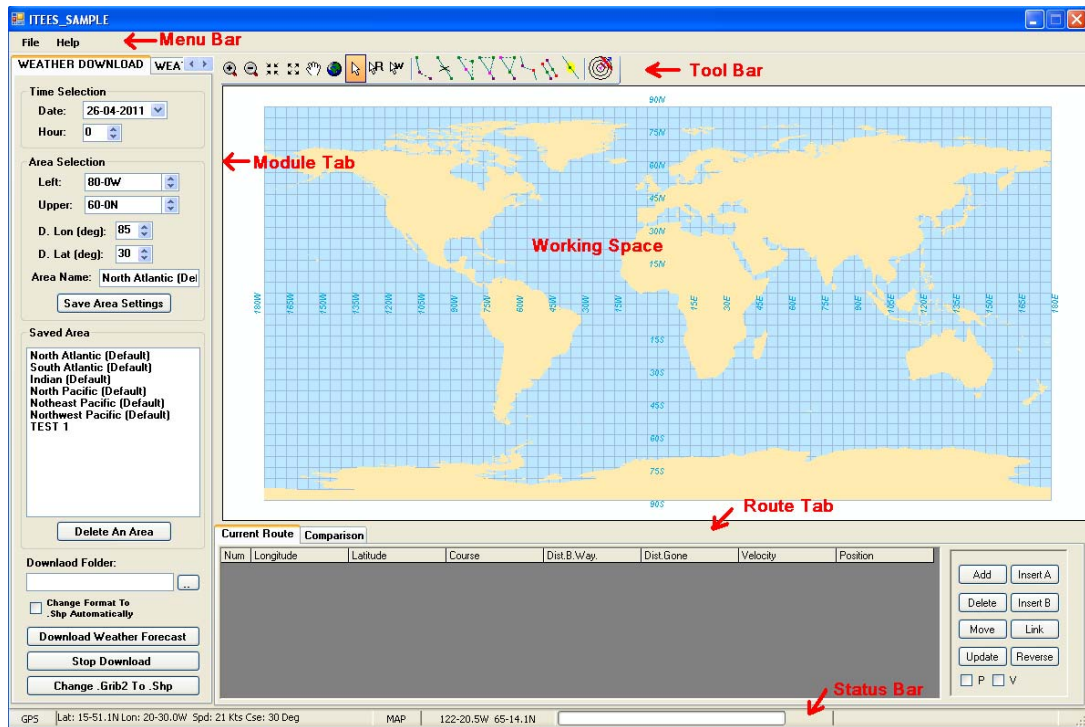


Figure 7.1 Interface of ITEES

The main items on the ITEES window are:

1) Menu bar

The menu bar is just below the title bar. It includes two menus. One is File menu and the other one is Help menu. By choosing “Propeller File...” and “Resistance File...” from the File menu, the propeller characteristics and ship resistance information can be input into ITEES. The suffix names of the propeller characteristics file and resistance database file are “.pc” and “.hyd” respectively. Click the “Help” to display the version information about ITEES.

2) Toolbar

The toolbar is below the menu bar. The toolbar consists of a series of buttons with different icons to describe different common functions. The name of the button appears in a box just below the icon by placing the mouse pointer on it, and the operator can quickly determine what a toolbar icon does.

3) Working space

The program working space is in the middle of the screen. A world map is displayed in the working space. The weather forecast and ship routing can be laid on the world map on demand.

4) Status bar

The status bar is at the bottom of the screen and includes helpful information. The latitude and longitude position of the mouse pointer on the working space is displayed in the status bar and updated to keep track of the mouse position. The status bar can also give some information of the next step of the operation. A progress bar in the status bar can be used to convey the progress of certain tasks.

5) Module tab

The module tab is an important part of ITEES. It includes the weather forecast download module, weather viewer module, input module, route design module, optimising a route module and optimising from a grid module. The descriptions of the functions of these modules will be presented in Section 7.2.

6) Route tab

The route tab includes the current route information table, the comparison of different passages table, and some route operating buttons. The current route information table gives detailed descriptions of the current operational route. It includes the positions of the way points, the route course and distance between two adjacent waypoints, the distance that the ship has already travelled, ship speed in calm water at the waypoint and so on. The comparison of different passages table allows the operator to compare different simulated routes against each other and

determine the most efficient route for the planned passage under the expected weather forecast.

7.2 Main modules of ITEES

ITEES is established based on object-oriented software development theory and consists of several independent functional modules. Each module can handle certain specific aspects for weather routing. Figure 7.2 gives a schematic to represent the structure of ITEES.

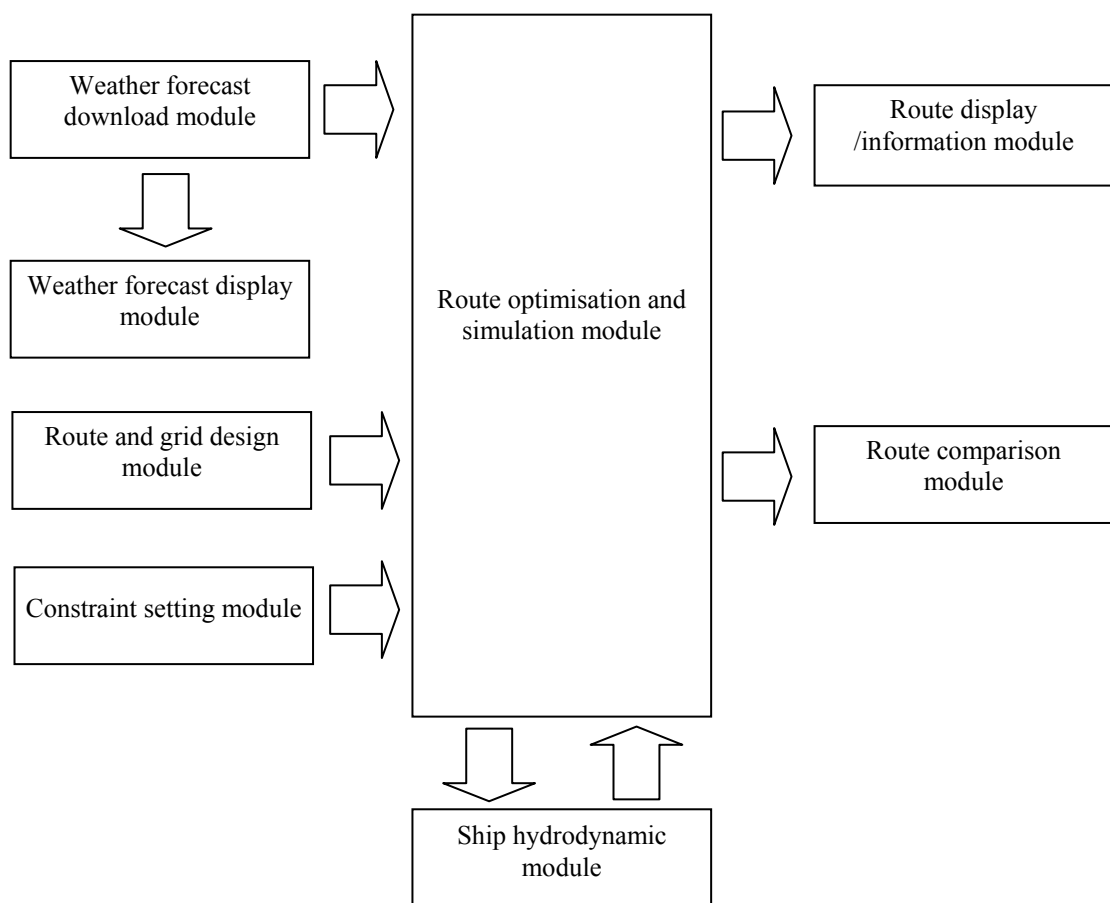


Figure 7.2 Structure of ITEES

1) Weather forecast download module

ITEES allows the operator to free download the weather forecast in GRIB format from the NOMADS as described in Chapter 3. However, at present, the GRIB file

cannot be read by ITEES directly. The GRIB file is automatically converted into a .shp file by ITEES, and then the weather display module reads the .shp file to display the weather forecast.

2) Weather forecast display module

The Weather Viewer is an important module of ITEES allowing the operator to view the weather forecast which has been downloaded, to animate and transfer them into the route optimisation and simulation module of ITEES for the optimisation or simulation of the route.

3) Route and grid design module

Design of a route or a grid system will become very easy by using this module. Several buttons or other widgets can be employed by the operator to create a new route, add, delete, move or insert way points for a route, link two routes, delete or reverse a route, create a grid system and so on. The created route or grid system can be saved by ITEES as a “.rou” file. The “.rou file” can also be loaded by ITEES. The designed route or grid by this module will be used by the route optimisation and simulation module.

4) Constraint setting module

This module allows the operator to set ship departure and arrival time, engine information and weather constraints. The scheduled departure and arrival time of the ship can be set by the time picker. The engine information includes the maximum continuous rating of the main engine, the maximum propeller rotation speed, the maximum and minimum allowed ship speed over the ground in calm water. These values will be treated as the constraints condition during the optimisation of the ship routing. “Max. Power” and “Max. RPM” should be determined according to the engine specifications given in the engine operational manual. This module allows the operator to specify sea wave height limit in different directions and the wind speed

limit that the operator wants to avoid. The operator also can choose the IMO “Guidance to the master for avoiding dangerous situations in adverse weather and sea conditions” to ensure ship safety during the voyage. There is a check box for each of the above listed items. If the operator removes the check mark from the check box, ITEES will no longer take this category into account during the route optimisation process.

5) Ship hydrodynamic module

The ship hydrodynamic and propeller characters can be read from the database by this module to calculate the ship speed reduction and propeller rotation speed. The module can also inspect the ship safety during the voyage according to the sea state information transferred by the route optimisation and simulation module.

6) Route optimisation and simulation module

This module includes all the optimisation algorithms mentioned in the above chapters. It will collect the weather forecast, route or grid information and the constraint conditions from other modules to finish the ship routing optimisation process. Furthermore, this module can also allow the operator to simulate a route during which the course and the engine power setting of the voyage are specified by the operator. During the route optimisation or simulation process, this module will call the functions of the Ship Hydrodynamic module to determine what effects the forecast weather will have on the route planned and what speed reduction would be required if the limits specified in the constraint setting module are to be maintained and if the limits could be maintained. This module is the core of the whole software.

6) Route display /information module

After finishing the optimisation process, the information of the optimised solutions can be given by this module. The information includes the predicted arrival time and position of certain way points, ship course, ship speed, engine delivery power,

propeller rotation speed to the next way point, fuel consumption and distance from departure at this way point, wind speed and direction, wave height and direction at this way point and so on. The optimised solutions can be saved as a “.irou” file and read by this module.

7) Route comparison module

This module allows the operator to compare different simulated or optimised solutions against each other to assist the operator in determining the most efficient route for the planned passage in the expected weather forecast.

Further detailed description of ITEES and how to use it are given in Appendix B.

Chapter 8.

CASE STUDIES AND DISCUSSION

The capability of ITEES are analysed in this chapter. A 54,000 DWT container ship as a case ship is brought in for the investigation. The principle characteristic of the case ship is given in Appendix A and the performance calculations of the case ship have already been presented in Chapter 2. Driven by increasing fuel oil prices and environmental considerations most shipping companies have started to show more interest in reducing fuel consumption and maintaining a certain time schedule specified in the chartering contract. The research in this chapter is focused on the minimum fuel route optimisation.

Section 8.1 involves two case studies which are corresponding to medium and rough sea conditions respectively. Additionally, comparisons between the 2DDP method, the novel 3DDP method and the MOEAs are given in this section. The extent to which the solutions are affected by the constraint conditions are analysed in Section 8.2.

8.1 Case studies

The following two studies consider a North Atlantic voyage between Le Havre and New York. Since the route optimisation focuses on the open water area, the pilot time and estuary travelling section of the route are deliberately removed from the consideration. For this reason, the point (5-14.5 W, 49-21.1 N) at the western end of the English Channel and the point (71-14.3 W, 40-35.6 N) near the estuary of New York are used as the departure and the destination respectively for the grid system

creation. All the parameters used in ITEES are given first before two case studies are discussed.

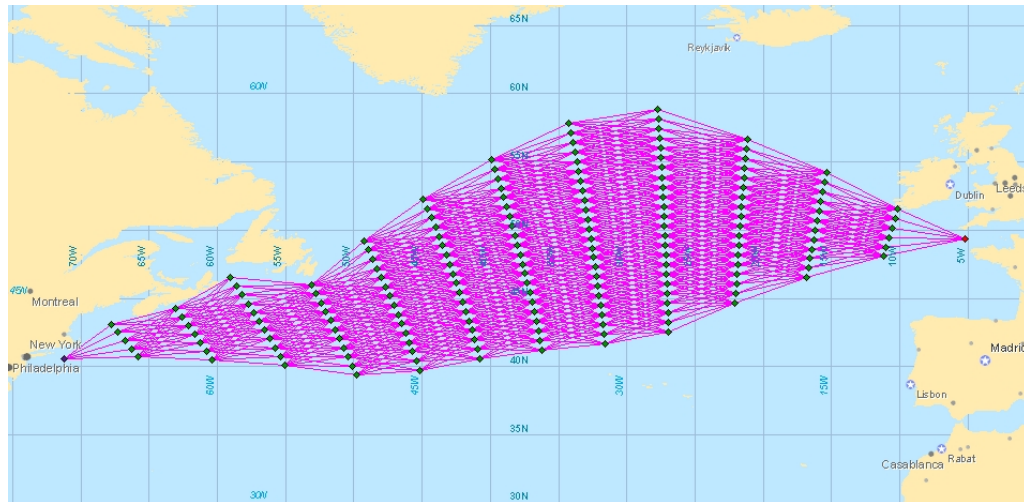


Figure 8.1 Grids system used in the case study

1) The parameter settings for the grid system in ITEES are given as follows:

- Departure from: 5-14.5 W, 49-21.1 N
- Arrival at: 71-14.3 W, 40-35.6 N
- Total stage number: $K = 14$ (stage space: $\Delta X = 212$ miles)
- The proportion between the breadth of one stage and the length of RGC: 20%
- The total number of states on one stage in geographic position: $N = 27$ (State space: $\Delta Y = 46$ miles), so Is_i should be chosen from 1 to 27 for using the MOEAs.
- The integer which indicates how many headings the ship can choose from one stage to the next stage: 9

The grid system used in the case studies is shown in Figure 8.1.

2) The common parameter settings for all the optimisation algorithms.

- Time step for fuel consumption calculation between two stages $\Delta t = 3$ hours. (Mentioned in Section 5.6)
- Calm water ship speed: $u = 5$ to 25.4 knots. The scope of this value corresponds to the index of the hydrodynamic database so I_{S_i} can be chosen from 1 to 250 for using the MOEAs.
- Ship speed change step: $\Delta u = 0.1$ knots.
- Maximum continuous rating of a main engine (MCR): 48598 kW (corresponding to 25.4 knots in calm water)
- Specific fuel oil consumption: 170 g / kWh (125 g / PSh)

3) The parameters used in the 2DDP method are same as the common parameter settings.

4) The exclusive parameters used in the novel 3DDP method:

- Time interval between states on a stage: $\Delta \bar{t} = 0.1$ hour

5) The exclusive parameters used in the MOEAs method:

- NSGA II: Crossover distribution indexes η_c is 20; mutation distribution indexes η_m is 20; crossover probability P_c is 0.9; mutation probability P_m is 0.3; population size is 200 and generation size is 1000.
- MOPSO_CD: Mutation probability p_m is 0.3; external archive number is 500; population size is 200 and generation size is 1000.
- SPEA: Crossover distribution indexes η_c is 20; mutation distribution indexes η_m is 20; crossover probability P_c is 0.9; mutation probability P_m is 0.3; population size is 200; external population size is 50 and generation size is 1000.

6) Safety constraints:

- The maximum wave height is 7 m.

- Compliant with the IMO guidance (IMO, 2007)

By using the variation method, it can be easily proved that in calm sea conditions the minimum fuel route is the shortest route between departure and destination with a constant ship speed. So, the route optimisation in calm water is beyond the scope of this research and the following two case studies only focus on solving the minimum fuel route in medium and rough sea conditions respectively. The weather forecasts used in the case studies are downloaded by ITEES from the NOAA website according to the OPeDAP technique.

8.1.1 Case study in medium sea condition

The North Atlantic weather forecast with the time period from midnight of June 28th, 2011 until noon of July 5th, 2011 is used in this case. It is assumed that the ship departed at the same time when the forecast become available and hoped to arrive at the destination at eight o'clock on July 3rd which corresponds to the specified en-route time of 128 hours. The sequence of Figure 8.2 (a) to (e) illustrates the significant wave height changing of the weather forecast during the en-route time of the ship. The contour lines represent the significant wave height in these figures. No waves with significant height more than 5m occur in this time period, so the wave height constraints can be neglected during the optimisation process in this case. Actually, referring to the WMO (World Meteorological Organisation) sea state code (WMO, n.d.), this kind of wave should be classified as a very rough wind sea condition. However, since the operator did not need to change the ship's course or engine power setting frequently in this weather condition for the safety consideration of the case ship, this weather is referred to as a medium sea condition in this research in contrast with the rough sea condition as mentioned in the next section.

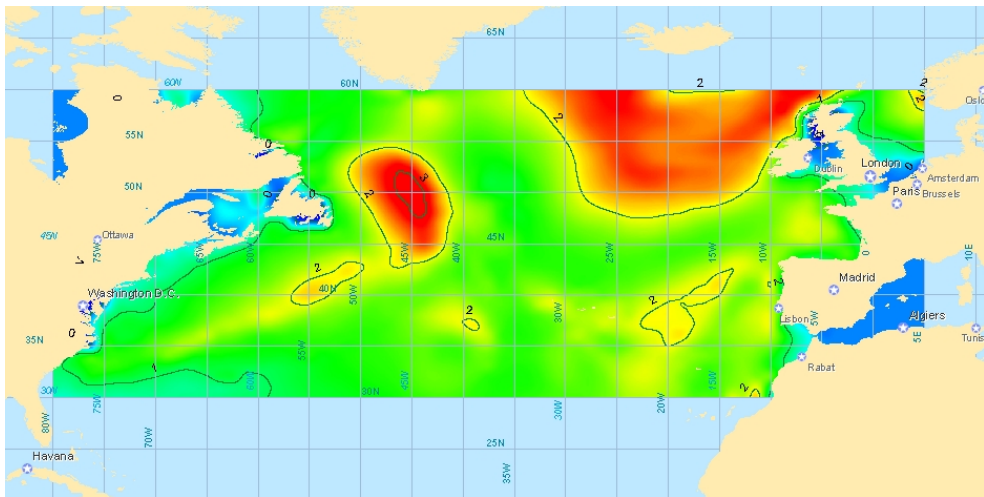


Figure 8.2 (a) Significant wave height at 09:00 28/ 06/ 2011

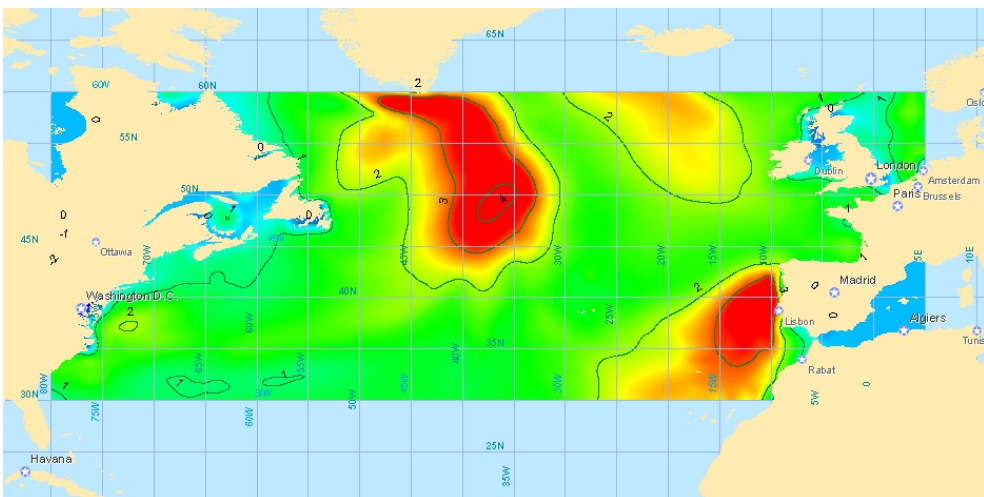


Figure 8.2 (b) Significant wave height at 03:00 29/ 06/ 2011

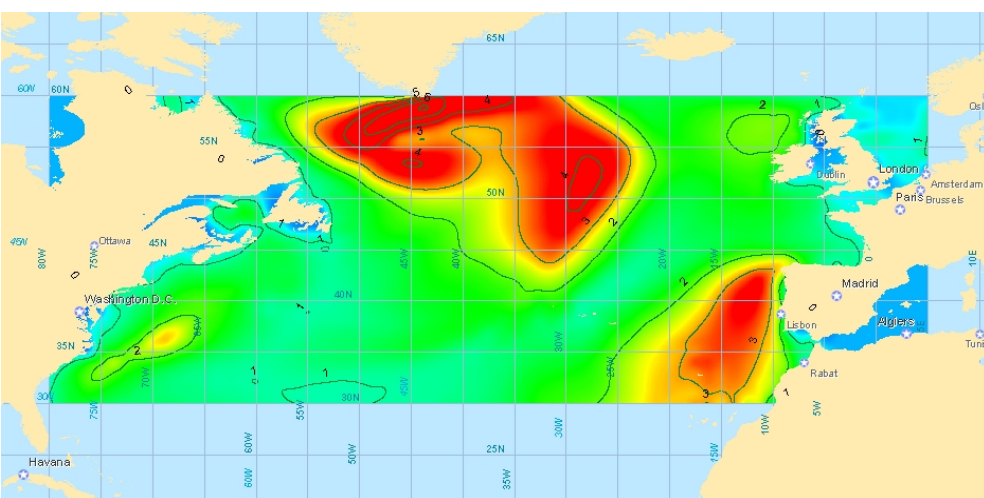


Figure 8.2 (c) Significant wave height at 21:00 29/ 06/ 2011

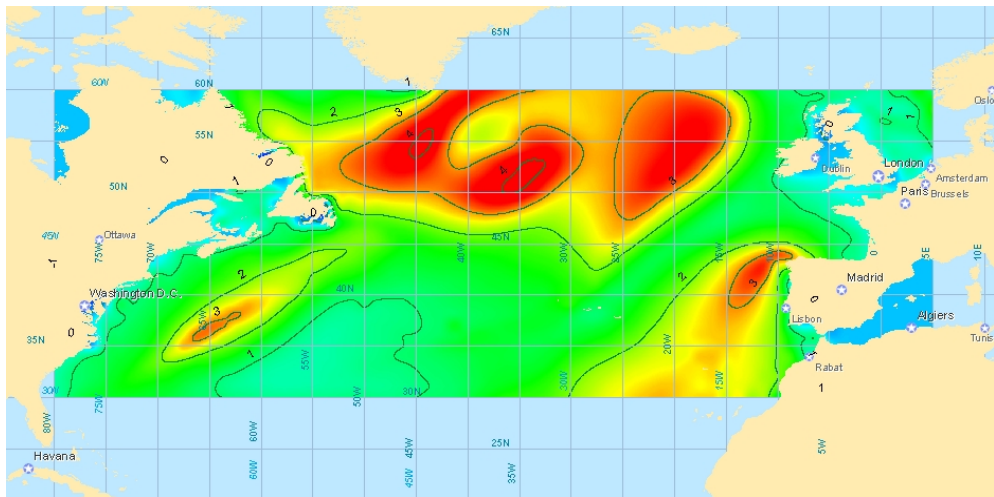


Figure 8.2 (d) Significant wave height at 15:00 30/ 06/ 2011

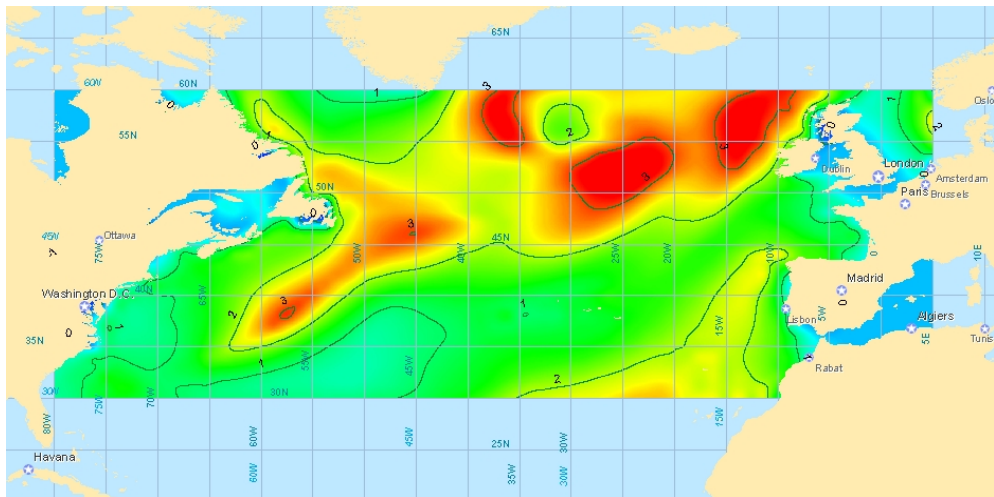


Figure 8.2 (e) Significant wave height at 09:00 01/ 07/ 2011

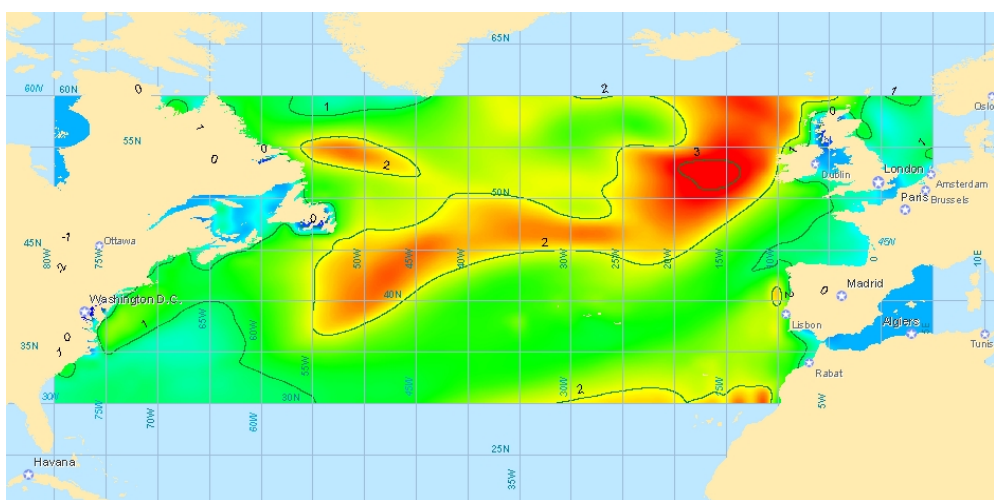


Figure 8.2 (f) Significant wave height at 03:00 02/ 07/ 2011

Figure 8.3 shows the fuel consumption of the optimised results for different estimated times of arrival (ETA) from 116 to 140 hours, 12 hours before and after the specified arrival time. The simulation results by using the shortest route (the shortest route can be calculated by using any optimisation algorithms under calm sea conditions) with constant engine power settings (except when reducing the ship's speed for ship safety considerations in certain weather conditions) are also included in this figure for the purpose of comparison. Each dot in this figure represents a feasible route solution. Figure 8.4 is a cut-out of the region around the specified arrival time from Figure 8.3 to illustrate the problem clearly. From these two figures it can be seen that nearly all the results obtained from the novel 3DDP method dominate the results obtained by other optimisation algorithms and the shortest route, but the superiority of the 3DDP method is not obvious. Because the initial population of the MOEAs are generated based on the random selection of the results from the 2DDP method, the results from the MOEAs should, apparently, dominate all the results obtained by the 2DDP method theoretically. On the other hand, since the shortest route, the course and the engine setting of the case ship are totally fixed during the whole voyage, in theory the results from the shortest route should be the worst and dominated by all the other solutions. Surprisingly, the results between MOEAs, 2DDP and the shortest route are almost non-dominated with each other. The fuel saving by the optimisation algorithms compared with the shortest route are listed in Table 8.1. The performance of NSGA II is a little better than other MOEAs, whereas the average fuel saving for one voyage by MOEAs are all less than 1 ton, indicating that there is already no improvement for the solutions during the optimisation process of the MOEAs since the results of the 2DDP method and the shortest route are already near the real Pareto front. The 3DDP method can have the most fuel saving almost for every ETA as illustrated in Table 8.1. As a result, even though the room for improvement is small, an average of 1.9 tons of fuel has been saved by using the 3DDP method for one voyage.

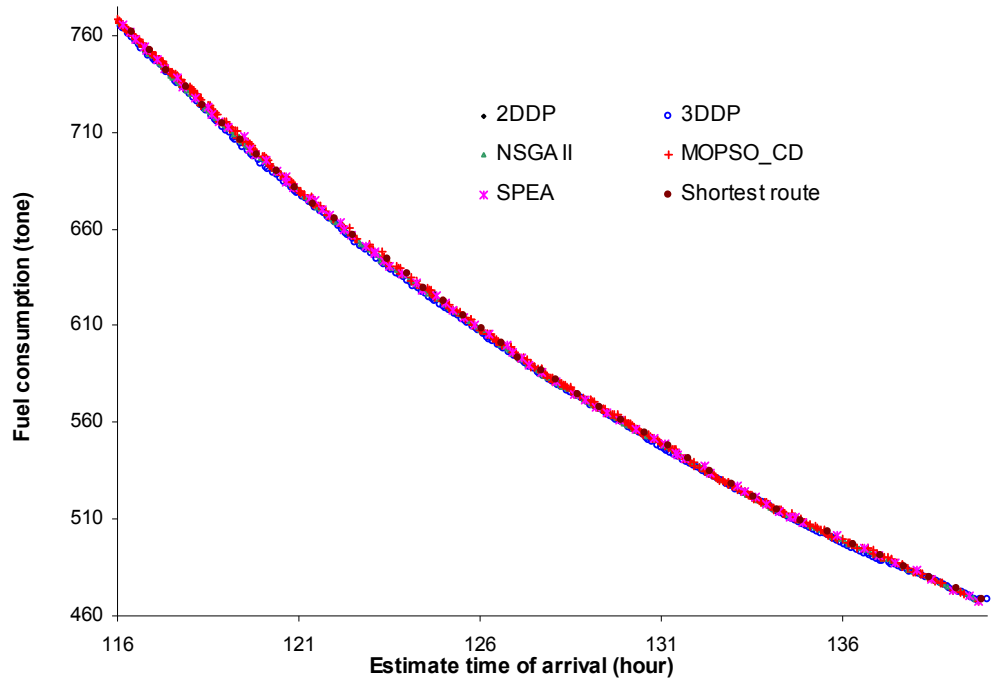


Figure 8.3 Fuel consumption for different ETAs

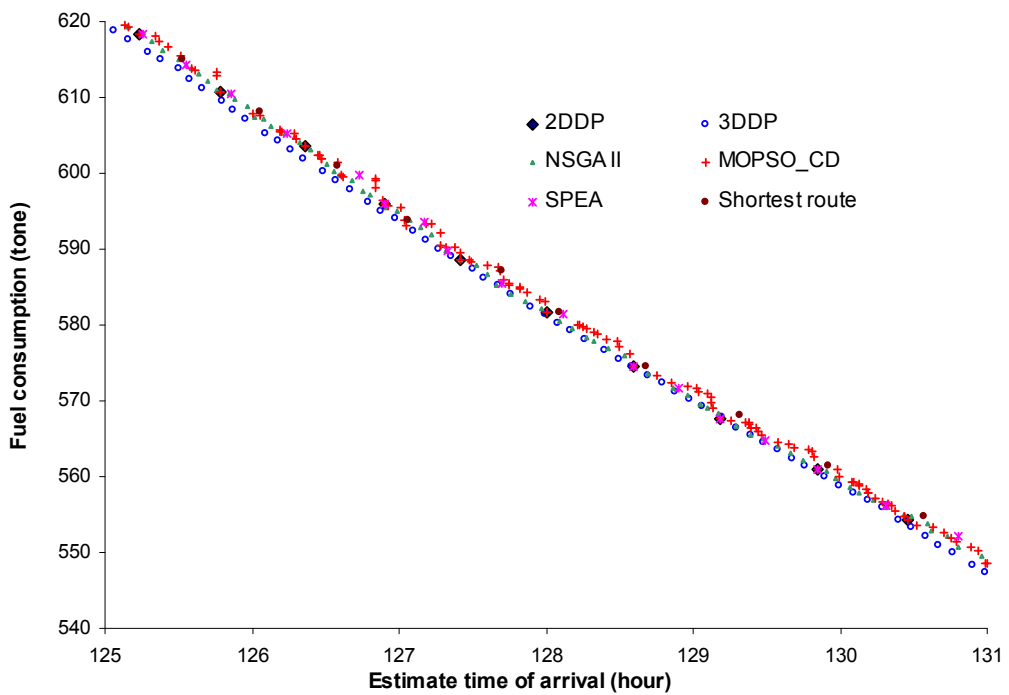


Figure 8.4 Fuel consumption for different ETAs (cut-out of figure 8.3)

Table 8.1 Fuel saving by the optimisation algorithms compared with the shortest route

| ETA (hour) | Fuel consumption of the shortest route (ton) | Fuel saving by 2DDP (ton) | Fuel saving by 3DDP (ton) | Fuel saving by NSGA II (ton) | Fuel saving by MOPSO_CD (ton) | Fuel saving by SPEA (ton) |
|---------------------------|--|---------------------------|---------------------------|------------------------------|-------------------------------|---------------------------|
| 140 | 468.2 | 0.2 | 0.1 | 0.2 | 0.2 | 0.2 |
| 139 | 473.9 | 0.2 | 1.1 | 1.0 | 0.2 | 0.2 |
| 138 | 485.5 | 0.2 | 1.2 | 0.0 | 0.2 | 0.0 |
| 137 | 491.4 | 0.2 | 2.7 | 1.1 | 0.5 | 0.2 |
| 136 | 497.2 | 0.2 | 1.9 | 1.5 | 0.6 | 2.1 |
| 135 | 508.9 | 0.0 | 1.2 | 0.0 | 0.2 | 1.0 |
| 134 | 515.1 | 0.3 | 0.8 | 0.1 | 0.3 | 1.0 |
| 133 | 527.9 | 0.3 | 1.2 | 1.2 | 0.4 | 0.6 |
| 132 | 541.3 | 0.4 | 2.6 | 1.6 | 1.2 | 0.4 |
| 131 | 548.1 | 0.4 | 2.8 | 1.3 | 1.3 | 0.0 |
| 130 | 561.4 | 0.3 | 1.3 | 0.6 | 0.3 | 0.3 |
| 129 | 568.0 | 0.4 | 1.5 | 1.4 | 0.9 | 0.4 |
| 128 | 581.6 | 0.0 | 1.3 | 1.1 | 0.0 | 0.1 |
| 127 | 593.8 | 0.0 | 1.5 | 0.0 | 0.8 | 0.3 |
| 126 | 608.1 | 0.0 | 2.7 | 1.0 | 0.4 | 2.8 |
| 125 | 622.3 | 4.0 | 2.5 | 0.7 | 0.0 | 0.6 |
| 124 | 637.0 | 3.7 | 4.1 | 2.7 | 2.4 | 0.2 |
| 123 | 644.0 | 3.2 | 2.3 | 1.9 | 1.3 | 3.2 |
| 122 | 665.1 | 0.2 | 2.2 | 1.7 | 0.2 | 1.5 |
| 121 | 681.4 | 0.3 | 1.5 | 0.3 | 0.3 | 0.3 |
| 120 | 698.3 | 0.3 | 3.1 | 0.3 | 0.3 | 0.3 |
| 119 | 714.5 | 0.0 | 1.6 | 0.0 | 0.0 | 0.0 |
| 118 | 733.0 | 0.0 | 1.9 | 0.8 | 0.0 | 0.0 |
| 117 | 752.0 | 0.0 | 2.1 | 1.5 | 0.4 | 0.0 |
| 116 | 762.0 | 0.4 | 3.1 | 1.6 | 1.1 | 0.4 |
| Average fuel saving (ton) | | 0.6 | 1.9 | 0.9 | 0.5 | 0.6 |

The optimised routes corresponding to specified arrival time, ETA = 128 hours shown in Figure 8.5. Figure 8.6 and Figure 8.7 show the ship speed over ground and the engine power of these solutions respectively. All the optimised routes have a slight deviation to the north from the shortest route at the beginning and end of the voyage, but only the solutions from 3DDP and NSGA II can have certain fuel saving (1.3 and 1.1 tons respectively) compared with the shortest route. All the solutions

reduce the ship's speed around midnight on 30th of July for safety considerations since the ship will encounter a wave state which may have a more probability to cause the synchronised rolling of the ship, as shown in Figure 8.8.

In this case study it can be seen that the improvement by using the MOEAs for minimum fuel route in medium sea conditions is negligible in comparison with the shortest route. The novel 3DDP method can give certain fuel saving and perform better than all MOEAs but the superiority compared to the shortest route is not obvious. Furthermore, unlike other solutions which need frequent changes of the engine power during the voyage, as shown in Figure 8.7, the shortest route with a constant engine setting can give more convenience for the operators on board. It can be concluded that below a certain sea state the route optimisation is not necessary and the shortest route with constant engine power can be used for real navigation.

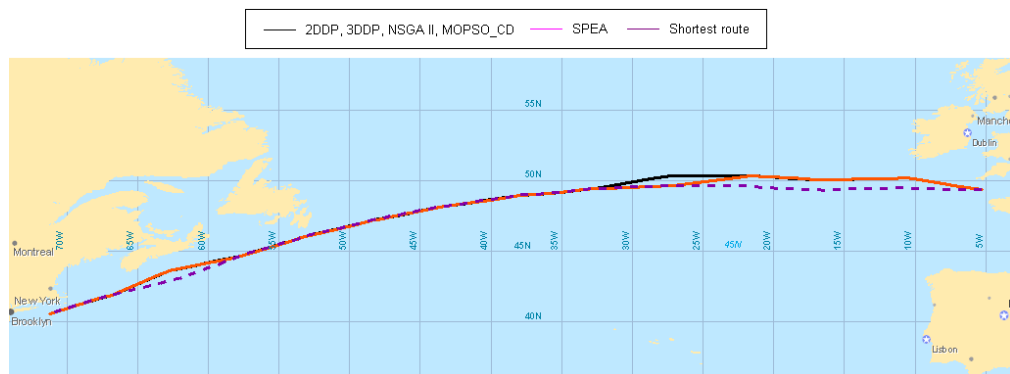


Figure 8.5 Optimised route under specified arrival time
(EAT = 128 hours, medium sea condition)

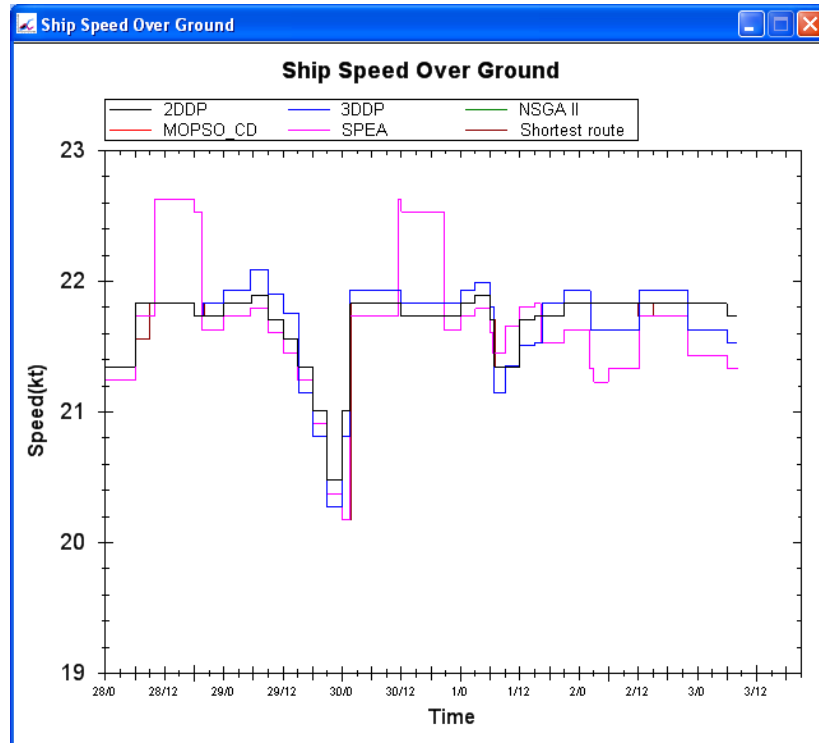


Figure 8.6 Ship speed over ground of the optimised routes
(EAT = 128 hours, medium sea condition)

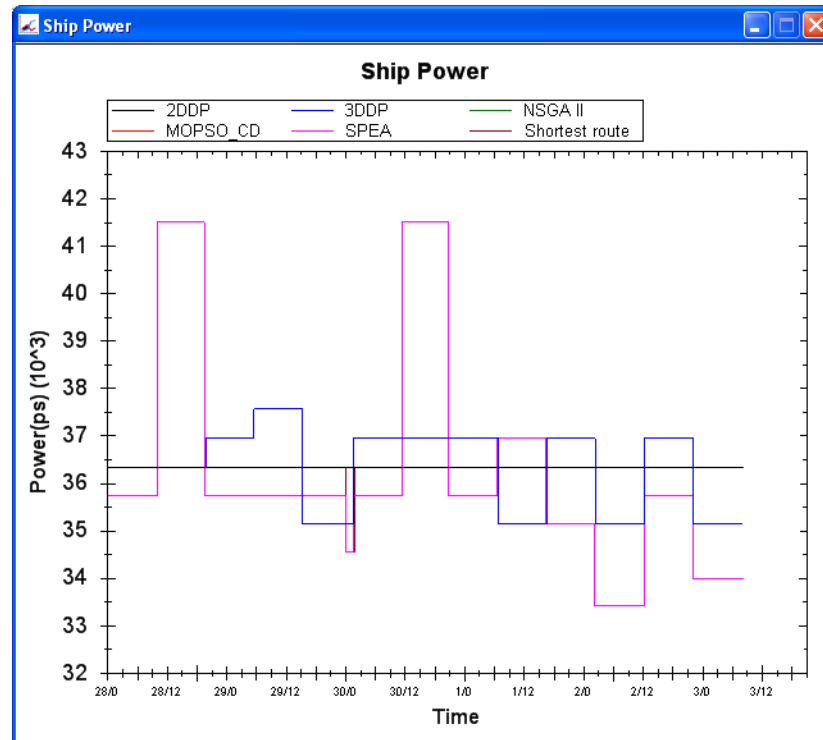


Figure 8.7 Ship engine power of the optimised routes
(EAT = 128 hours, medium sea condition)

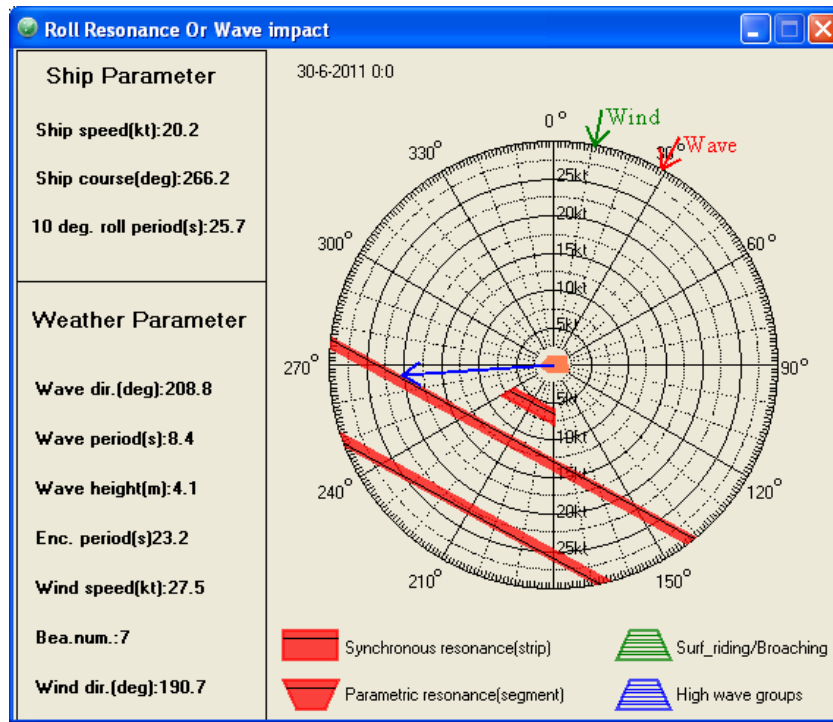


Figure 8.8 Polar diagram according to IMO guidelines at midnight on July, 30th
(Shortest route, medium sea condition)

8.1.2 Case study in rough sea condition

The North Atlantic weather forecast with rough sea condition from 6:00 a.m., 24th January 2011 to 6:00 p.m., 31st January 2011 is used for this study. The rough sea condition is moving towards northeast. Significant waves with a height more than 11m occur at times. The ship must avoid the rough sea area for safety operation. The ship departure time is 3:00 p.m., 25th January and hope to arrival at the destination 128 hours after departure. The en-route time scope, which allows 12 hours before and after the specified arrival time, will be considered during the optimisation process. Unlike in the medium sea condition in which the shortest route with a constant engine setting can be used for real navigation, the route optimisation is absolutely necessary in the rough sea state not only for fuel saving but, most importantly, for ensuring ship safety during the voyage.

Two route optimisation strategies, optimisations based on the grid system and the shortest route, are used to assess the capability of different optimisation algorithms for fuel saving in rough sea conditions.

1) Optimisation based on the grid system

To give a clear comparison between the capabilities of the different optimisation techniques, the fuel consumptions of the optimised results under different estimated times of arrival (ETA) are shown in Figure 8.9 to 8.11 separately. In contrast to the case study in medium sea condition, no solutions from the shortest route with a constant engine setting can satisfy ship safety considerations so they are reasonably excluded in the comparison.

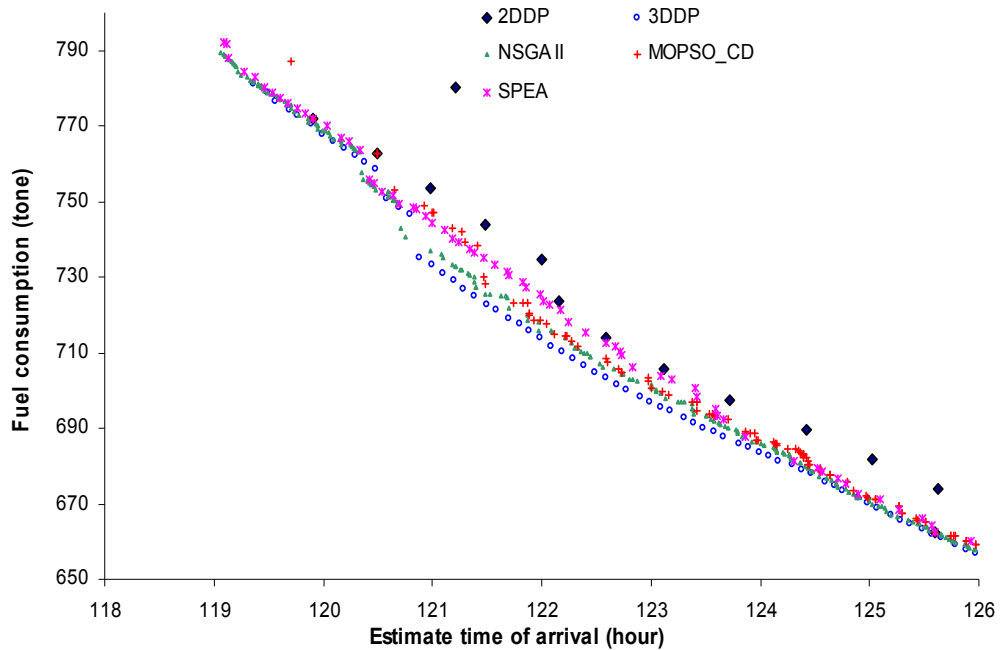


Figure 8.9 Fuel consumption for different ETAs (optimise the grid)

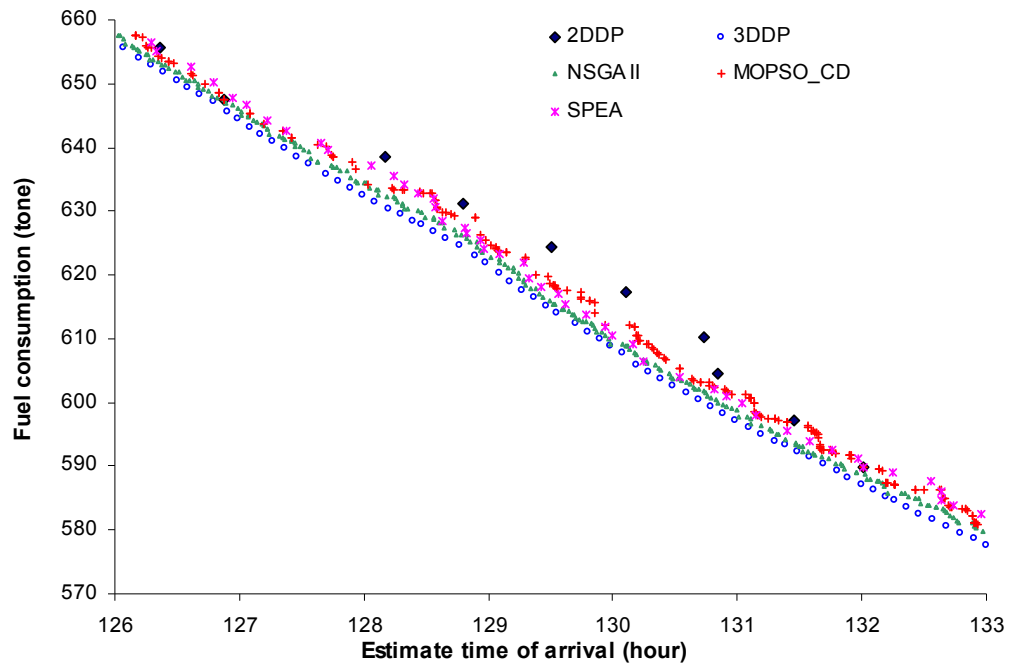


Figure 8.10 Fuel consumption for different ETAs (optimise the grid)

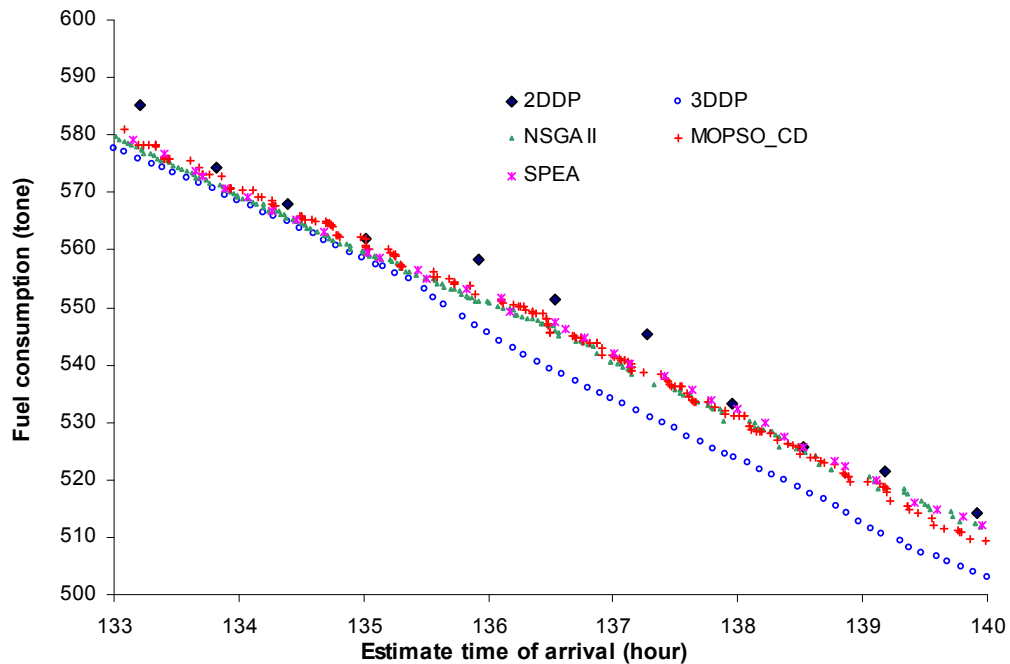


Figure 8.11 Fuel consumption for different ETAs (optimise the grid)

From these three figures it can be seen that the 3DDP method obtains the best results with a very uniform distribution. Nearly all the results obtained from the 3DDP dominate the results gotten by other optimisation algorithms, and the superiority of

the 3DDP method is very obvious in some part. All the MOEAs perform better than the 2DDP method but these methods converge to the local optimised results especially after ETA of 135 hours, as shown in Figure 8.11. Actually, after 1000 generations, the results from all the MOEAs already have no significant improvement. NSGA II is the second best method as it in the medium sea state. For most ETAs, this method can obtain better results and a finer distribution than those calculated by MOPSO_CD and SPEA but worse than the results obtained by the 3DDP method. The optimisation capabilities of MOPSO_CD and SPEA are well matched, most of the time they are better than 2DDP and worse than 3DDP and NSGA II, with a dispersed distribution. The results optimised by the 2DDP method are the worst for most ETAs. Unlike the last case study, the optimised results cannot completely cover the whole considered range of the ETAs. This suggests that, in rough sea conditions, as the ship speed has to be reduced significantly, an arrival under a short ETA is impossible. The ETAs of fastest attainable routes achieved by 3DDP, NSGA II and SPEA are about 119 hours whereas the ETA of fastest routes by 2DDP and MOPSO_CD are near 120 hours.

The fuel saving by the 3DDP and the MOEAs methods, compared with the 2DDP method, are listed in Table 8.2. Better performances from the 3DDP and MOEAs methods than they are in the medium sea condition can be shown. Optimising the engine power and ship course simultaneously in rough sea condition can give certain contribution towards fuel savings in comparison with the traditional 2DDP method which only optimises the ship's course and uses a fixed engine power during the whole voyage. Especially by using the novel 3DDP method, an average of more than 1.5% fuel can be saved for one voyage. Under certain ETA, 3DDP can even offer fuel savings of more than 20 tons (\$14000 at \$700/ton) in comparison with the optimised solution by the 2DDP. It can be seen that the novel 3DDP method presented in this paper can give better results than the 2DDP and the MOEAs methods for weather routing. In addition, less parameter settings give some convenience for operators onboard.

Table 8.2 Fuel saving by the optimisation algorithms compared with 2DDP method

| ETA (hour) | Fuel consumption by 2DDP (ton) | Fuel saving By 3DDP (ton) | Fuel saving by NSGA II (ton) | Fuel saving by MOPSO_CD (ton) | Fuel saving by SPEA (ton) |
|---------------------------|---|---------------------------------|------------------------------------|-------------------------------------|---------------------------------|
| 140 | 514.1 | 10.1 | 1.6 | 4.4 | 2.1 |
| 139 | 521.5 | 8.7 | 3.2 | 2.8 | 1.6 |
| 138 | 533.2 | 9.3 | 3.1 | 2 | 0.9 |
| 137 | 545.2 | 11.2 | 8.7 | 6.7 | 7.1 |
| 136 | 558.3 | 13.1 | 7.2 | 6 | 5.1 |
| 135 | 561.8 | 3.3 | 2.4 | 0 | 2.2 |
| 134 | 574.4 | 5.8 | 3.1 | 1.8 | 3.8 |
| 133 | 585.3 | 7.8 | 7.7 | 7 | 6.2 |
| 132 | 589.8 | 2.6 | 1.1 | 0 | 0 |
| 131 | 610.2 | 10.9 | 8.3 | 7 | 8.1 |
| 130 | 617.3 | 9.6 | 8.3 | 5.2 | 8.1 |
| 129 | 631.2 | 6.5 | 5 | 1.9 | 3.8 |
| 128 | 638.5 | 8.1 | 6.3 | 5 | 2.9 |
| 127 | 647.5 | 1.9 | 0 | 0 | 0 |
| 126 | 673.7 | 12.7 | 11.5 | 11.2 | 11.2 |
| 125 | 681.6 | 12.7 | 11.8 | 10.6 | 10.5 |
| 124 | 697.2 | 9.4 | 7 | 5 | 5.1 |
| 123 | 705.5 | 9.8 | 7.8 | 5.9 | 1.6 |
| 122 | 734.7 | 20.9 | 18.9 | 16.4 | 10.9 |
| 121 | 753.3 | 20.2 | 16.4 | 6.1 | 9.2 |
| 120 | 772 | 1.4 | 1.4 | 0 | 0 |
| Average fuel saving (ton) | | 9.3 | 6.7 | 5.0 | 4.8 |

Table 8.3 Fuel consumption and distance of the optimised routes (ETA = 128 hours)

| | 2DDP | 3DDP | NSGA II | MOPSO_CD | SPEA |
|------------------------|--------|--------|---------|----------|--------|
| Fuel consumption (ton) | 638.5 | 630.4 | 632.2 | 633.5 | 635.6 |
| Distance (sea mile) | 2799.1 | 2791.5 | 2791.7 | 2791.5 | 2791.8 |

The optimised routes corresponding to specified arrival time, ETA = 128 hours, are shown in Figure 8.12. Figure 8.13 and Figure 8.14 show the ship speed over ground and the engine power of these solutions respectively. All the optimised routes have a deviation to the south from the shortest route during the voyage. Since the 2DDP

method uses a constant engine power during the voyage, the ship has to circumnavigate the bad weather to ensure ship safety. As a result, more fuel consumption and longer distance is needed by 2DDP as shown in Table 8.3. Temporary speed reduction is necessary to avoid synchronous resonance as shown in the red circle area on Figure 8.14 and Figure 8.15 (a polar diagram according to IMO guidelines). In contrast to the 2DDP, the 3DDP and the MOEAs are very “smart” and three “tricks” are usually used: 1) Slowing down to let the bad weather pass by first, once the bad weather has passed, the ship increases her speed to ensure the desired arrival time is achieved. 2) Speeding up to pass the region before the bad weather arrives. Once the ship has passed the region that the bad weather is going to pass through, the speed of the ship is reduced and maintains the desired arrival time. 3) Bypassing the rough sea to ensure ship safety. All these three “tricks” can be used for one voyage since the ship may encounter several rough sea conditions during the whole voyage. These “smart” methods will balance the fuel saving due to the reduced speed and additional fuel consumption due to the increased ship speed for catching-up the schedule. As a result, fuel can be saved and shorter distance is needed as shown in Table 8.3. The novel 3DDP method is “No.1” of these “smart” methods. Two routes variations obtained by the 2DDP (red line) and 3DDP (green line) method under 128 hours of ETA and the weather conditions changing are shown in the sequence of Figure 8.16 (a)-(f). The contour lines represent the significant wave height during the voyage and the red (2DDP) and black dots (3DDP) represent the ship’s current positions (simulation progression). During the first one third of the distance, the sea condition is moderate and the 3DDP method chooses the same course strategy as used by 2DDP but with a higher engine power setting. As a result higher fuel consumption is needed by the 3DDP in the first one third of the voyage. These two routes will separate before encountering the bad weather conditions. The route by 3DDP chooses a track with a slight deviation to the north from the route by 2DDP. Once the ship encounters the rough sea condition, the 3DDP method reduces the engine power setting and passes the rough sea safely but the route by 2DDP must circumnavigate the rough sea to ensure ship safety. Finally, certain fuel saving is achieved by the 3DDP when the ship encounters the rough sea. These two routes converge again in the final one third of the voyage once the rough sea is passed.

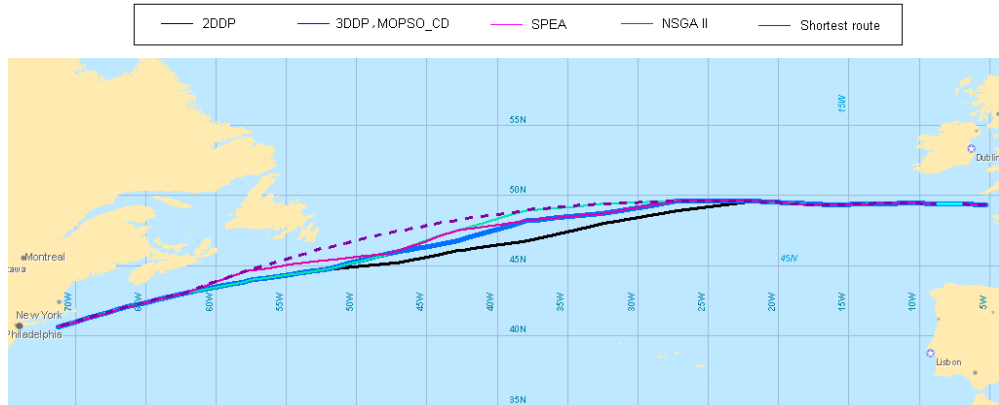


Figure 8.12 Optimised route under specified arrival time
(EAT = 128 hours, medium sea condition)

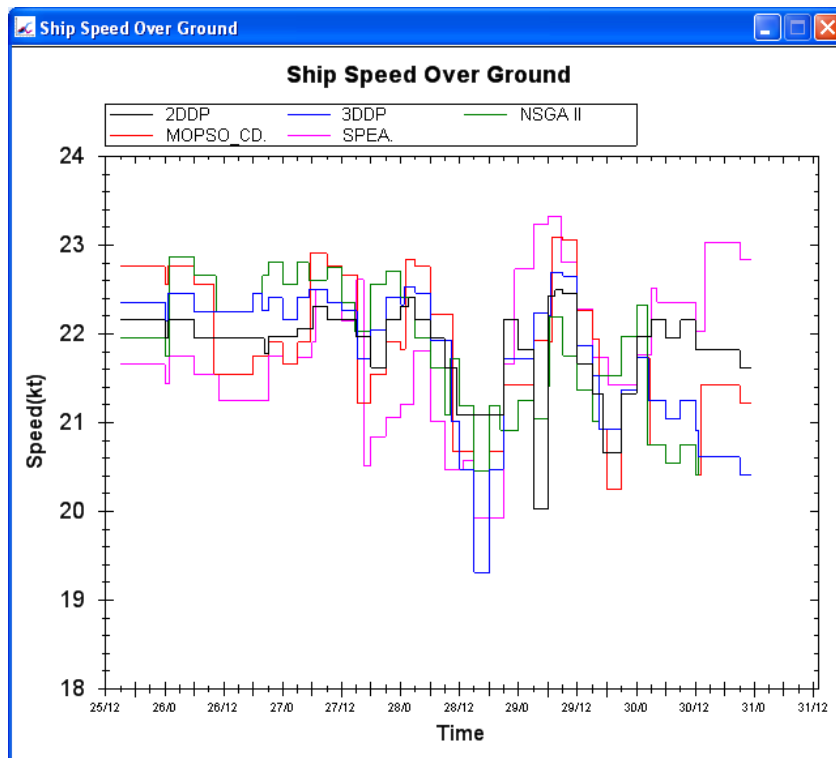


Figure 8.13 Ship speed over ground of the optimised routes
(EAT = 128 hours, rough sea condition)

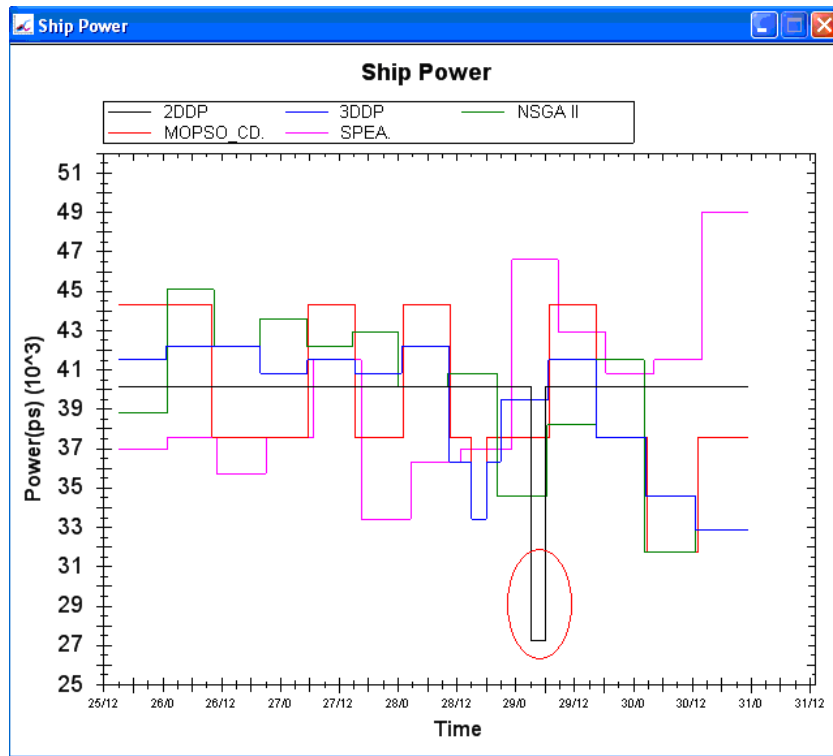


Figure 8.14 Ship engine powers of the optimised routes (EAT = 128 hours, rough sea condition)

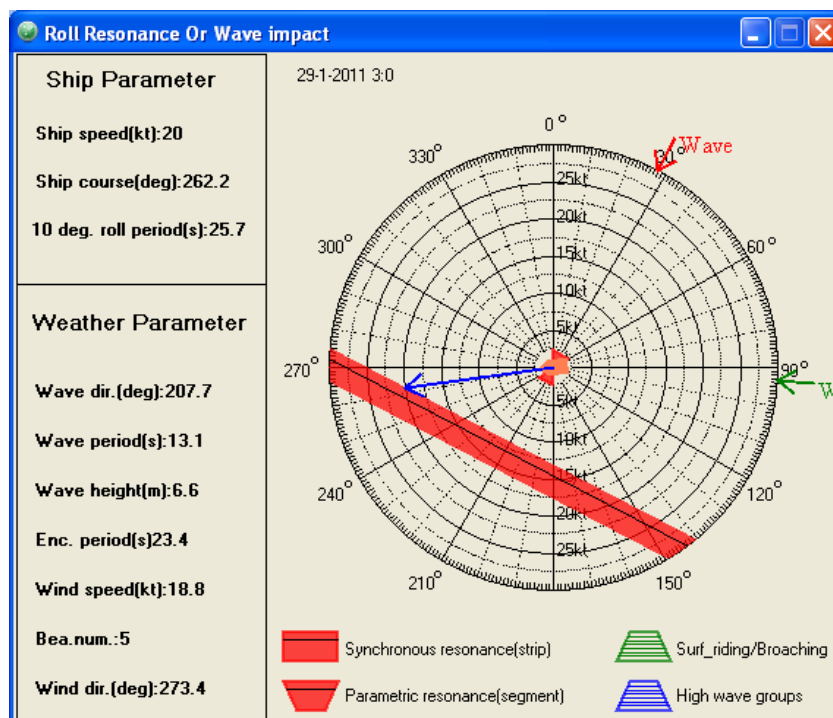


Figure 8.15 Polar diagram according to IMO guidelines at midnight on July, 30th (route from 2DDP, rough sea condition)

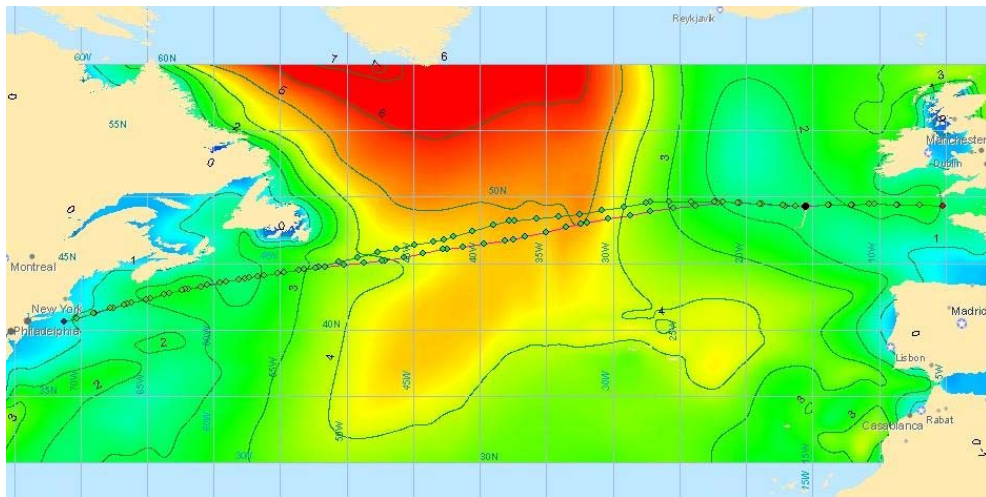


Figure 8.16 (a) Ship position and significant wave height at 09:00 26/ 01/ 2011

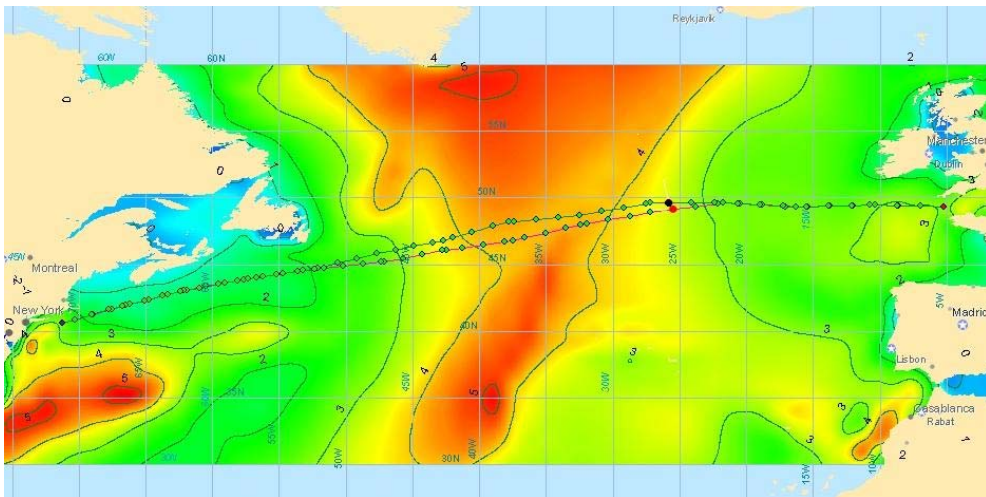


Figure 8.16 (b) Ship position and significant wave height at 03:00 27/ 01/ 2011

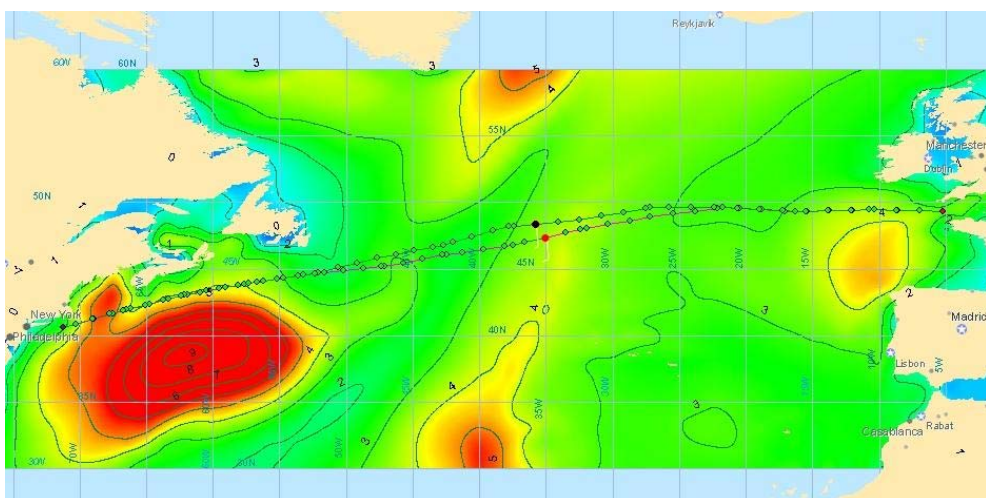


Figure 8.16 (c) Ship position and significant wave height at 21:00 27/ 01/ 2011

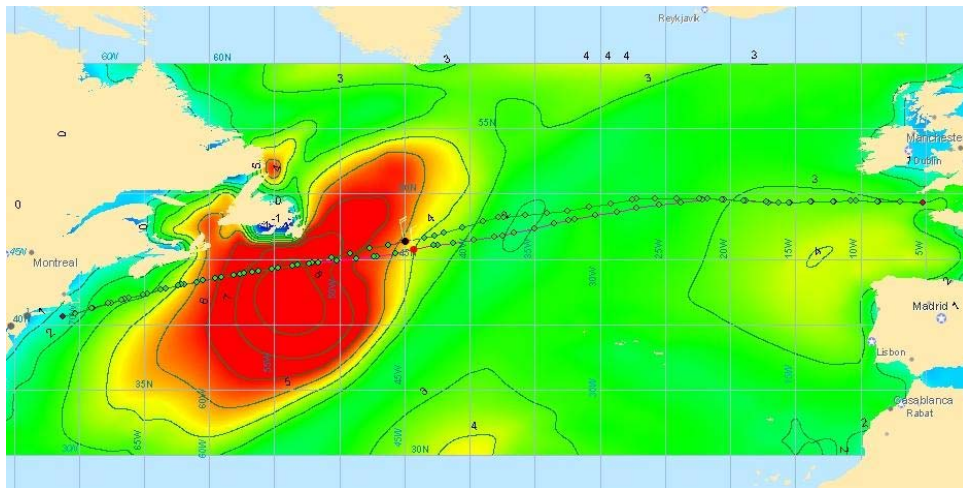


Figure 8.16 (d) Ship position and significant wave height at 15:00 28/ 01/ 2011

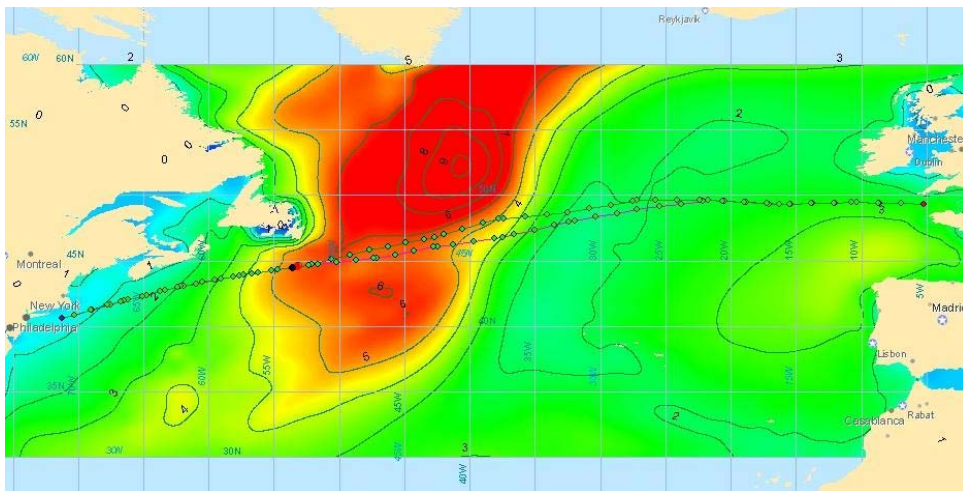


Figure 8.16 (e) Ship position and significant wave height at 09:00 29/ 01/ 2011

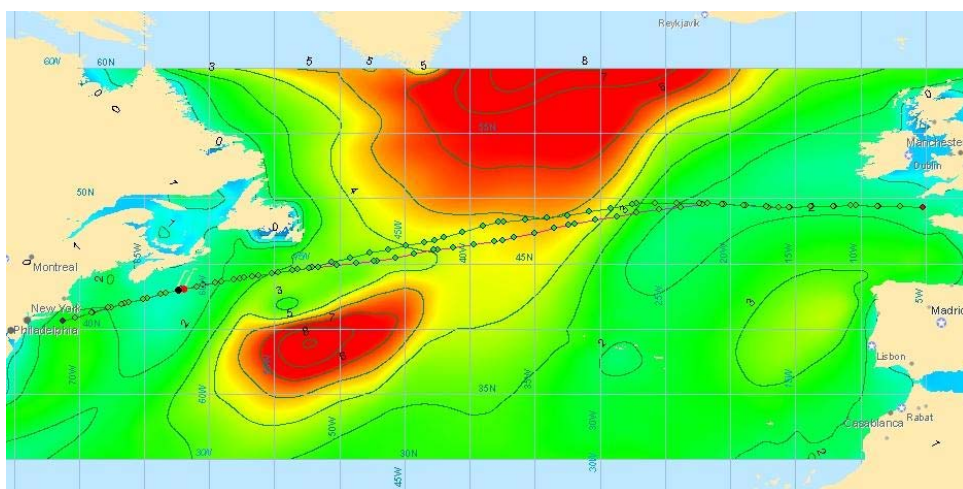


Figure 8.16 (f) Ship position and significant wave height at 03:00 30/ 01/ 2011

2) Optimisation of ship engine power based on the shortest route

When following a fixed course only the parameters of engine power are used as the free variables in this optimisation. The shortest route can be considered as a special case of the grid system in which there is only one state on a stage in geographic position. Except for the grid system, all the parameter settings for this optimisation are the same as mentioned above.

Under the shortest route, the 2DDP method will be degraded as using the shortest route with a constant engine setting for the voyage. Unlike in the last section, no solution can be found by using the shortest route with a constant engine setting since the ship will encounter the adverse weather situations during the voyage which have a significant wave height more than the allowed limit (7m) as shown in Figure 8.17. The purple dot represents the actual position of the ship in this figure. It is evident that the route optimisation in rough sea conditions is absolutely necessary not only for fuel saving but, most importantly, for ensuring ship safety during the voyage.

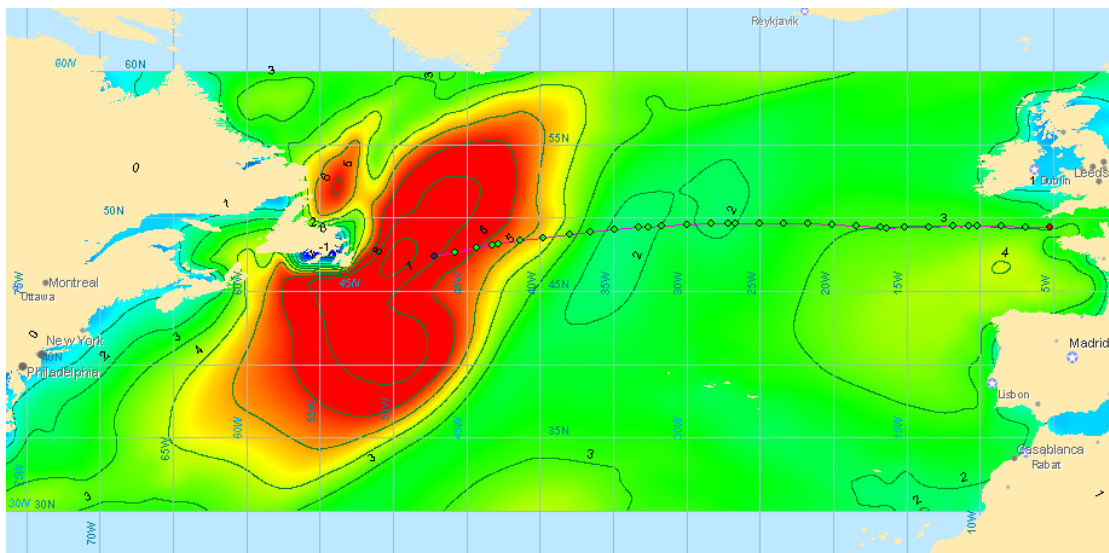


Figure 8.17 Encounter of rough sea conditions by following the shortest route with constant engine power setting (ship speed in calm water = 21.8 knot)

When using the MOEAs, a constant engine power for the whole voyage should be randomly selected for creating the initial population. Otherwise the optimisation process of MOEAs will become slow and very difficult to converge to the real Pareto front and, sometimes, no solutions can be obtained by the MOEAs especially for MOSPO_CD which should use a non-dominated solution archive to update the search direction during the optimisation process. The fuel consumptions of the optimised results for different ETAs are shown in Figure 8.18 to 8.19 separately. In contrast to the case study of optimising the grid system, the superiority of the 3DDP is not obvious. The results of 3DDP and NSGA II nearly coincide with each other. For most ETAs, the SPEA method can obtain better results and a finer distribution than those calculated by MOPSO_CD but a little worse than the results obtained by the 3DDP and NSGA II method. The results optimised by the MOPSO_CD method are the worst for most ETAs. There are no solutions for the specified arrival time to be obtained by all the optimisation algorithms and the ETAs of fastest routes obtained by all algorithms are about 132 hours except MOPSO_CD which gives the fastest route with an ETA of 133 hours. These values are less than those achieved in the case study of optimising the grid system. The more fuel consumption by MOEAs compared with the 3DDP method are shown in Table 8.4. Most of the time the 3DDP gives the least fuel consumption, but the difference of fuel consumption between each method is very small. It can be seen that, since the number of control variables are less than the case of optimising the grid system, the optimisation capability of the novel 3DDP is restricted. However, when considering the computing time, the 3DDP method offers a much greater advantage compared with the MOEAs. The computing time (less than 30 seconds) used by the 3DDP is much less than the time (approximately 5 minutes) used by MOEAs to converge to the Pareto front.

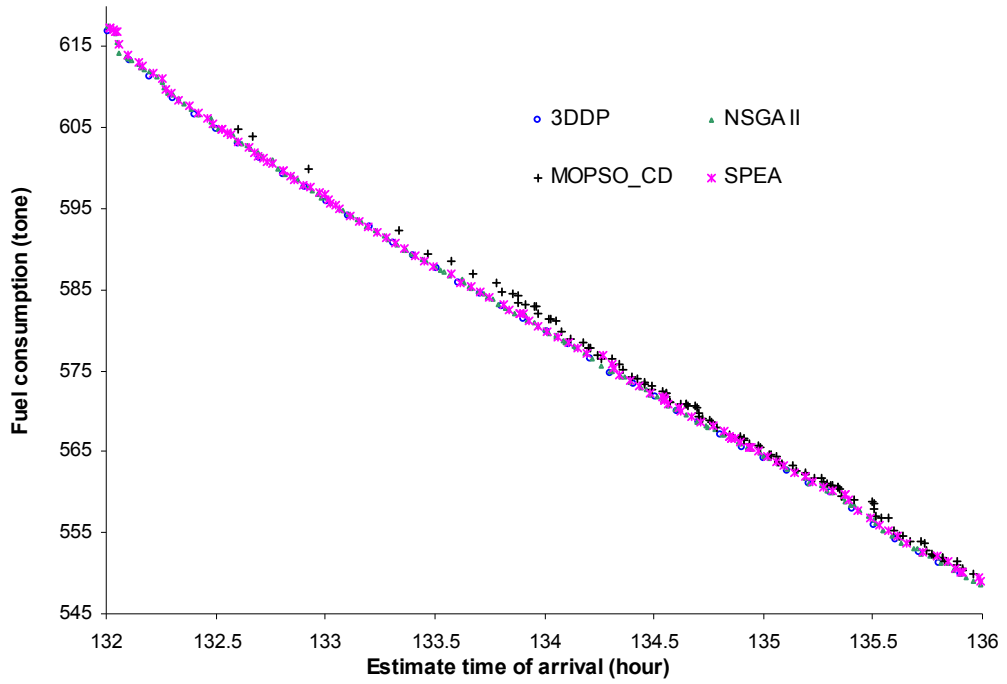


Figure 8.18 Fuel consumption for different ETAs
(Optimise the engine power based on the shortest route)

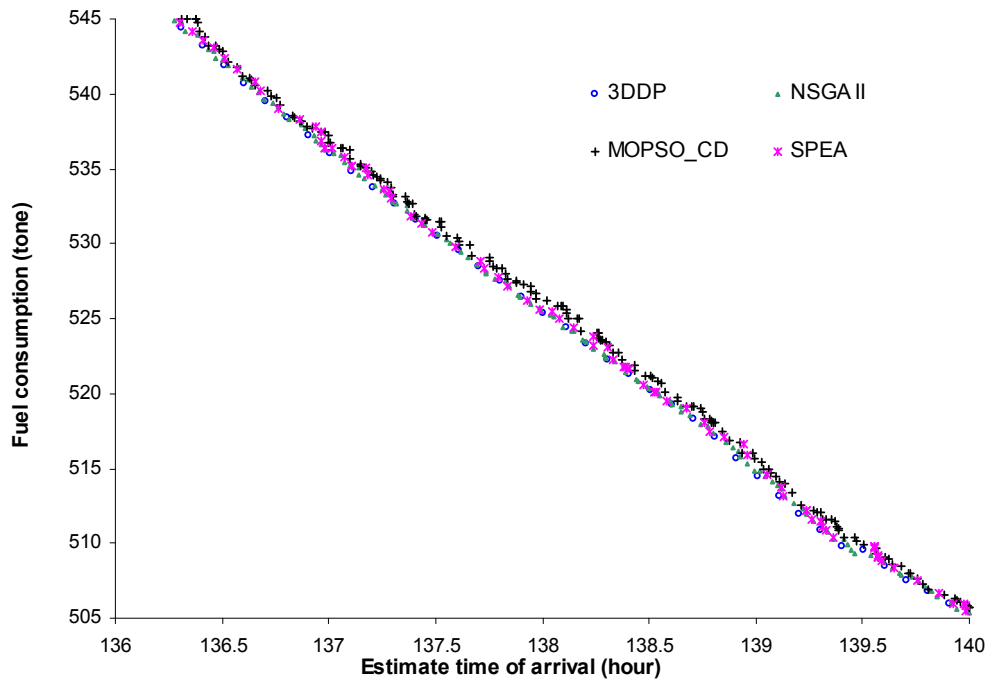


Figure 8.19 Fuel consumption for different ETAs
(Optimise the engine power based on the shortest route)

Table 8.4 Fuel consumption used by the MOEAs and 3DDP methods

| ETA (hour) | Fuel consumption by 3DDP (ton) | More fuel consumption by NSGA II (ton) | More fuel consumption by MOPSO_CD (ton) | More fuel consumption by SPEA (ton) |
|-------------------------------------|-----------------------------------|---|--|--|
| 132 | 616.9 | 0.5 | X | 0.5 |
| 133 | 597.7 | 0.1 | 2.3 | 0.2 |
| 134 | 581.3 | 0.8 | 1.7 | 0.6 |
| 135 | 565.6 | 0.4 | 1.2 | 0.6 |
| 136 | 548.3 | 0.1 | 1.5 | 0.7 |
| 137 | 536.1 | -0.1 | 0.6 | 0.3 |
| 138 | 525.4 | 0.1 | 0.8 | 0.2 |
| 139 | 514.4 | 0.4 | 1.3 | 1.4 |
| 140 | 505.9 | 0.2 | 0.6 | 0.1 |
| Average more fuel consumption (ton) | | 0.2 | 1.3 | 0.5 |

The difference of the optimised fuel consumptions by the 3DDP method based on the grid system and the shortest route are shown in Figure 8.20. At smaller ETAs, optimising the grid system can save more fuel than simply optimising the engine power based on the shortest route, but as the ETA increases, the difference between the fuel consumption gradually becomes smaller. It is because that with the ETA increases, the average ship speed during the voyage will be reduced. For longer ETAs, most of the time changing the ship speed to avoid the rough sea condition can save more fuel than bypassing the rough sea to ensure ship safety. As a result, the optimised routes based on the grid system will be close to the shortest route with the ETA increase and the difference of the fuel consumptions become smaller as illustrated in Table 8.5.

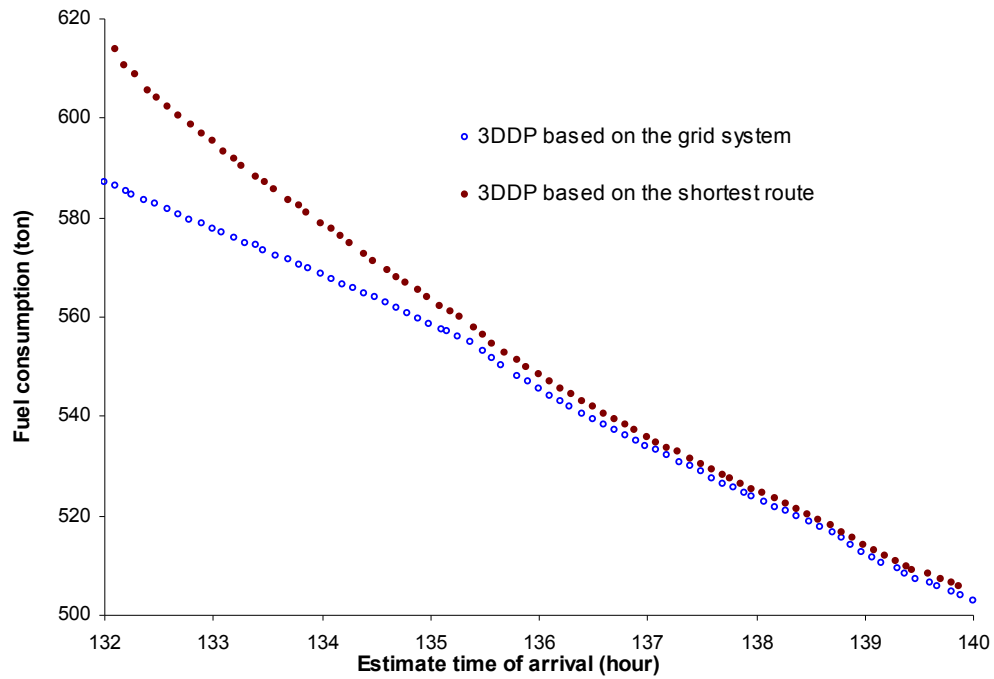


Figure 8.20 Optimised fuel consumptions by the 3DDP method based on the grid system and the shortest route

Table 8.5 Fuel and distance saving based on the grid system compared with the shortest route by the 3DDP method

| ETAs (hour) | 132 | 133 | 134 | 135 | 136 | 137 | 138 | 139 | 140 |
|-----------------------------|------|------|------|------|-----|-----|-----|-----|-----|
| Fule saving (ton) | 29.6 | 20.2 | 12.7 | 7.1 | 3.1 | 2.1 | 1.5 | 1.6 | 1.9 |
| distance saving (sea mile) | 16.4 | 16.4 | 16.2 | 16.4 | 0.3 | 0.3 | 0.3 | 0.3 | 0.3 |

8.2 The influence of constraint conditions

This section discusses the influence of the variation of the constraint conditions on the optimisation results. Since the 3DDP method has the best performance in the case studies above, for this reason only the 3DDP method is employed for the sensitive study of the constraint conditions. In the other sides, the route optimisation in rough sea conditions is the pivotal case for weather routing. As a consequence, only the rough sea condition is considered in this section.

Figure 8.21 shows the Pareto fronts under the different limit setting of the encountered wave height (the IMO guideline (IMO, 2007) is also applied to ensure ship safety). The limit of the wave height is varied from 6 to 8 meters with 0.5 meter intervals. It can be seen that relaxing the limit of encounter wave height can improve the optimisation results. The fuel consumption decreases along with the wave height limit increase under certain ETA. The Pareto front for wave height limit of 7.5 m is very close to the one with wave height limit of 8 m and some parts of these two Pareto fronts even coincide with each other. Since higher waves can cause more fuel consumption and the solution with higher encounter waves will be deleted during the optimisation process, among most of the optimised solutions under the wave height limit of 8 m, the encountered wave heights are already smaller than 7.5 m. Actually there is already no difference between the Pareto front with wave height limit of 8 m and the Pareto front in which the wave limit is deactivated. The tightening wave height limit can increase the en-route time of the attainable fastest route significantly. When the wave height limit is smaller than 6 m, a solution under the specified arrival time (ETA = 128 hour) is already impossible.

Synchronous rolling, parametric rolling, riding on the wave crest of wave groups and surf-riding and broaching-to are four of main reasons for ship capsizing in adverse weather conditions. The IMO guidelines (IMO, 2007), as mentioned in Section 2.5, are used for predicting and avoiding these dangerous phenomena during route optimisation. Figure 8.22 (a) to (e) show the influence of the application of the IMO guidelines on the route optimisation results. By applying the IMO guidelines, some optimised solutions which should be available when these dangerous phenomena are neglected during the optimisation process will be deleted and this additional constraint will degrade the optimisation results. As a result the ETA of the attainable fastest route is increased when applying the IMO guidelines. Nevertheless, except in the low ETA region (except Figure 8.22 f), the optimised solutions with the application of IMO guidelines and solutions with deactivation of IMO guidelines nearly coincides with each other. This suggests that the influence of the application of IMO guidelines on the optimised results are not obvious unless considering the time minimum route and the proportion of the en-route time which encounters these

four dangerous phenomena are small. Even so, as ship safety is the first considerable factor and more important than the fuel consumption in ship weather routing it is strongly advised to employ the IMO guidelines as a constraint condition during the optimisation process.

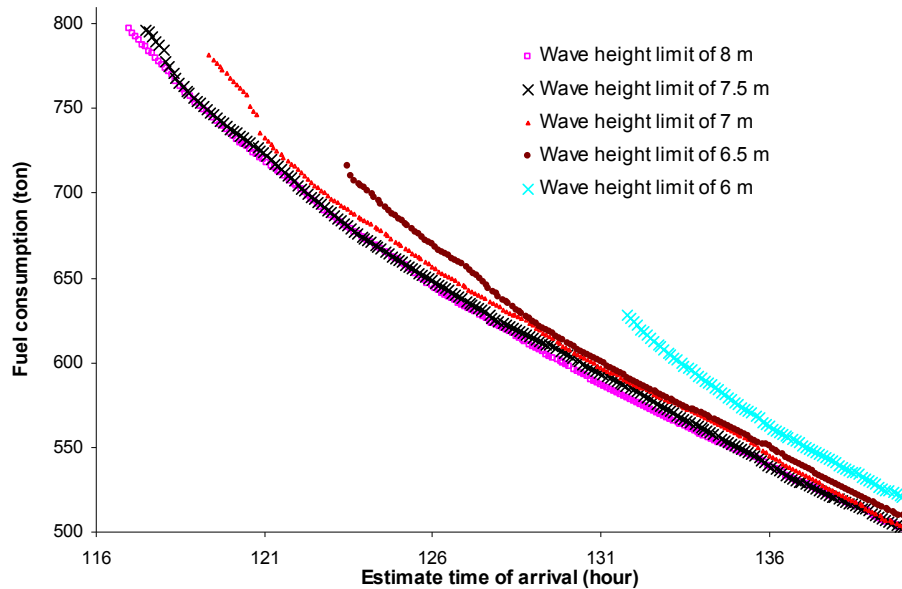


Figure 8.21 Pareto fronts for different limit setting of the encountered wave height

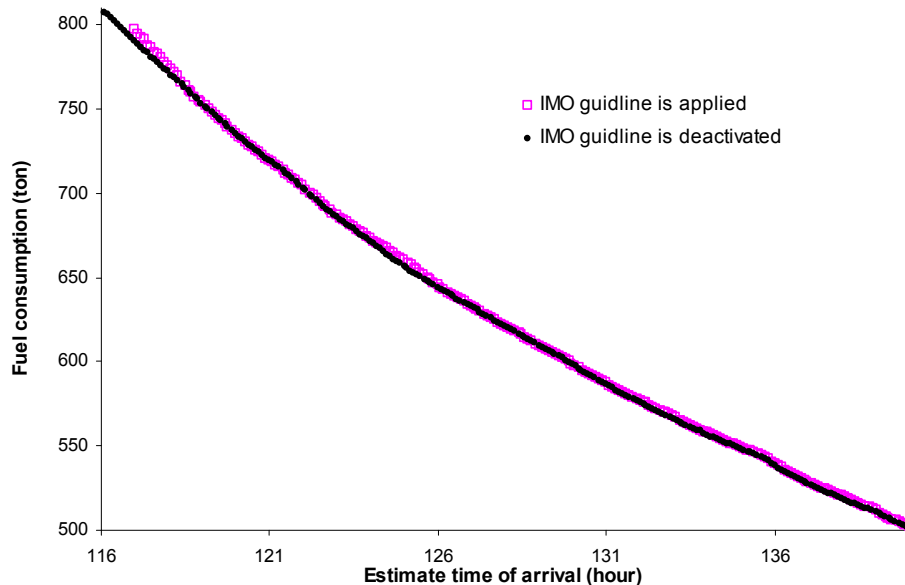


Figure 8.22 (a) Influence of the application of the IMO guidelines (wave height limit of 8 m)

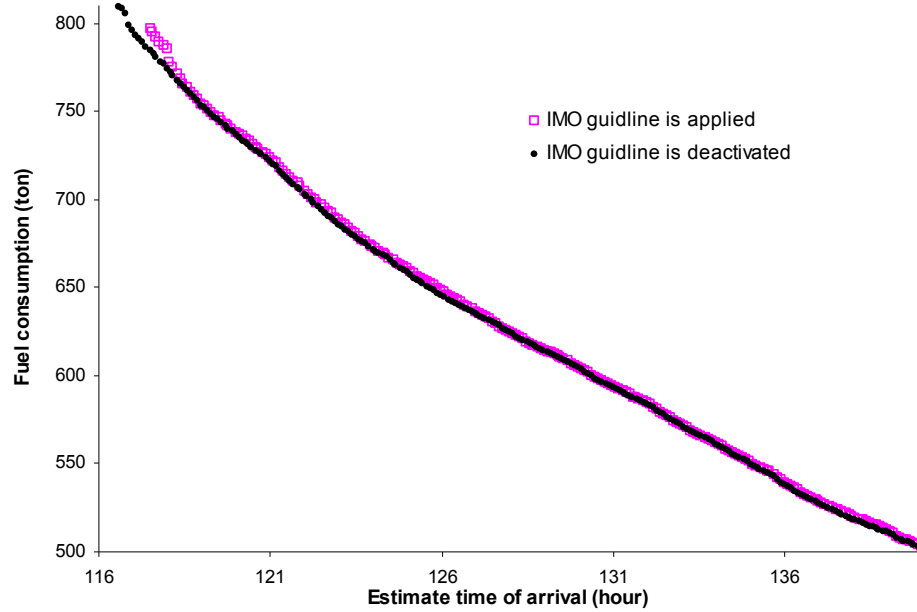


Figure 8.22 (b) Influence of the application of the IMO guidelines (wave height limit of 7.5 m)

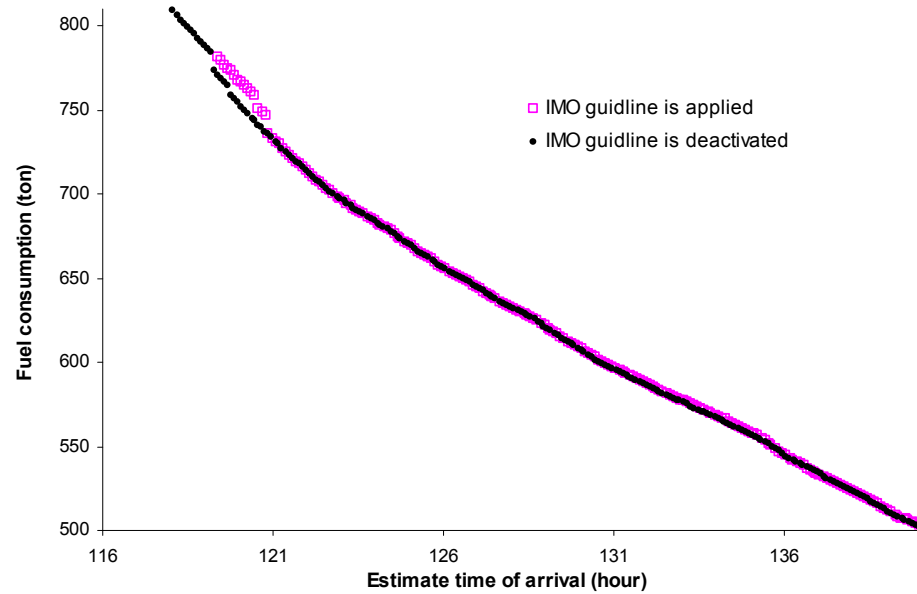


Figure 8.22 (c) Influence of the application of the IMO guidelines (wave height limit of 7 m)

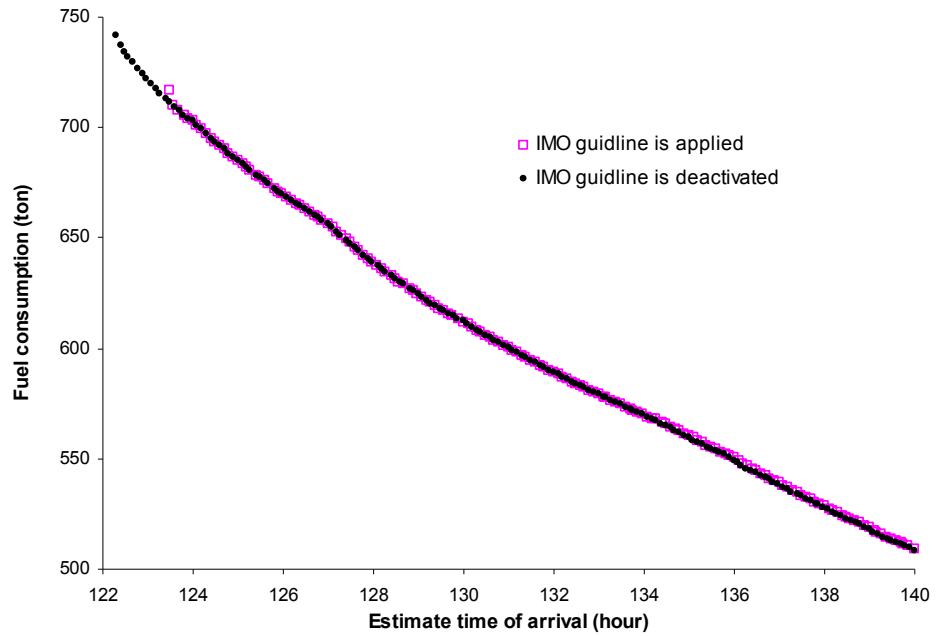


Figure 8.22 (d) Influence of the application of the IMO guidelines (wave height limit of 6.5 m)

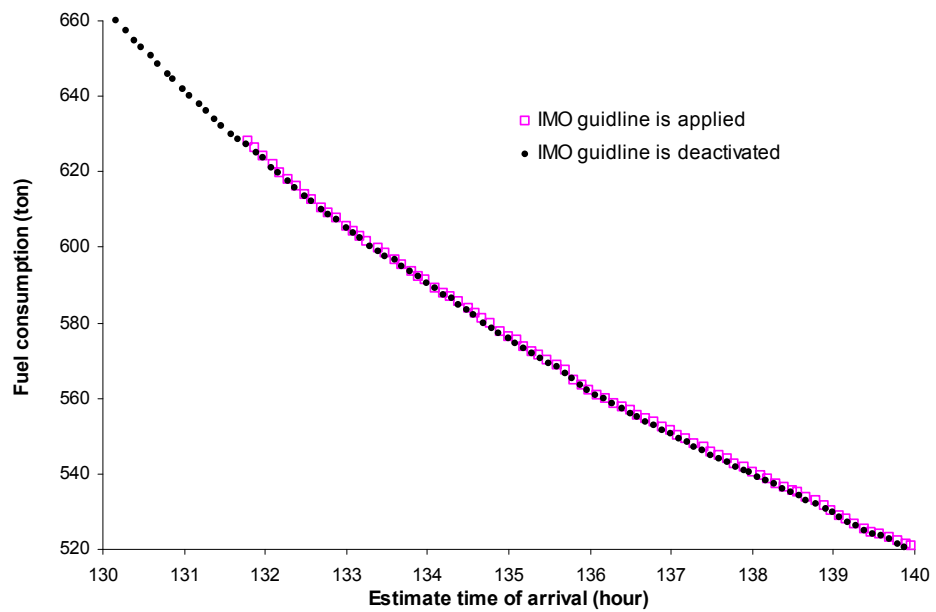


Figure 8.22 (f) Influence of the application of the IMO guidelines (wave height limit of 6 m)

Chapter 9.

CONCLUSIONS AND RECOMMENDATIONS FOR FURTHER WORK

9.1 Conclusions

The following conclusions can be drawn based on this research work as described above:

1. In this study, a novel three dimensional dynamic programming method (3DDP) was formulated to determine the optimised ship's course and its corresponding engine power for minimum fuel route. Compared with the traditional two dimensional dynamic programming (2DDP) which only optimises the ship's heading, while the engine power or propeller rotation speed is set as a constant throughout the voyage, this new method considers both the ship power settings and heading controls. The 3DDP method employs voyage progress as the stage variable together with the use of the forward algorithm. In the forward algorithm, the initial departure time is fixed; the arrival time at a location where the optimisation calculation has progressed to can be treated as a flexible parameter. This allows a set of route with a minimum fuel consumption to be obtained corresponding to different arrival times at the current location where the optimisation has been concerned. This is a logical process in line with the ship's operations along a voyage course. Compared with the use of time as the stage variable, the advantages of using voyage progress as the stage variable are a less finer grid system is required which will save much computing time. When voyage progress is chosen as the stage variable, the headings of the ship are pre-

defined by the grid points already, hence the engine delivery power becomes the only control variable. A float state technique is used by 3DDP to reduce the iteration on the process of optimisation for computing time saving. This novel 3DDP method could lead to a quasi-global optimal routing in comparison with the traditional weather routing methods.

2. A grid system which specifies the spatial and temporal layout of stages and states is needed by the 3DDP method in the algorithm calculation. A new automatic creation method for the grid system is presented in this study. This new technique requires only few parameters to define a route which makes the grid construction understandable and easy to tune. Unmeaning states in every stage in the grid system will be deleted to reduce the computing time in this algorithm.
3. In addition to the 3DDP method, three multi-objective evolutionary algorithms (MOEAs) are also applied for weather routing by treating it as a multi-objective and constrained optimisation problem. In the comparison with the parameters used by 3DDP method, much more parameters setting are needed by the genetic algorithm. These more parameters definitely give some inconvenience to the operator, and how to set these parameters gives another problem. The other disadvantage of the genetic algorithm is that this method is a kind of stochastic method and cannot ensure the same results can be achieved in every run.
4. A simpler and easier approximate method established by Kwon (2008) is used for the prediction of involuntary drop in speed in irregular waves and wind and an IMO guideline is employed to ensure ship safety during the voyage. The adoption of these two simplification processes ensures the program is performed in a reasonable computing time and is practically used onboard.

5. The OpeNDAP technology is employed to provide a transparent and free access to the distributed online oceanographic and meteorological datasets.
6. Based on the ship performance algorithm, environmental data and optimisation algorithm, a weather routing model was constructed and according to all this knowledge, an intelligent tool for energy efficient and low environment impact shipping software (ITEES) was developed during this research. As an onboard software, ITEES emphasises on solving the minimum fuel route by considering the weather conditions, ship engine characteristics, ship hydrodynamic responses in different weather conditions and their impact on fuel consumption. It can advise ship operators with shipping courses, engine power/speed in advance of and also during a voyage. Following the instruction offered by the system will ensure ship's fuel consumption is minimal, whilst increasing the ship's safety and reducing CO₂ emissions.
7. The case studies demonstrated that, in medium sea conditions route optimisation is not necessary and the shortest route with constant engine power can be used for real navigation. However, route optimisation is absolutely necessary in rough sea states not only for fuel saving but, most importantly, for ensuring ship safety during a voyage. Among the optimisation algorithms evaluated by the research, the 3DDP can give a better performance for fuel saving than other methods. In addition, it has the characters of using straightforward theory and less parameter settings compared with MOEAs, making the 3DDP method easy and convenient for operators onboard to use.
8. The limit of wave height has a great affect on the optimised results but the influences of the application of IMO guidelines are not obvious unless considering the time minimum route. Even so, as ship safety is the first considerable factor and more important compared with fuel consumption for ship weather routing it is strongly advised to employ the IMO guidelines or

other constraint conditions to ensure the ship safety during the optimisation process.

9.2 Recommendations for further work

1. The sophisticated ship performance database is required for further work. The ship performance responses to different sea conditions can be investigated in three ways: a) numerical simulation; b) experiment in towing tank tests; c) data analysis according to the data recorded by the ship response monitor system onboard. The ship specific responses and behaviour should be added to a database and then used by ITEES. The wave effects on the performance of the propeller should also be considered in order that more accurate engine power estimation can be made.
2. The current influence as an important factor for weather routing in certain sea areas should also be considered in the future.
3. Additional safety constraint conditions such as slamming, deck wetness, propeller racing, motion sickness and other hazards in adverse weather should be considered in future studies.
4. The parallel techniques can be applied on ITEES to reduce the computing time.
5. ITEES will be installed in several ships for validation and software tuning.

Reference

Adda, J, Cooper, R.(2003) *Dynamic Economics*. Massachusetts: MIT Press.

Aligne, F., Papageorgiou, M. and Walter, E. (1998) ‘Incorporating Power Variations Into Weather Routing and Why It May Lead to Better Results’. *Ifac Control Applications in Marine Systems*, Fukuoka, Japan, pp. 269-274.

Bellman, R.E. (1957) *Dynamic Programming*. Princeton: Princeton University Press.

Benedict, E.K. et al. (2008) *Development of ARROW software for decision support to avoid roll resonance and wave impact for ship operation in heavy seas*. Available at <http://212.201.38.20/siw/paper/heft6/benedict1> (Accessed: 28 November 2011).

Bijlsma, S.J. (1975) *On Minimal-Time Ship Routing*. PhD Thesis. Royal Netherlands Meteorological Institute, Delft University of Technology.

Bijlsma, S.J. (2001) ‘A Computational Method for the Solution of Optimal Control Problems in Ship Routing’. *Navigation*, 48 (3), pp. 145-154.

Bijlsma, S.J. (2002) ‘On the Applications of Optimal Control Theory and Dynamic Programming in Ship Routing’. *Navigation*, 49 (2), pp. 71-80.

Bijlsma, S.J. (2004) ‘A Computational Method in Ship Routing Using the Concept of Limited Maneuverability’. *Journal of Navigation*, 57 (3), pp. 357-369.

Bleick, W.E. and Faulkner, F.D. (1965) 'Minimal-Time Ship Routing'. *Journal of Applied Meteorology*, 4 (2), pp. 217-221.

Bullo, F., Lewis A.D. (2004) *Geometric Control of Mechanical Systems: Modeling, Analysis, and Design for Simple Mechanical Control Systems*. Springer.

Buttazzo, G. and Fredian, A. (2009) 'Variational Analysis and Aerospace Engineering'. *Springer Optimization and Its Applications*.

Calvert, S. (1990) *Optimal Weather Routeing Procedures for Vessels on Trans-Oceanic Voyages*. PhD Thesis. Polytechnic South West.

Calvert, S., Deakins, E. and Motte, R. (1991) 'A Dynamic System for Fuel Optimisation Trans-Ocean'. *Journal of Navigation*, 44 (2), pp.233-265.

Chen, H. (1978) *A Dynamic Program for Minimum Cost Ship Routing Under Uncertainty*. PhD Thesis. Dept. of Ocean Engineering, Massachusetts Institute of Technology.

Chen, H., Cardonne, V. and Lacey, P. (1998) 'Use of Operation Support Information Technology to Increase Ship Safety and Efficiency'. *SNAME Trans.* 106, pp.105–127.

Chen, R., Zou, Y. and Hou, S. (2011) 'Energy Management Strategy for Hybrid Electric Tracked Vehicle Based on Dynamic Programming'. *Electrical Engineering and Control, Lecture Notes in Electrical Engineering*, 98, pp843-851.

Coello, C.A. et al. (2007) *Evolutionary Algorithms for Solving Multi-Objective Problems*. New York: Springer

Cornillon, P. et al. (2003) 'OPeNDAP: Accessing Data in a Distributed, Heterogeneous Environment'. *Data Science Journal*, 2, pp. 164-174.

Dadebo, S.A, Mcauley, K.B. (1995) 'Dynamic optimization of constrained chemical engineering problems using dynamic programming'. *Computers & Chemical Engineering*, 19(5), pp. 513–525.

Darwin, C. (1895) *The Origin of Species*. London: John Murray.

De Wit, C. (1968) *Mathematical Treatment of Optimal Ocean Ship Routing*. PhD Thesis. Delft University of Technology.

De Wit, C. (1990) 'Proposal for Low Cost Ocean Weather Routeing'. *Journal of Navigation*, 43 (3), pp. 428-439.

Deb, K. (2001) *Multi-Objective Optimisation using Evolutionary Algorithms*. New York: Wiley, pp. 518.

Deb, K, et al. (2002) 'A fast and elitist mult-objective genetic algorithm: NSGA-II'. *IEEE Transactions on Evolutionary Computation*, 6, pp. 182-197.

Eiben, A.E. and Smith, J.E. (2003) *Introduction to evolutionary computing*. Springer.

ESRI (1998) *Esri Shapefile Technical Description*. Available at <http://www.esri.com/library/whitepapers/pdfs/shapefile.pdf> (Accessed: 28 November 2011).

Froude, W. (1955) 'The Papers of William Froude Trans'. *RINA*.

GMN (n.d.) *GFS/AVN vs. Wwave3 GRIB Files*. Available at http://www.globalmarinenet.com/grib_whatism.htm (Accessed: 28 November 2011).

Hagiwara, H. and Spaans, J.A. (1987) 'Practical Weather Routeing of Sail-Assisted Motor Vessels'. *Journal of Navigation*, 40, pp. 96-119.

Hagiwara, H. (1989) *Weather Routing Of (Sail-Assisted) Motor Vessels*. PhD Thesis. Delft University of Technology.

Haltiner, G.J., Hamilton, H.D. and Arnason, G. (1962) 'Minimal-Time Ship Routing'. *Journal of Applied Meteorology*, 1 (1), pp. 1-7.

Harries, S., Heinmann, J. and Hinnenthal, J. (2003) 'Pareto-Optimal Routing Of Ships'. *International Conference on Ship and Shipping Research*, Palermo.

Harries, S., Hinnenthal, J. (2004) 'A Systematic Study on Posing and Solving the Problem of Pareto Optimal Ship Routing'. *3rd International Conference on Computer Applications and Information Technology in the Maritime Industries*, Siguenza, Spain.

Hinnenthal, J. (2010) *Robust Pareto-Optimum Routing of Ships Utilising Deterministic and Ensemble Weather Forecasts*. PhD Thesis. Technische Universität Berlin.

Holtrop, J. and Mennen, G.G.J. (1978) 'A Statistical Power Prediction Method'. *International Shipbuilding Progress*, 25, October, 1978.

Holtrop, J. and Mennen, G.G.J. (1982) 'An Approximate Power Prediction Method'. *International Shipbuilding Progress*, 29, July, 1982.

Holtrop, J. (1984) 'A Statistical Re-Analysis of Resistance and Propulsion Data'. *International Shipbuilding Progress*, 31, November, 1984.

IMO (2007) *Revised Guidance to the Master for Avoiding Dangerous Situations in Adverse Weather and Sea Conditions*, Msc / Circ. 1228.

International Chamber of Shipping (2009) *Shipping, World Trade and the Reduction of CO₂ Emissions* [Online]. Available at: <http://www.shippingandco2.org/CO2%20Flyer.pdf> (Accessed: 28 November 2011).

James, R.W. (1957) *Application of wave forecasts to marine navigation*. Washington DC: Navy Hydr. Office.

Klompstra, M.B. et al. (1992). 'The Isopone Method in Optimal Control'. *Dynamics and Control*, 2 (3), pp. 281-301.

Kwon, Y.J, (2008) 'Speed Loss Due to Added Resistance in Wind and Waves'. *The Naval Architect*, 3, pp.14–16.

Marie, S. and Courteille, E. (2009) 'Multi-Objective Optimization of Motor Vessel Route'. *8th International Symposium on Marine Navigation and Safety of Sea Transportation*, Gdynia, Poland, pp.411-418.

Motte, R.H. and Calvert, S. (1990) 'On the Selection of Discrete Grid Systems for On-Board Micro-Based Weather Routing'. *The Journal of Navigation*, 43, pp. 104-117.

Osborne, P. (2008) *The Mercator Projections*. Available at <http://mercator.myzen.co.uk/mercator.pdf> (Accessed: 10 January 2013).

Osyczka A. (1985) 'Multi-Criteria Optimisation for Engineering Design'. In *Design Optimization*, Gero John S (Ed.), New York: Academic Press, pp.193-227.

Padhy, C.P, Sen, D. and Bhaskaran, P.K. (2008) 'Application of wave model for weather routing of ships in the North Indian Ocean'. *Nat Hazards*, 44, pp. 373–385.

Panigrahi, J.K. and Umesh, P.A. (2008) 'Minimal Time Ship Routing Using IRS-P4 (MSMR) Analyzed Wind Fields'. *Marine Geodesy*, 31, pp.39–48.

Perakis, A.N. and Papadakis, N.A. (1990) 'Deterministic Minimal Time Vessel Routing. Operations Research', 38 (3), pp. 426-438.

Raquel, C.R and Naval, P.C. (2005) 'An Effective Use of Crowding Distance in Multi-objective Particle Swarm Optimisation'. *In Proc. of Genetic and Evolutionary Conference*, pp. 257–264.

Rawson, K.J., Tupper, E.C. (2001) *Basic ship theory. [Volume 2]. Ship dynamics and design*. Boston: Butterworth-Heinemann.

Samsung Heavy Industries Co. LTD (n.d.) *Samsung-sulzer Engine Repor*.

Samsung Shipbuilding and Heavy Industries (1996) *Hull Form Study For SAMSUNG 54,000 DWT Container*.

Sgouros, T. (2004) *OPeNDAP User Guide Version 1.14*. Available at <http://www.opendap.org/user/guide-html/guide.html> (Accessed: 28 November 2011).

Spaans, J.A. (1995) 'New Developments in Ship Weather Routing'. *Navigation*, 169, pp. 95-106.

Spaans, J.A. and Peter, Stote. (2000) 'Shipboard Weather Routing'. *Proceedings of the IAIN World Congress and the 56th Annual Meeting of The Institute of Navigation*, San Diego, CA, June.

Szłapczyńska, J. and Smierzchalski, R. (2007) 'Adopted Isochrones Method Improving Ship Safety in Weather Routing With Evolutionary Approach'.

International Journal of Reliability, Quality and Safety Engineering, 14(6), pp. 635-645.

Szłapczyńska, J. and Smierzchalski, R. (2009a) 'Multi-criteria Optimisation in Weather Routing'. *8th International Symposium on Marine Navigation and Safety of Sea Transportation*, Gdynia, Poland, 2009, pp. 423-429.

Szłapczyńska, J. (2009b) *Application of Evolutionary Algorithms and Ranking Methods to the Weather Routing For Ships with Hybrid Propulsion*. PhD Thesis. Zachodniopomorski University of Technology.

Tolman, H.L. (2009) 'User Manual and System Documentation of WAVEWATCH-III version 3.14'. *NOAA / NWS / NCEP / OMB*, Technical Note pp. 276.

V. Pareto. (1896) *Cours d'économie politique*, Lausanne, Switzerland.

Van Manen J.D and Van Oossanen, P. (1988) *Principles of Naval Architecture, Propulsion*. s, Jersey City: Society of Naval Architects and Marine Engineer.

Vessel Optimization and Safety System. (2010) Available at: <http://www.ocean-systems.com/VOSS.htm> (Accessed: 29 November 2011).

WMO (2010) *NCEP WMO GRIB2 Documentation*. Available at http://www.nco.ncep.noaa.gov/pmb/docs/grib2/grib2_doc.shtml (Accessed: 28 November 2011).

WMO (n.d.) *Sea state*. Available at http://en.wikipedia.org/wiki/Sea_state (Accessed: 28 November 2011).

Zitzler, E. (1999) *Evolutionary Algorithms for Multi-objective Optimization: Methods and Applications*. PhD Thesis. ETH Zurich, Switzerland.

Appendix A.

PRINCIPAL DIMENSIONS OF THE HULL FORM OF THE CASE SHIP

| Designation | Symbol | Unit | Value |
|------------------------------|--------|----------------|---------|
| Length between perpendicular | LPP | m | 261.2 |
| Beam | B | m | 40 |
| Depth | D | m | 24.3 |
| Number of propeller | NOPROP | - | 1 |
| Draft (normal) | T | m | 12.5 |
| Length of water line | L | m | 260.55 |
| Wet surface area | S | m ² | 12449.0 |
| Displacement volume | DISV | m ³ | 76250 |
| Block coefficient | CB | - | 0.5836 |
| Load waterline coefficient | CW | - | 0.7940 |
| Mid-ship section coefficient | CM | - | 0.9826 |
| Prismatic coefficient | CP | - | 0.5939 |

Appendix B.

USER MANUAL OF ITEES

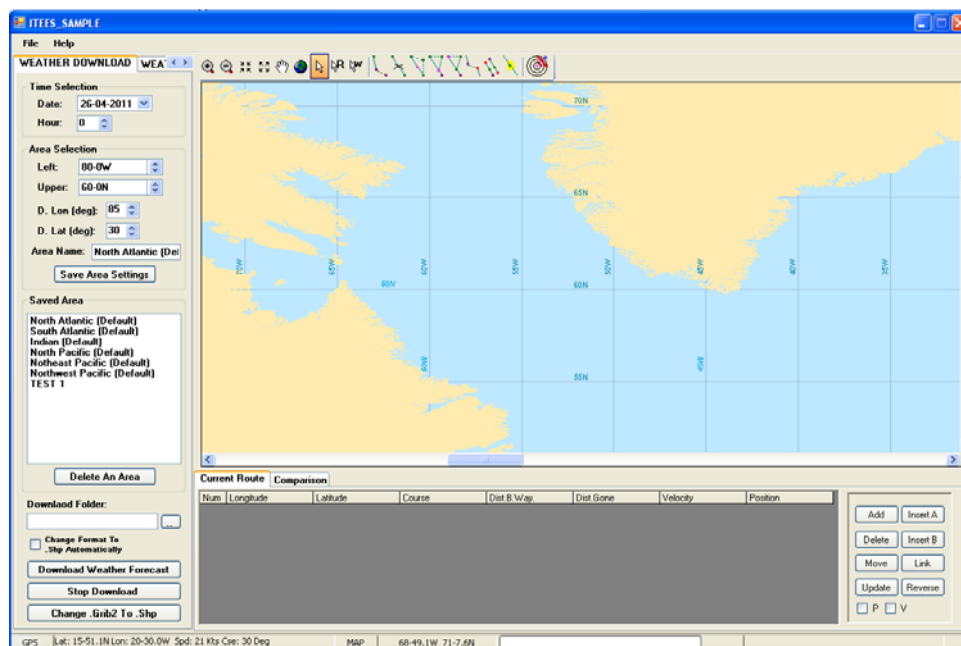
B.1 Weather forecast download

ITEES can allow the operator to free download the weather forecast directly from the NOMADS (National Oceanic and Atmospheric Administration Operational Model Archive Distribution System). The weather forecast is based on WAVEWATCH III model. The properties of this model are:

- Providing 180 hours' forecast.
- Coverage from 77°S - 77°N.
- The resolution is 1.25°x1°
- Including wind direction (degree), wind speed (m/s), wind speed component in true north direction (m/s), wind speed component in true east direction (m/s), significant wave height (m), mean wave direction (degree), mean wave period (s), peak wave direction (degree), peak wave period (s), wind sea direction (degree) corresponding wind sea period (s).
- With a 3 hours time step.
- The weather forecasts are generated 4 times a day.
- The weather forecasts are only for ocean waters.

The weather forecast is described by the GRIB format. GRIB (GRIdded Binary) is in a mathematically concise data format commonly used in meteorology to store historical and forecast weather data. It is standardized by the World Meteorological Organization's Commission for Basic Systems. Almost every conceivable weather and ocean data variable is available in the GRIB format. It can store the weather forecast as numbers on longitude/latitude using the binary format to minimize the file size, so it is very convenience to download ocean weather forecasts via wireless which is bandwidth limited.

The weather forecast download module in the module tab is mainly used for weather forecast download. A screen of the weather forecast download module is shown in below.




B.1.1 Select the time of the weather forecast

Click “Date” time picker in “Time Selection” to choose the starting date of the weather forecast. The date with the blue back ground indicates the current date.

Time Selection

Date: 26-04-2011

Hour: 

Area Selection

Left:

Upper:

D. Lon (d):


D. Lat (d):

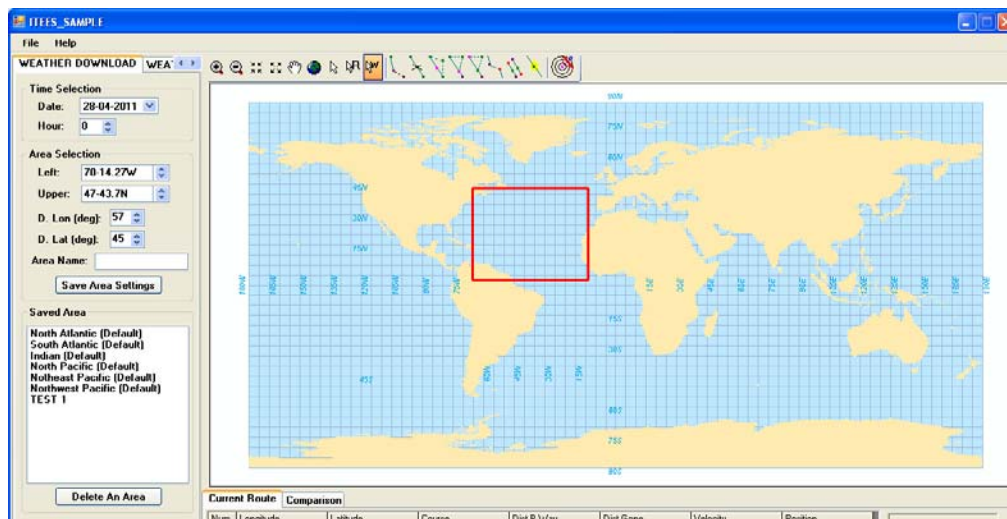
Today: 26/04/2011

Click “Hour” in “Time Selection” to choose the starting hour of the weather forecast. The weather forecasts are issued 4 times every day at GMT 00:00, 06:00, 12:00, 18:00 by NOAA (National Oceanic and Atmospheric Administration).

Hour:

B.1.2 Select the area of the weather forecast

Click “Select Weather Area” button in the tool bar. This button will be shown in highlight as . Then the operator can use the mouse to click and drag a red rectangle in the working space to cover an area in which the operator wants to download the weather forecast. The data in the “Area Selection” will be changed automatically to match the rectangle. When click “Select Weather Area” button again, this button can be shown in normal, and the red rectangle will disappear.



Area Selection

Left:

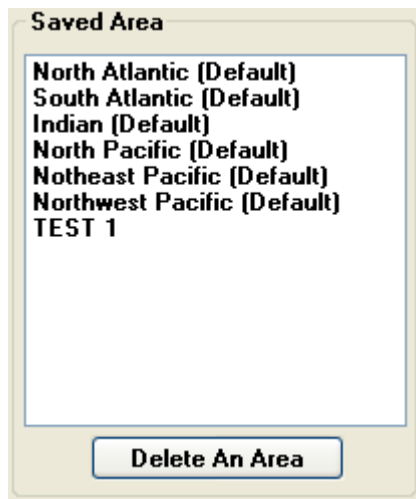
Upper:

D. Lon (deg):

D. Lat (deg):

Area Name:

In “Area Selection”, “Left” can control the longitude position of the left boundary of the rectangle and “Upper” decides the latitude position of the upper boundary of the rectangle “D. Lon (deg)” is the width of the rectangle and “D. Lat (deg)” is the height of the rectangle. The operator can also use these four numerical up-down widgets to set the size and position of the rectangle and the rectangle in the working space will be changed simultaneously. After set the download area, the “Area Name” textbox names this area and the position attribution of this area can be saved in ITEES by clicking the “Save Area Settings” button. Then this saved area will be listed in “Saved Area” list box. Once the area is saved in ITEES, the saved area information will be stored when close ITEES, and they will be listed when open ITEES again.




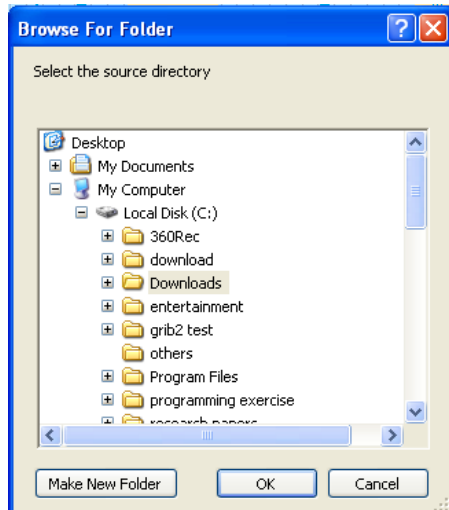
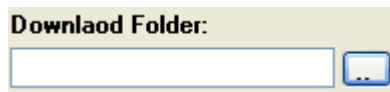
There are six default areas in ITEES which are most popular for operators to download the weather forecast. The operator can delete the selected area and its information in “Saved Area” list box by using “Delete an Area” button except for the default areas. When use the mouse to select an area, its position and size information can be shown in the correlative widgets in “Area Selection” and a corresponding red rectangle is drawn in the working space automatically.

The usage of “Left” and “Upper” numerical up down widgets are necessary to be presented here:


When the cursor is on the left of the hyphen, the up and down button can change the integer part of the value of longitude or latitude. When the cursor is between the hyphen and the letter, the up and down button can change the decimal fraction part of the value of the longitude and latitude. If the cursor is on the right of the letter, the up and down button can control the change between “W” and “E” for longitude and the change between “S” and “N” for latitude respectively, where the letters “W, E, N, S” mean the west longitude, the east longitude, the north latitude and the south latitude, respectively.

B.1.3 Select the down load folder


Click button , “Browse For Folder” dialog box is shown and enables the user to select a folder to which the weather forecast can be saved.



B.1.4 Download the weather forecast

After selecting the time, area and folder for the weather forecast. The weather forecast can be downloaded by clicking  button. Of course, the connection with the internet is necessary for downloading the weather forecast. The larger the area chosen the longer the time the download takes. If the chosen weather forecast is not available, a dialog will be shown as following.



Once the download begin, the text of  will be changed to display how many KB already be downloaded as shown like:

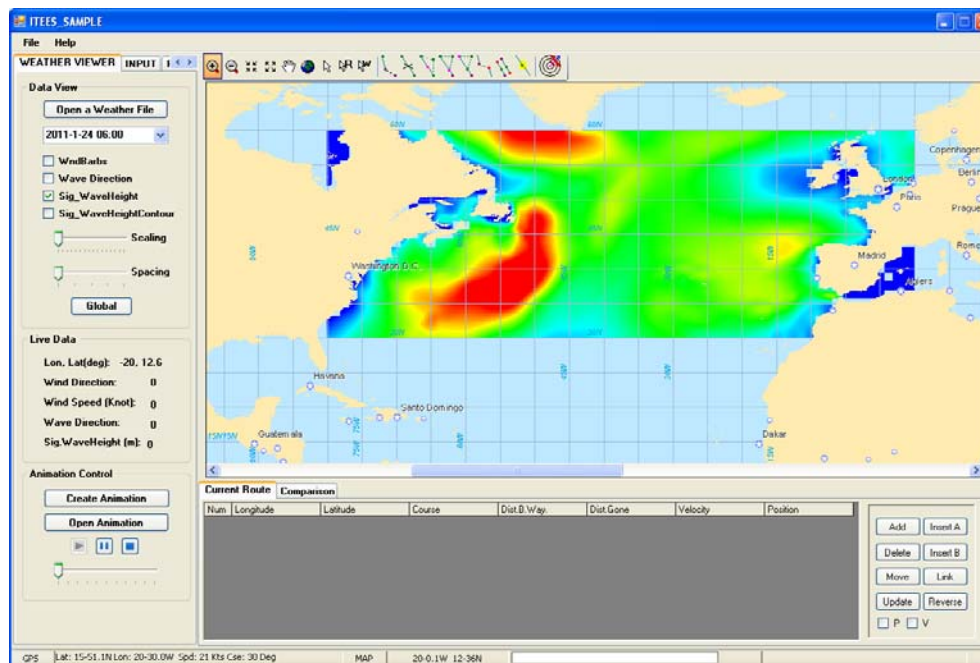
76KB

Click **Stop Download** can stop the download.

The download weather forecast file is described by Grib2 format, and must be converted to Shp format to be read by ITEES. Button **Change .Grib2 To .Shp** can be used to finish this transformation. If the checkbox **Change Format To .Shp Automatically** is checked, this format transformation will be performed automatically once the weather forecast download is finished.

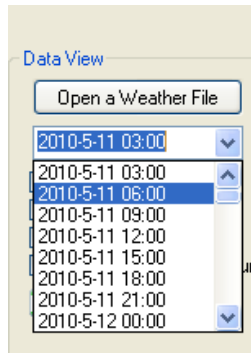
B.2 View weather forecast

The Weather Viewer as an important module of ITEES allows the operators to view the weather forecast which has been downloaded, to animate and transfer them into the dynamic programming module of ITEES for the optimisation of the route. A full screen of the Weather Viewer is shown in below.









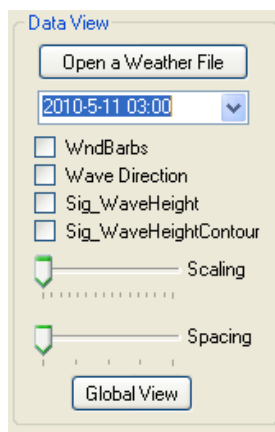
B.2.1 Load weather forecast

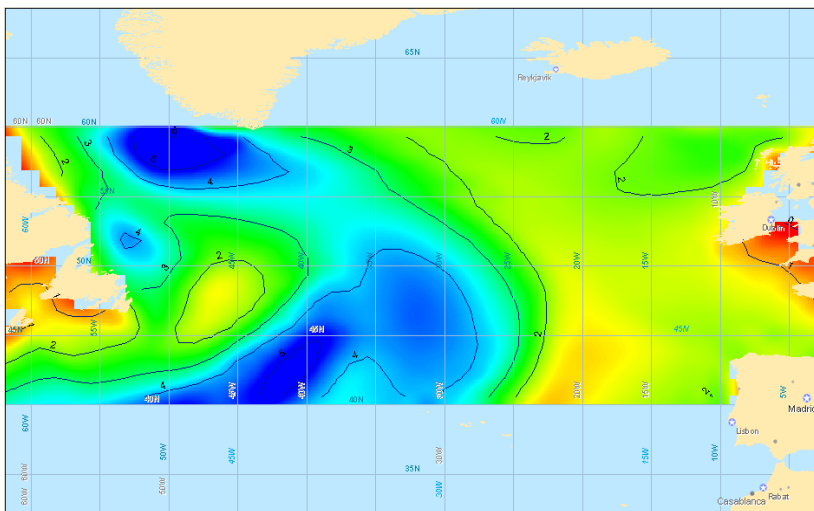
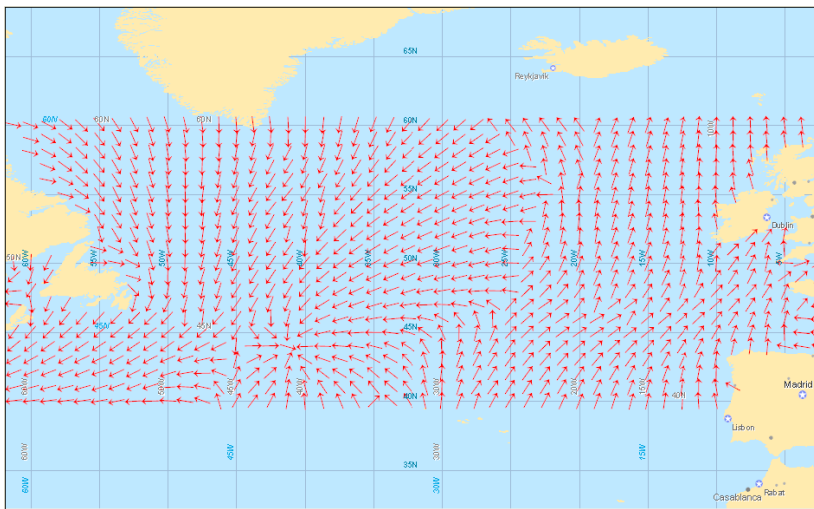
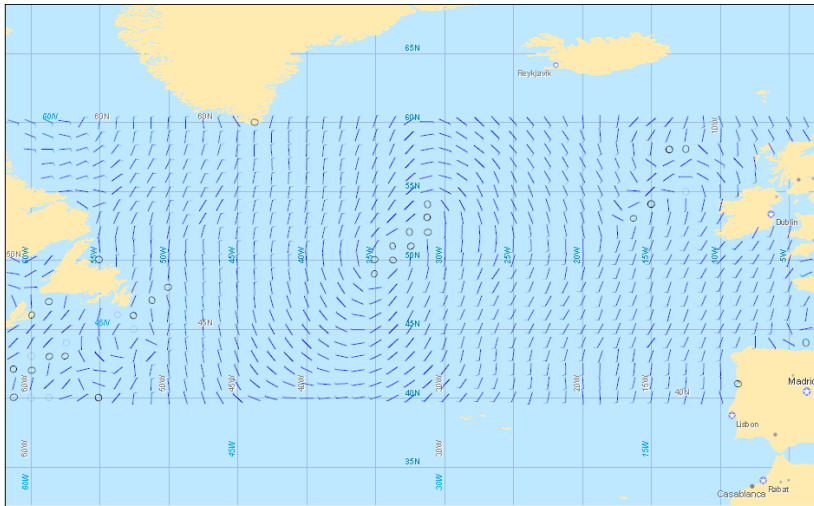
Click button **Open a Weather File** to load weather forecast to ITEES, once being loaded, the date and time of the weather forecast will be listed.



B.2.2 Select the display items

The check boxes decide whether or not to display the wind barbs, the wave direction, the significant wave height with colour filled and the significant wave height with contour lines. A red arrow is used for representation of the wave direction. The number on the contour line is the wave height, Some buttons in the tool bar like “Zoom In” , “Zoom Out” , “Fixed Zoom In” , “Fixed Zoom Out” , “Pan” , “Full extend”  are very convenient for operator to view the weather forecast.



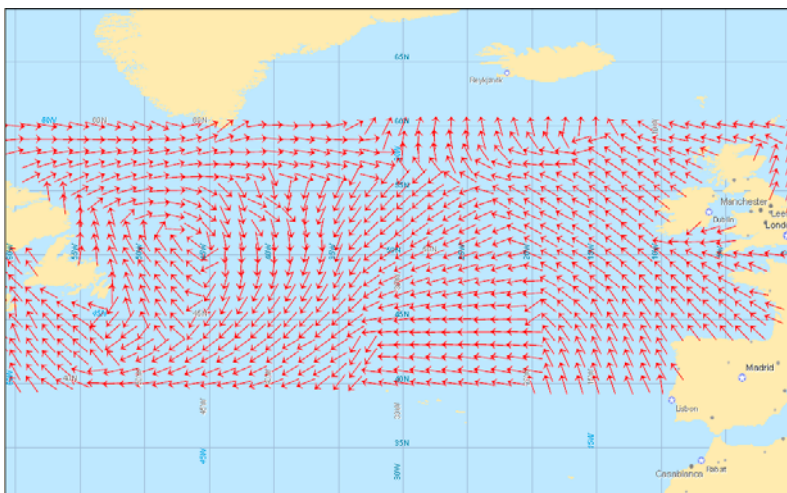


B.2.3 Change the scale and space of the wind barbs and wave arrow

The track bar “Scaling” can be used to decide the scale of the wind barbs and the arrow of wave direction.



The track bar “Spacing” can be used to decide the space of the wind barbs and the arrow of wave directions.



B.2.4 Weather parameters

“Live Data” displays the cursor position on the earth and the parameters of the weather forecast correspondingly.

Live Data

Lon, Lat(deg): -31.06, 48.88

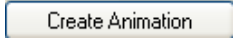
Wind Direction: 166.81

Wind Speed (Knot): 10.58

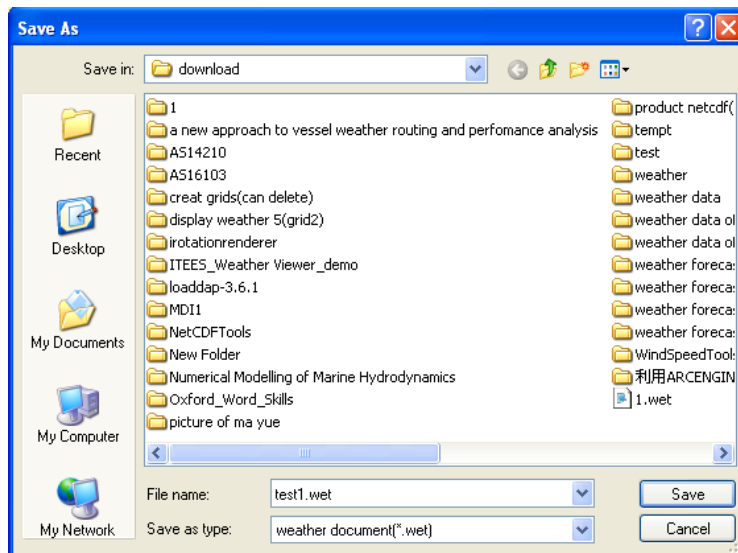
Wave Direction: 240.68

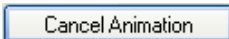
Sig_WaveHeight(m): 3.57

B.2.5 Create animation

Click the button . An animation file can be created according the weather forecast download.

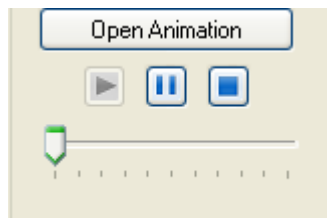
The animation can be saved as a file with the extension “.wet”



Click the button  to cancel the animation function.

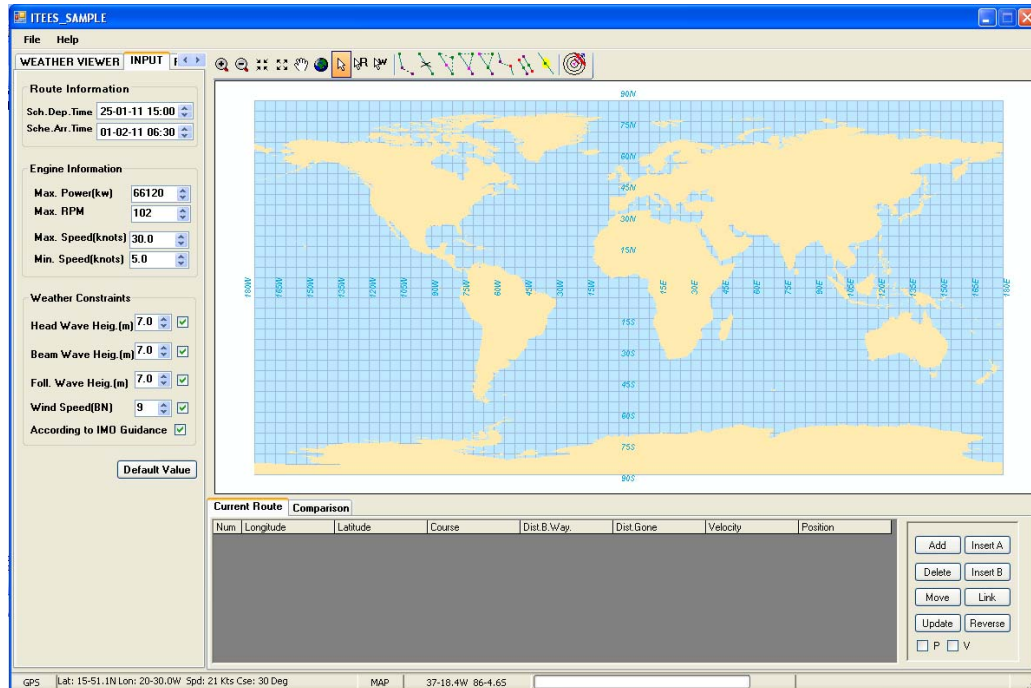
B.2.6 Display animation

Click the button “Open Animation” to display an animation file. The operator can start, pause or stop the animation; the operator can also choose the start point of the animation.



B.3 Set up the input module

The input module allows the operator to set ship departure and arrival time, engine information and weather constraints. A full screen of the Input Module is shown below.



B.3.1 Set departure and arrival time

The schedule departure and arrival time of the ship can be set by the time picker as below.

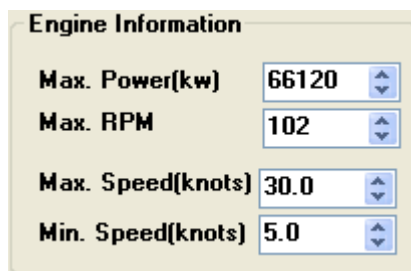
Route Information

Sch. Dep. Time

Sche. Arr. Time

B.3.2 Set engine information

The engine information includes the maximum continuous rating of the main engine, the maximum propeller rotation speed, the maximum and minimum allowed ship speed over the ground in calm water. These values will be treated as the constraints condition during the optimisation of the ship routing. “Max. Power” and “Max. RPM” should be determined in a consultation with engine specifications given in the engine operational manual. Engine should be not allowed to be overloaded to exceed the maximum value for ship safety concerns. “Max. Speed” and “Min. Speed” must be in the range of speed value of the resistance database file already input into ITEES. ITEES will search the optimal ship speed between the maximum and minimum speed value. The large the speed range is, the longer the computing time ITEES will take.

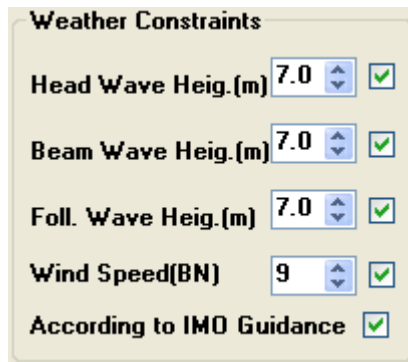


| Engine Information | |
|--------------------|-------|
| Max. Power(kw) | 66120 |
| Max. RPM | 102 |
| Max. Speed(knots) | 30.0 |
| Min. Speed(knots) | 5.0 |

B.3.3 Set weather constraints

The Weather Constraints screen window is where the operator enters the environment constraints to be applied to the passage under planning. It allows the operator to specify sea wave height limit in different directions and the wind speed limit that the operator wants to avoid. The operator also can choose the IMO “Guidance to the master for avoiding dangerous situations in adverse weather and sea conditions” to ensure the ship safety during the voyage. There is a check box for each of the above listed items. If the operator removes the check mark from the check box, ITEES will no longer take this category into account during the route optimisation process. This will speed up program operation. With the limit values filled in the text box and check marks in the check boxes. The route optimised or simulated by ITEES will either avoid violating the constraints or inform the operator

that it is being exceeded. 7.0 meters of wind speed of all direction and 9 BN wind speed are the default constraint limits by ITEES.



| Constraint | Value | Checked |
|---------------------------|-------|---------|
| Head Wave Heig.(m) | 7.0 | Yes |
| Beam Wave Heig.(m) | 7.0 | Yes |
| Foll. Wave Heig.(m) | 7.0 | Yes |
| Wind Speed(BN) | 9 | Yes |
| According to IMO Guidance | | Yes |

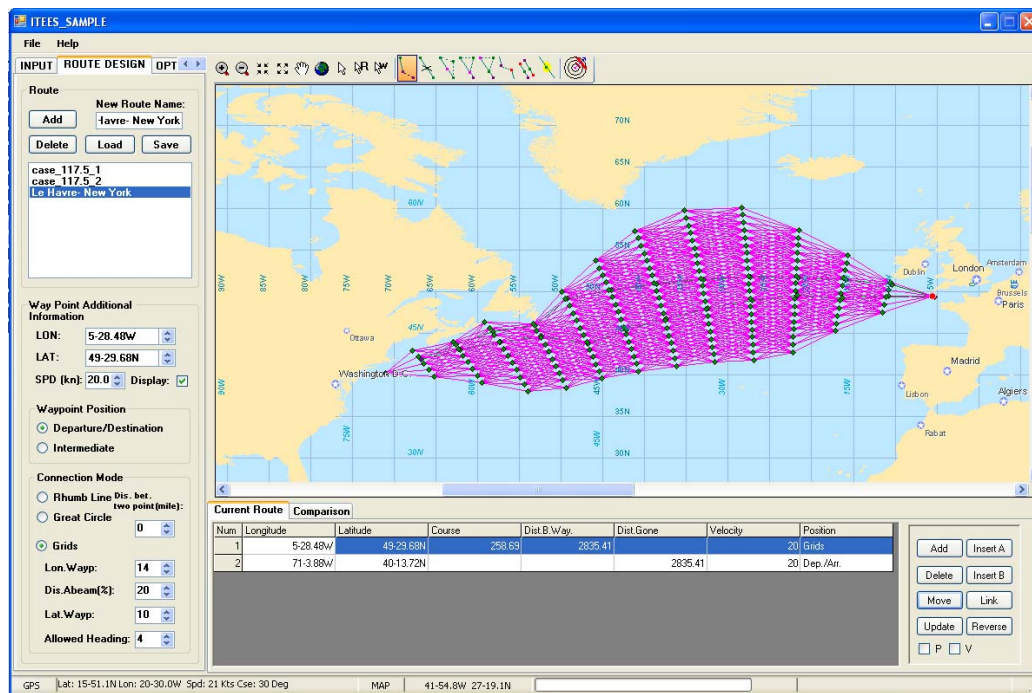
4. Route and grids design

There are three main functions of ITEES: A) Simulate a route. B) Optimise a route. C) Optimise a grid.

Detailed descriptions about the function A, B, and C will be given in section B.5, B.7 and B.8 respectively.

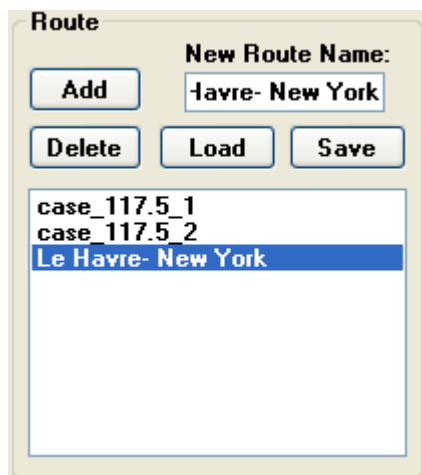
Before using function A and B a route must be designed by the operator. And a grids system is necessary before operation of function C. This section will present how to design a route and grids.

“Route Design” module is mainly a widget for the route and grids design. Beside this module, several buttons in “Tool Bar” and “Route Tab” are commonly used for this purpose. A full screen of the “Route Design” module is shown below.

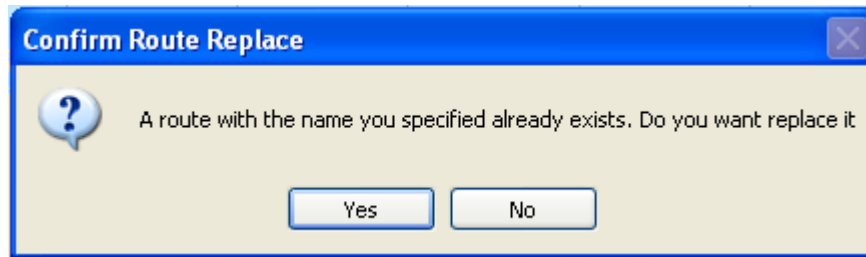


B.4.1 Add a new route

Before add a new route, the operator must name the new route in the “New Route Name” text box. After click “Add” button, a new route will be list in the list box.





The name of the new route must differ from a route that already exists in the system. Otherwise, a message box will be shown as following. Click “Yes” button to replace the existent route with the new route or click “No” to give up the operation.



After add a new route, the new route will become the current route and its name will be highlighted in the route list. At present there is no waypoint on this route and the “Current Route” table in “Route tab” becomes blank. Here, the “current route” is the current chosen route or grids which ITEES will simulate or optimise for and all the route operations are just valid for the current route. That means that the operator can design many routes or grids using ITEES, but only the “Current Route” will be considered when operate simulation or optimisation function.

B.4.2 Add new way point for a route

Click add way point  button in the toolbox and then click select the way point  button, next, position the mouse pointer over the approximate location on the chart where the new added way point should be, after click the left mouse button, a new way point will be added on the current route. The operator can continue to use the mouse to position way points on the chart; a course line will connect the way points in the order when they have been positioned. If the route has already had some way points, the new way points will join the route after the last way point is set. After adding a new way point, the information of the new way point will be listed in the “Current Route” table, and the new added way point will be in the selecting status (see “select the way point” of this section)

| Current Route | | Comparison | | | | | | |
|---------------|-----------|------------|--------|-------------|-----------|----------|--------------|--|
| Num | Longitude | Latitude | Course | Dist.B.Way. | Dist.Gone | Velocity | Position | |
| 1 | 5-14.54W | 49-21.1N | | 271.86 | 216.46 | | 28 Dep./Arr. | |
| 2 | 10-47.06W | 49-28.12N | | 267.6 | 216.43 | 216.46 | 28 Dep./Arr. | |
| 3 | 16-19.3W | 49-19.06N | | 274.67 | 212.19 | 432.9 | 28 Dep./Arr. | |
| 4 | 21-44.69W | 49-36.35N | | 270.44 | 212.2 | 645.09 | 28 Dep./Arr. | |
| 5 | 27-12.22W | 49-37.99N | | 266.21 | 212.2 | 857.29 | 28 Dep./Arr. | |
| 6 | 32-38.35W | 49-23.95N | | 262.02 | 212.2 | 1069.49 | 28 Dep./Arr. | |
| 7 | 37-59.66W | 48-54.49N | | 257.95 | 212.19 | 1281.69 | 28 Dep./Arr. | |
| 8 | 42-12.88W | 48-12.12N | | 251.88 | 212.2 | 1493.88 | 28 Dep./Arr. | |

Information of the way point list includes the longitude, latitude of the location, the course to the next way point, the distance to the next way point, the distance already gone before this waypoint, the speed of the ship to the next way point (it is just used when simulating a route) and position information. The speed of the ship on the way point can be set by using **SPD (kn): 28.0** widget in “Way Point Additional Information” panel. Click on another item on the toolbox to turn off the “add new waypoint” function.

The above method is a quick way to add the way points, but it is not accurate to position the way points. There is another way that can be chosen to add a way point with an accurate position: direct set the accurate position of the way point in the position setting widget.

Way Point Additional Information


LON:

LAT:


And then click the “Add Way Point” button on the right of the “Current Route” table. By using this method, just one new way point can be added at a time.

For the way points on the chart, a red diamond indicates the first way point of the route, the black diamond indicates the last waypoint of the route and the green diamond indicates the intermediate way points.



B.4.3 Select the way point

The way point can be selected by clicking the left mouse button on the chart after clicking “Select Way Point” button  on the toolbox. The selected way point on the chart is indicated by pink colour and a blue band is drawn on the row which corresponds to the selected way point in the “Current Route” table. The operator also can select the way points by selecting multiple rows in the “Current Route” table. This allows the operator to select multiple way points one time.


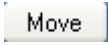
B.4.4 Delete a way point

After a way point on the chart or multiple way points by using the “Current Route” table has been selected, the operator can delete a way point by clicking the “Delete Way Point” button  or button on the right of the “Current Route” table. The information of the way points in the “Current Route” table will be update automatically.

B.4.5 Insert a way point

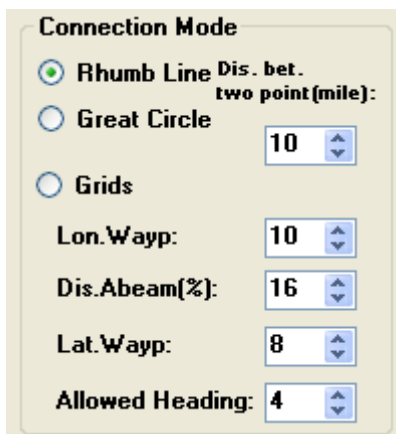
Additional way points can be inserted either before or after a selected way point. Select a way point first; click “Insert Way Point after Selected Way Point” button  or “Insert Way Point before Selected Way Point” button . Next, position the mouse pointer over an approximate location on the chart where the new added way point should be, after click the left mouse button, a new way point will be added after or before the selected way point on the current route. The operator can continue to insert new way points on the chart. After inserting new way points, the information of current route will be updated automatically in the “Current Route” table. The operator can also insert a way point with an accurate position value by using the way point position setting widget and then click (Insert Way Point after Selected Way Point) and (Insert Way Point before Selected Way Point) button.

B.4.6 Move a way point

Select the way point which is intended to be moved first, click move a way point  button, and then use the mouse to point a new position of the way point on the chart. The position of the way point also can be moved accurately: select a way point; set a new position value in position setting widget and then click  button. After moving a way point, the information of current route will be updated automatically in the “Current Route” table.

B.4.7 Use the “Connection Mode”

After setting the way points like adding, inserting deleting or moving the waypoint(s), the connection between the operating way point(s) and its adjacent way points can be performed by three “Connection Mode”: a) rhumb line; b) great circle; and c) grids. The detailed description of grids mode will be given in subsequent sections.



Connection Mode

Rhumb Line **Dis. bet. two point (mile):** 10

Great Circle

Grids

Lon. Wayp: 10

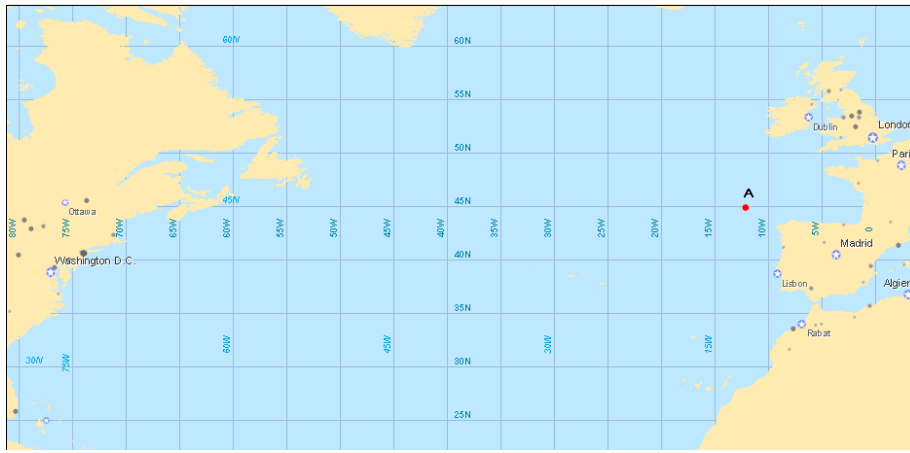
Dis. Abeam(%): 16

Lat. Wayp: 8

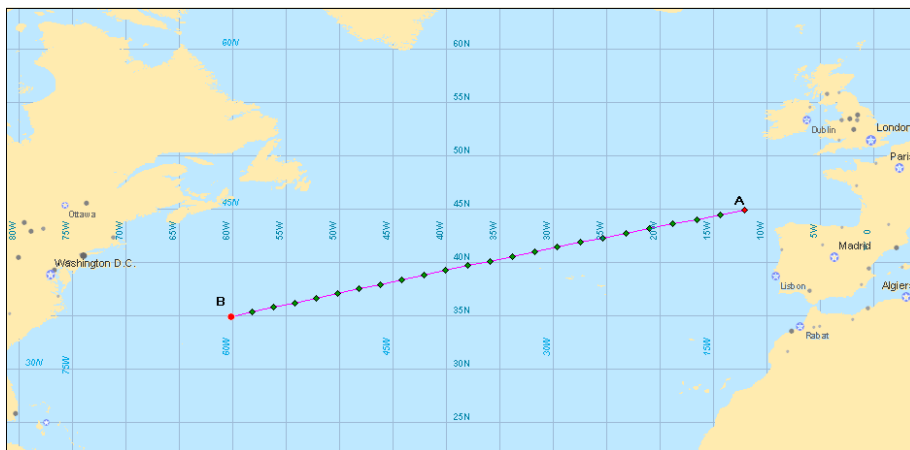
Allowed Heading: 4

When use the Rhumb line or great circle mode, the connection between the operating way point(s) and its adjacent way points will be separated into several sections and additional waypoints will be added in the route according to the value in the “Dis. Bet two points” numerical up down widget.

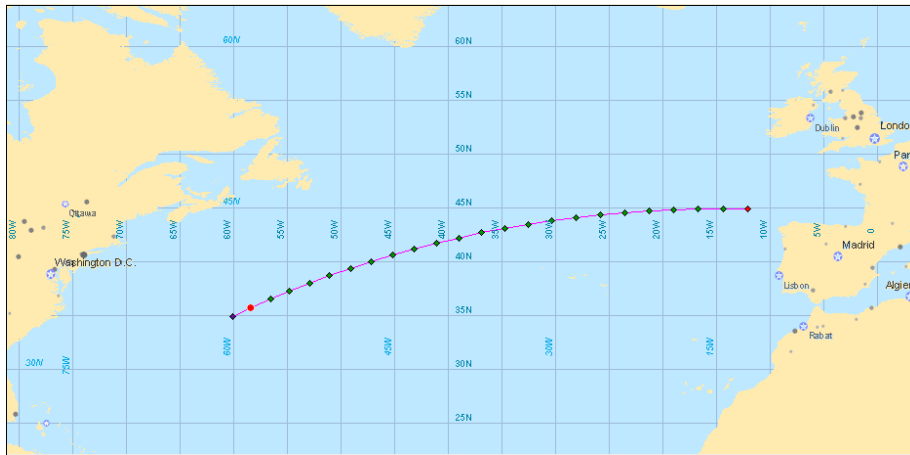
For example, the current route already has the first way point A as shown below.



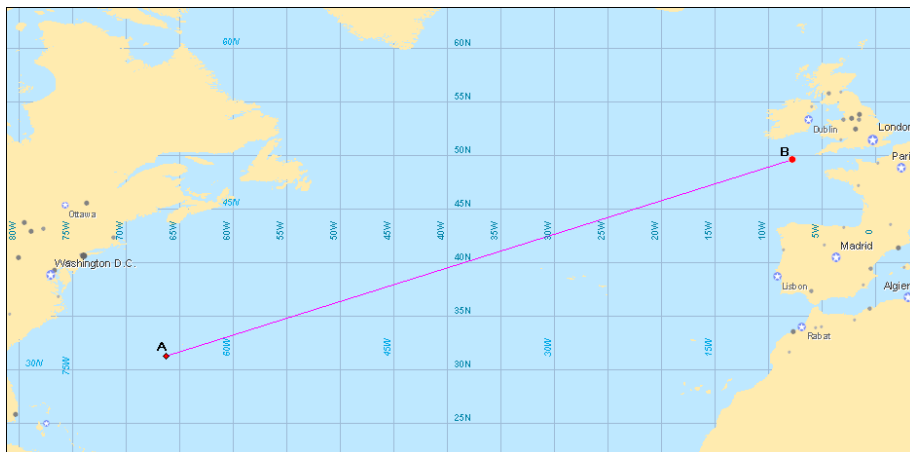
Chose the “Rhumb Line” mode and set the value of the distance between the two way points as 100 nautical miles, then add a new way point B at the end of the route. The connection between the way point A and B is a rhumb line and several additional way points will be inserted in this line with interval 100 nautical miles automatically.



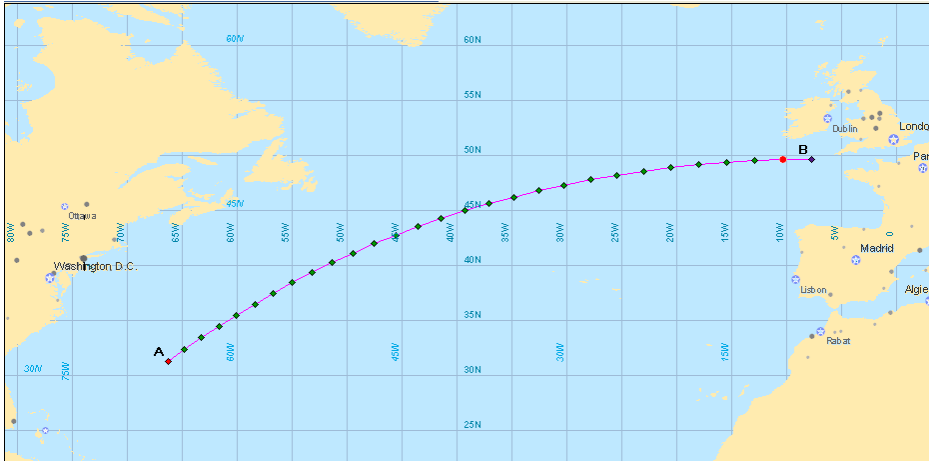
If “Great Circle” mode is chosen, the connection between way point A and B will be a great circle, and several additional way points will be inserted in this circle with interval 100 nautical miles. But the connection between the additional way points is the rhumb line.




For another example, the current route consists of two way point, the first way point is A and another way point is B as shown below.

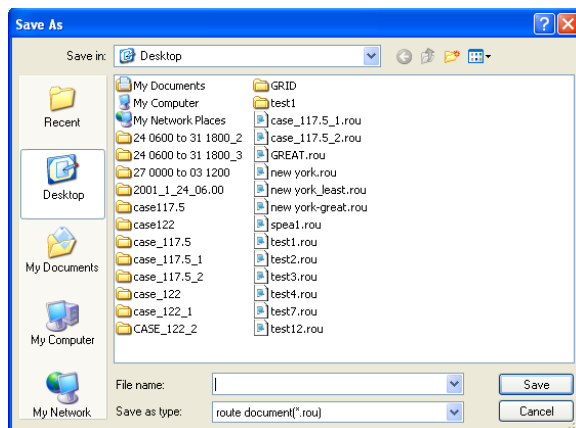



Select the first way point A, choose “Great Circle” mode, set the distance between the additional way points is 100 nautical miles, click the button, the current route will be shown as below.



B.4.8 Save as or load a route file

After completing a route design, the route can be saved as a file with suffix .rou file by using  button.



The route information also can be read from the route file by clicking the load  button. The new added route has the same name with the file.

B.4.9 Select a route

Many routes can be designed in ITEES, but only one can be treated as the current route. Use the mouse to choose an item in the route list to make it as the current route. The information of the chosen route will be listed in “Current Route” table

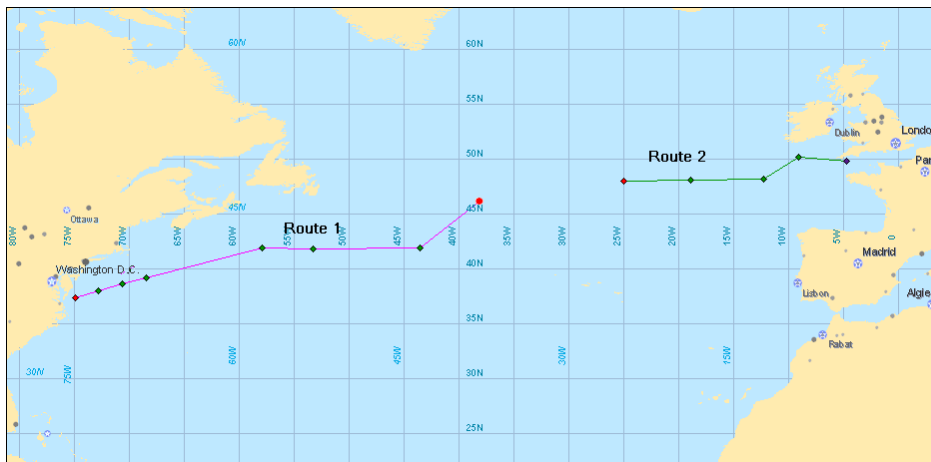
immediately. The connection line of the current route is in pink to differentiate with other routes in green.

B.4.10 Hide or display a route

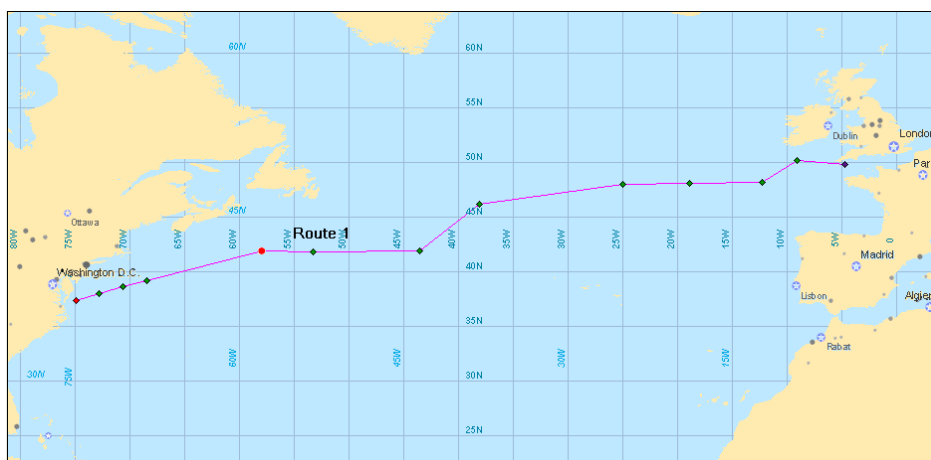
Many routes on the chart may give some inconvenience for the operator. The display check box **Display:** allows the operator to hide or display the current route.



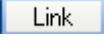
B.4.11 Link two routes

ITEES allows the operator to link two existent routes. For an example, route 1 and route 2 are already designed by the operator as shown below.


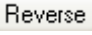


Chose route 1 as the current route first, click the button  in the tool box or




button on the right of the “Current Route” table, the information  Please select the second route,click Esc to cancel will be given in the right corner of the status bar. Select Route 2 by using the mouse on the chart or by using the route list. Click button  or  button again. Route 2 will be copied and merged into Route 1 and the last way point of Route 1 is connected with the first way point of the copy of Route 2. Note that, Route 2 has no change after this operation.


B.4.12 Reverse a route

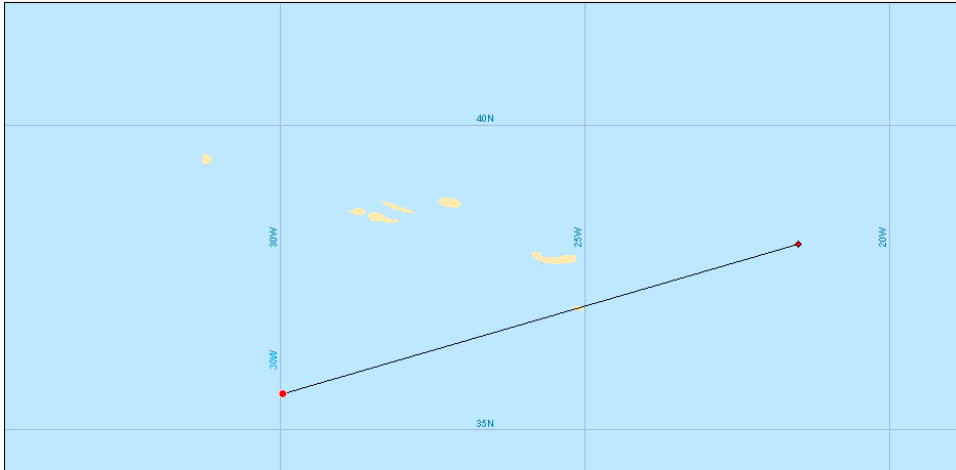
For a route designed in ITEES, the first way point of the route is the departure position, and last way point is the destination. The operator can use the “Reverse Route” button  or  button to reverse a route. After doing this operation, the sequence of the way point is reversed so that the former departure position of the route becomes the destination and the former destination becomes the departure position.

B.4.13 Delete a Route

Select a route first and then use the “Delete a Route”  button in “Route Design” module to delete a route.

B.4.14 Check a route

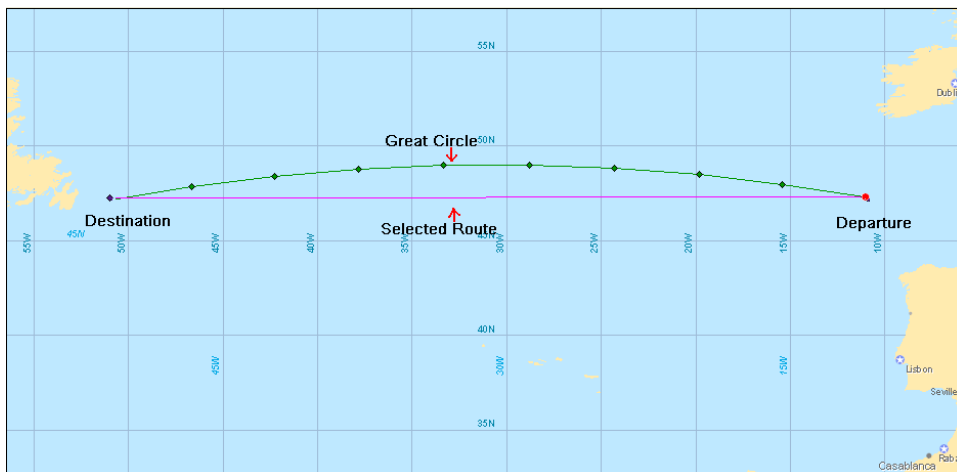
Some time, a designed route may cross an island which is not allowed in the navigation. Click “Check a Route” button . If the course line’s colour becomes black, it means that the route cross the land and is forbidden to be used in the navigation.



B.4.15 Create a grids system

A grids system is needed for optimising a grid function when using 3 dimensional dynamic programming (3DDP) method. The grids system makes up the boundaries within which the ship could be operated. The boundary can be treated as geographic constraints.

Select a route first. A route is needed to design a grids system as shown below. Choose one way point (it doesn't need to be the first way point of the current route) as the departure point of the grids.

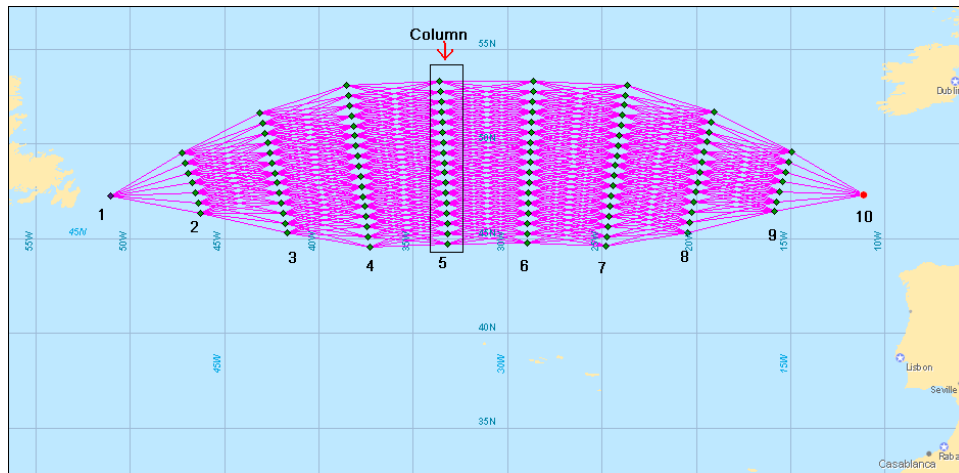


Grids
Lon. Wayp: 10
Dis. Abeam(%): 16
Lat. Wayp: 8
Allowed Heading: 4

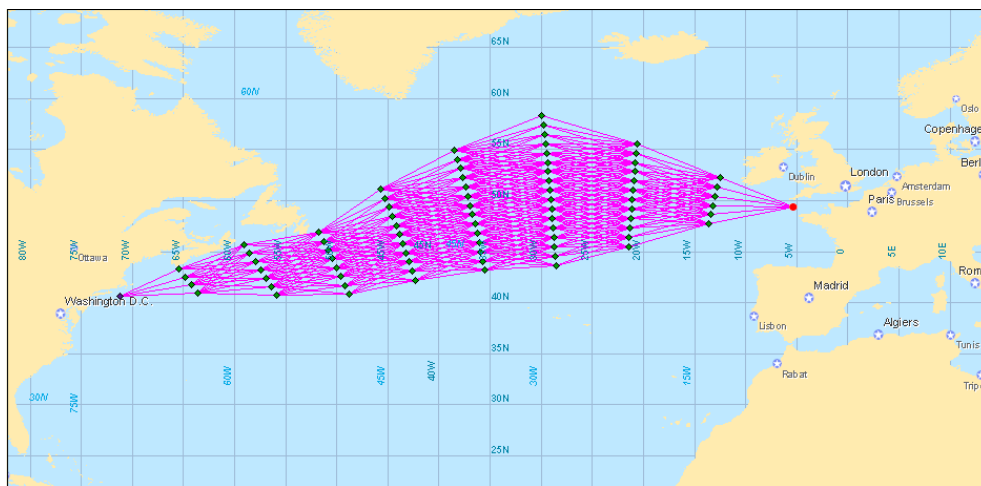
Choose “Grids” in “Connection Mode”, and then set the parameters for the grid design.

Since the great circle is the optimum route under calm water from the departure to the destination, it is chosen as a reference route for the construction of the grids. The grids are laid on both side of great circle according to the grids parameters. In one column, the grids are on a further great circle which perpendicular to the great circle between and destination.

“Lon. Wayp” is the column number of the grids. “Dist. Abeam” decides how many percent of the great circle the transverse scope of the grids from the great circle on either sides covered. It depends where the ship may pass to avoid a bad weather or sea conditions. “Lat. Wayp” is the maximum number of the grids lying on one side of the great circle. “Allowed Heading” decide the maximum number of tracks from one grid point to the next column grid points. Click “move” button, a grids system will be created and as shown below. In the current route table, the way points in which the item “Dep. / Arr.” is marked as the “Grids” indicated the departure way point of the grids.



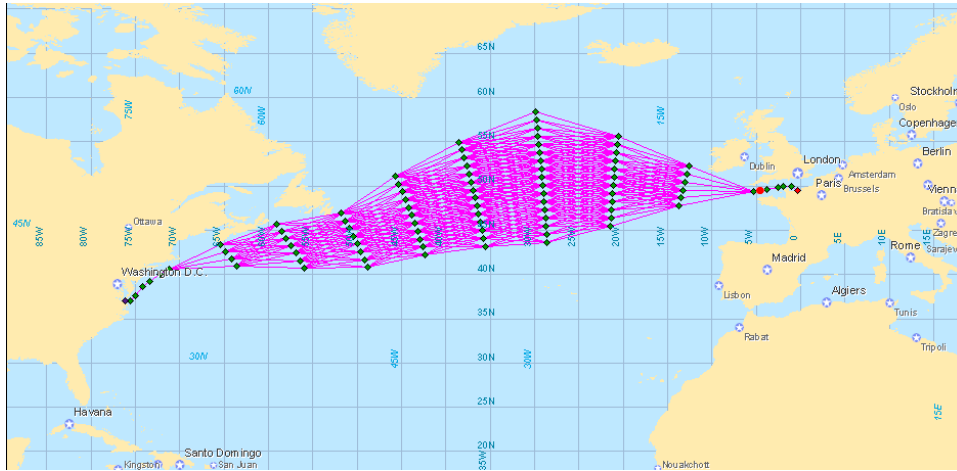
The grids or tracks, which cross island, will be deleted automatically by ITEES.



Generating grids is somewhat of a trial and error process. If a grids system that was automatically generated has too many gaps or open spaces, change the input parameters to generate another grids system. Too little number of column and (or) grids in one column and not enough “Allowed Heading” will result in to many gaps or open space in the grids. Too much number of column and (or) grids in one column and “allowed Heading” will make the mesh of a grid system too dense, as a result, too much time is needed to get an optimised route.

A grids system can also contain a single track lines at the departure or destination. The example below shows a grids system which was developed for a passage from

Le Havre to New York. This grids system is made up of two single tracks at the departure and destination which the operator wants to maintain and an expanded operating area cross the Atlantic which the operator want to stay within.



A grids system can be treated as the common route to do some route operations mentioned before, like “Select a Route”, “Hide or Display a Route”, “Link Two Routes”, “Reverse the Route”, and “Delete a Route”. Please note that, a grids system can only link with a single track, two grids systems cannot be link together.

B.5 Simulate a route

Simulation allows the operator to determine what effects the forecast weather will have on any route planned and what speed reduction would be required if the IMO guideline selected in the “Input” module are to be maintained and if the constraint condition could be maintained.

B.5.1 Select a route

Select a designed route which the operator wants to simulate as the current route. The first way point is the departure point and the last way point is the destination point.

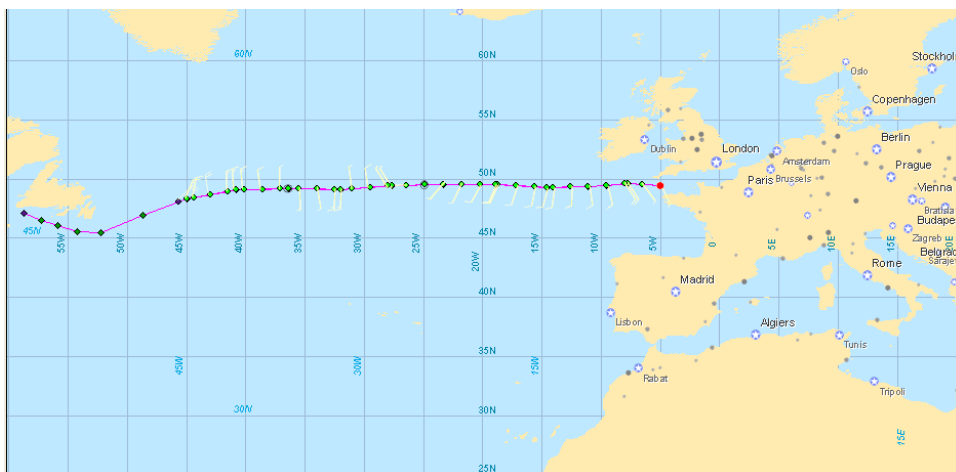
B.5.2 Specify the calm water ship speed

In “Current Route” table, “velocity” means the calm water ship speed which the operator plans the ship to sail between two adjacent way points. The specified calm water ship speed can be set by using **SPD (kn): 28.0** widget in “Way Point Additional Information” panel when adding the new way point. For a designed route, the “velocity” of the way point can also be updated by using the method below: specify the speed in **SPD (kn): 28.0** widget first; select the way point (s) in the chart or in the “Current Route” table; check the box which on the left of the “Current Route” table; after click the **Update** button, the speed of the selected way point(s) can be updated.

B.5.3 Simulation of the current route

Before simulate a route, must ensure that propeller file, resistance file and weather forecast are already downloaded into ITEES; the simulated route must be in the scope of the loaded weather forecast; the departure time set in the “Input” module should be in the time range of the loaded weather forecast.

Once the simulation process has been done, the “wind barbs” are displayed at every three hours increment along the simulated route to give the operator a quick indication of the wind direction and speed expected to be encountered. A “Route Information” window is also opened.



Click the **Simulate the current route** button to simulate the current route. If the simulation process cannot be finished for some reasons, the following prompt dialog box will be shown



And the “Wind barbs” will not be drawn along the route after the location where the constraint conditions could not be met.

B.6 Route information window

This window will display the simulation information of the route.

| Route Information | | | | | | | | | | | | | |
|---|----------|-----------|-----------|----------|---------|---------|-------|-----------|---------|-------|-------|------|-------|
| File | | | | | | | | | | | | | |
| Route name: <input type="text"/> Add to route design Add to compare <input type="text"/> Graphs Roll resonance | | | | | | | | | | | | | |
| Dep. time: 25-03:00 Arr. time: 29-12:00 Delay(hour): -78.5 ETA(hour): 81 Distance(nm): 1604.6 Fuel(ton): 288.9 Ave. speed(kt): 19.8 | | | | | | | | | | | | | |
| Ave./Max. W.S(kt): 17.5/41.3 W.S 34kt+(hour): 3 Ave./Max. W.H(kt): 2.7/7.7 W.H 4m+(hour): 6 W.H 8m+(hour): | | | | | | | | | | | | | |
| NUM | GMT | POSITION | | CSE(deg) | SPD(kt) | SHP(ps) | RPM | FUEL(ton) | DIS(nm) | WIND | | WAVE | |
| | | LN | LAT | | | | | | | kt | deg | m | deg |
| 1 | 25-15:00 | 4-59.17W | 49-26.01N | 276.1 | 20 | 27720.1 | 82.2 | | | 12.5 | 333.9 | 9 | 351.7 |
| | 25-18:00 | 6-30.78W | 49-32.41N | 276.1 | 20 | 27720.1 | 82.2 | 10.4 | 59.9 | 14 | 323.6 | 1.2 | 338.4 |
| | 25-20:24 | 7-44.64W | 49-37.55N | 263.9 | 19.7 | 27720.1 | 82 | 18.8 | 108 | 15.8 | 327.6 | 1.2 | 337.8 |
| 3 | 25-21:00 | 8-2.4W | 49-36.33N | 263.9 | 19.7 | 27720.1 | 82 | 20.8 | 119.6 | 15.8 | 327.6 | 1.2 | 337.8 |
| | 26-00:06 | 9-36.23W | 49-29.86N | 262.7 | 19.7 | 27720.1 | 82 | 31.5 | 180.8 | 16.9 | 346.8 | 1.3 | 354.1 |
| | 26-03:10 | 11-8.59W | 49-22.16N | 268.4 | 19.7 | 27720.1 | 82 | 42.2 | 241.4 | 16.6 | 351.7 | 1.4 | 354.9 |
| 4 | 26-06:00 | 12-34.36W | 49-20.57N | 268.4 | 19.7 | 27720.1 | 82 | 52 | 297.2 | 18.2 | | 2 | 354.9 |
| | 26-09:00 | 14-5.18W | 49-18.89N | 268.4 | 19.7 | 27720.1 | 82 | 62.4 | 356.5 | 18.7 | 7.7 | 1.8 | 1.1 |
| | 26-10:01 | 14-36.38W | 49-18.31N | 274.2 | 20.1 | 29683.1 | 83.8 | 65.9 | 376.8 | 18.2 | 15.4 | 1.8 | 7.4 |
| 5 | 26-12:00 | 15-37.07W | 49-21.19N | 274.2 | 20.1 | 29683.1 | 83.8 | 73.2 | 416.5 | 19.9 | 11.3 | 1.9 | 4.9 |
| | 26-15:00 | 17-9.65W | 49-25.58N | 274.2 | 20.1 | 29683.1 | 83.8 | 84.4 | 476.9 | 17.7 | 18.1 | 1.9 | 18.4 |
| | 26-18:00 | 18-42.37W | 49-29.98N | 274.2 | 20.1 | 29683.1 | 83.8 | 95.5 | 537.3 | 17.6 | 24 | 2.2 | 23.8 |
| 6 | 26-18:28 | 18-57.09W | 49-30.67N | 270.8 | 19.8 | 28199.4 | 82.4 | 97.3 | 546.9 | 17.5 | 23.3 | 2.1 | 271 |
| | 26-21:00 | 20-14.22W | 49-31.41N | 270.8 | 19.8 | 28199.4 | 82.4 | 106.2 | 597 | 15.7 | 29 | 2.5 | 270.7 |
| | 27-00:00 | 21-45.91W | 49-32.29N | 270.8 | 20.1 | 28199.4 | 82.7 | 116.7 | 656.5 | 14.2 | 25.6 | 2.7 | 262.8 |
| 7 | 27-03:00 | 23-19.12W | 49-33.19N | 267.5 | 20.2 | 29180.8 | 83.6 | 127.4 | 717 | 5.1 | 40.4 | 3.1 | 258.5 |
| | 27-06:00 | 24-52W | 49-30.59N | 267.5 | 20.1 | 29180.8 | 83.5 | 138.3 | 777.3 | 3.5 | 92.8 | 3.3 | 257.2 |
| | 27-09:00 | 26-24.97W | 49-27.99N | 267.5 | 20.1 | 29180.8 | 83.5 | 149.2 | 837.8 | 5.2 | 88 | 3.4 | 258.3 |
| 8 | 27-11:26 | 27-40.72W | 49-25.87N | 264.2 | 20 | 27248.3 | 82 | 158.1 | 887.1 | 8.8 | 148.5 | 3.4 | 259.9 |
| | 27-12:00 | 27-57.66W | 49-24.76N | 264.2 | 20 | 27248.3 | 82 | 160 | 898.1 | 8.8 | 148.5 | 3.4 | 259.9 |
| | 27-15:00 | 29-29.34W | 49-18.73N | 264.2 | 19.6 | 27248.3 | 81.5 | 170.2 | 958.1 | 17.4 | 171.8 | 3.6 | 262.4 |
| 9 | 27-18:00 | 30-59.17W | 49-12.81N | 264.2 | 20 | 27248.3 | 82 | 180.5 | 1017.1 | 10.5 | 172.6 | 3.7 | 270.6 |
| | 27-20:00 | 32-1.7W | 49-8.78N | 271.1 | 19.4 | 27720.1 | 81.5 | 187.3 | 1057.1 | 25.6 | 2.9 | 3.8 | 278.9 |
| | 27-21:00 | 32-29.72W | 49-9.16N | 271.1 | 19.4 | 27720.1 | 81.5 | 190.7 | 1076.5 | 25.6 | 2.9 | 3.8 | 278.9 |
| 10 | 28-00:00 | 33-58.72W | 49-10.32N | 271.1 | 20 | 27720.1 | 82.2 | 201.1 | 1134.7 | 13.7 | 350.3 | 3.3 | 286.6 |
| | 28-03:00 | 35-30.28W | 49-11.51N | 271.1 | 20.1 | 27720.1 | 82.5 | 211.5 | 1194.5 | 7.7 | 357.1 | 2.8 | 272.1 |
| | 28-04:45 | 36-24.46W | 49-12.21N | 267.8 | 20.4 | 28686.3 | 83.5 | 217.6 | 1230 | 4.8 | 175.3 | 2.3 | 261.2 |
| 28-06:00 | 37-3.11W | 49-11.26N | 267.8 | 20.2 | 28686.3 | 83.2 | 222.1 | 1255.2 | 12.9 | 180.3 | 2.2 | 232 | |

B.6.1 General information

General information of the simulated route is listed in the window above.


| | | | | | | |
|------------------------------|---------------------|----------------------------|------------------|----------------------|------------------|----------------------|
| Dep. time: 25-03:00 | Arr. time: 29-12:00 | Delay(hour): -78.5 | ETA(hour): 81 | Distance(nm): 1604.6 | Fuel(ton): 288.9 | Ave. speed(kt): 19.8 |
| Ave./Max. W.S(kt): 17.5/41.3 | W.S 34kt+(hour): 3 | Ave./Max. W.H(kt): 2.7/7.7 | W.H 4m+(hour): 6 | W.H 8m+(hour): | | |

General information includes departure time of the route, arrival time of the route, delayed hours, estimated time of arrival, total distance of the route, fuel consumption during the route, average speed of the ship, average and maximum speed of the wind, the en-route time of the wind speed more than 34 knot, average and maximum wave height, the en-route time of the wave height more than 4m and 8m.

B.6.2 En-route information

The en-route information is listed in a table of the window. This table displays the ship performance and weather condition at the way point locations and sub way point locations among which there are three hours segment along the planned route. The en-route information includes the predicted arrival time and position of (sub) way point, ship course, ship speed, engine delivery power, propeller rotation speed to the next (sub) way point, fuel consumption and distance from departure at this (sub) way point, wind speed and direction, wave height and direction at this (sub) way point. The row with a row number indicates this row is corresponding to the way point at that number, and the row without a number represents this row is corresponding to sub way points.

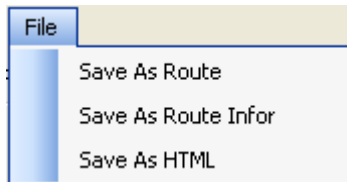
B.6.3 Select a way point or a sub way point on a simulated route

The way point or a sub way point on a simulated route can be selected by using the left mouse button after click the “Select Result Way point”  button in the tool box of the main window. The selected (sub) way point will be indicated by pink colour and the corresponding row in the en-route information table is highlighted by blue

colour. The way point or the sub way point of the simulated route can also be selected by clicking the corresponding row in the en-route information table.

B.6.4 Save a route

After click the “file” button in the upper right corner of the window, there three options for the operator to choose.



- “Save as Route” allows the operator to save the route as a “.rou” file which can be loaded in ITEES (discussed in section B.4). Only the position information of the way points is saved.
- When the operator is satisfied with a planned route, the en-route information can be saved by the “Save as Route Info” button as a “.roui” file. This file includes all the information of the simulated route and can be loaded in ITEES when use the “Compare Routes” function (Section B.9).
- “Save as HTML” saves the en-route information as a “.htm” file. This file can be read by any computer installed with web browser software.

Route Simulation Report

16/05/2011 21:15:03 By: master

Ship: APL England

Departure: 25/01/2011 15:00:00 Schedule: 01/02/2011 06:30:00 Early: 78.5 Hours

Total: 81 Hours, 1604.6 nm, 258.9 ton Average Speed: 19.8 knots

Ave./Max. Wind Speed: 17.5/41.3 knots Wind Speed 34knots+: 3.0 hours

Ave./Max. Wave Height: 2.7/7.7 m Wave Height 4m+: 6.0 hours Wave Height 8m+: 0.0 hours

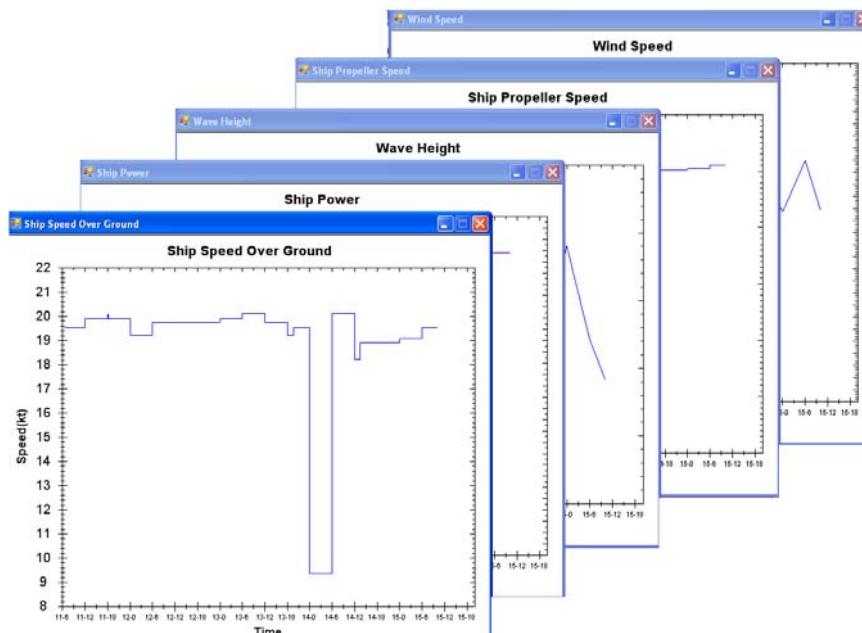
| WP # | GMT (dd hh:mm) | Latitude | Longitude | CSE (deg) | SPD (kt) | SHP (ps) | PRM | FUEL (ton) | DIS (nm) | Wi.Sp (kt) | Wi.Dir (deg) | Wa.H (m) | Wa.Dir (deg) |
|------|----------------|-----------|-----------|-----------|----------|----------|------|------------|----------|------------|--------------|----------|--------------|
| 1 | 25-15:00 | 4-59.17W | 49-26.01N | 276.1 | 20 | 27720.1 | 82.2 | | | 12.5 | 333.9 | 9 | 351.7 |
| | 25-18:00 | 6-30.78W | 49-32.41N | 276.1 | 20 | 27720.1 | 82.2 | 10.4 | 59.9 | 14 | 323.6 | 1.2 | 338.4 |
| 2 | 25-20:24 | 7-44.64W | 49-37.55N | 263.9 | 19.7 | 27720.1 | 82 | 18.8 | 108 | 15.8 | 327.6 | 1.2 | 337.8 |
| | 25-21:00 | 8-2.4W | 49-36.33N | 263.9 | 19.7 | 27720.1 | 82 | 20.8 | 119.6 | 15.8 | 327.6 | 1.2 | 337.8 |
| 3 | 26-00:06 | 9-36.23W | 49-29.86N | 262.7 | 19.7 | 27720.1 | 82 | 31.5 | 180.8 | 16.9 | 346.8 | 1.3 | 354.1 |
| 4 | 26-03:10 | 11-8.59W | 49-22.16N | 268.4 | 19.7 | 27720.1 | 82 | 42.2 | 241.4 | 16.6 | 351.7 | 1.4 | 354.9 |
| | 26-06:00 | 12-34.36W | 49-20.57N | 268.4 | 19.7 | 27720.1 | 82 | 52 | 297.2 | 18.2 | 2 | 1.6 | 354.9 |
| | 26-09:00 | 14-5.18W | 49-18.89N | 268.4 | 19.7 | 27720.1 | 82 | 62.4 | 356.5 | 18.7 | 7.7 | 1.8 | 1.1 |
| 5 | 26-10:01 | 14-36.38W | 49-18.31N | 274.2 | 20.1 | 29683.1 | 83.8 | 65.9 | 376.8 | 18.2 | 15.4 | 1.8 | 7.4 |
| | 26-11:00 | 14-27.07W | 49-17.10N | 274.2 | 20.1 | 29683.1 | 83.8 | 72.7 | 414.4 | 18.0 | 11.2 | 1.0 | 8.0 |

B.6.5 Add the optimised route to the “Route Design”

When use the “Optimise Grids” function, the optimised route with optimised speed can be determined by ITEES and the en-route information of the optimised route can be also shown by the “Route Information” window. The optimised route (Only the way points of the optimised route, exclude the sub way points) can be added in the “Route Design” module directly with the name specified in the textbox by clicking the button.

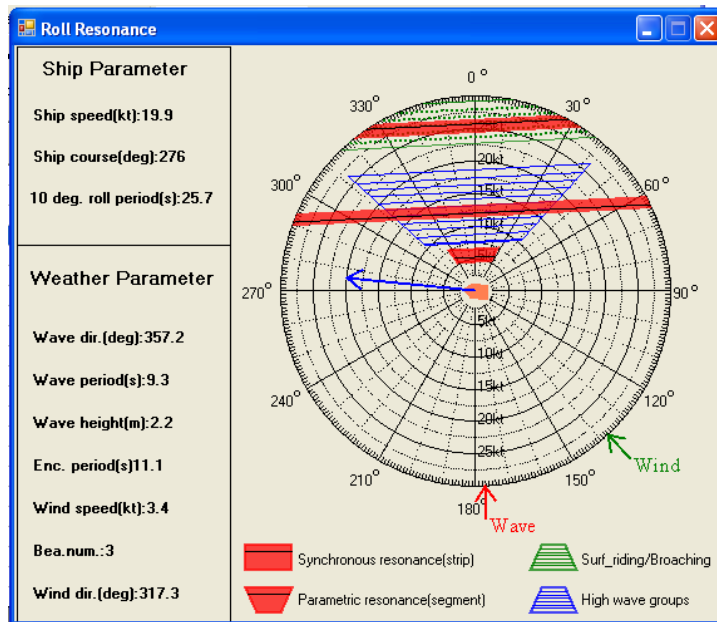
B.6.6 The route information displayed by a chart

Some route information which changes with time can also be displayed by a chart. Select the items to be displayed by using the drop-down list button on the top of the window, and then click the button, a chart will be shown. The format of the time in the chart is “Day / Hours”.



B.6.7 “Roll Resonance” polar diagram

Select a (sub) way point first, and then click the **Roll resonance** button, or select a (sub) way point first, click the right button of the mouse on the main window of ITEES, and then click **Roll Resonance** by using the left button of the mouse, the “Roll Resonance” polar diagram will be shown as below. This polar diagram can clearly display the potential dangers according to the ambient sea conditions around the ship.



B.6.8 Add the simulated route to “Compare Routes”

The operator can use the **Add to compare** button to add the simulated route to “Compare Routes” module. The compare program allows the operator to compare different simulated routes against each other. The detail description about “Compare Route” will be given in section B 9.

B.7 Optimise a route

When the operators “simulate” a route, ITEES attempts to reach, but not exceed, the calm water speed the operators have specified with the route plan. The specified calm water ship speeds are used as a reference only. When the operator uses the

“Optimise a Route” function of ITEES, ITEES tries to meet the schedule of arrival time the operator entered in the “Input” module disregarding the specified clam water ship speeds and insuring the calculated ship operations are optimised. Because of this difference, the operator may often find it is beneficial to “Optimise a Route”.

The “OPTIMUM_R” module in the module tab is mainly used for optimising a route. There are 5 methods allowing the operator to choose to optimise a route, including two dynamic programming methods, i.e. 2 dimensional dynamic programming (2DDP) and 3 dimensional dynamic programming (3DDP); and three evolution algorithms, i.e. NSGA II method, MOPSO_CD method, and SPEA method.

Optimize The Current Route

2DDP Method

3DDP Method

Time interval

Velocity interval

NSGA II Method

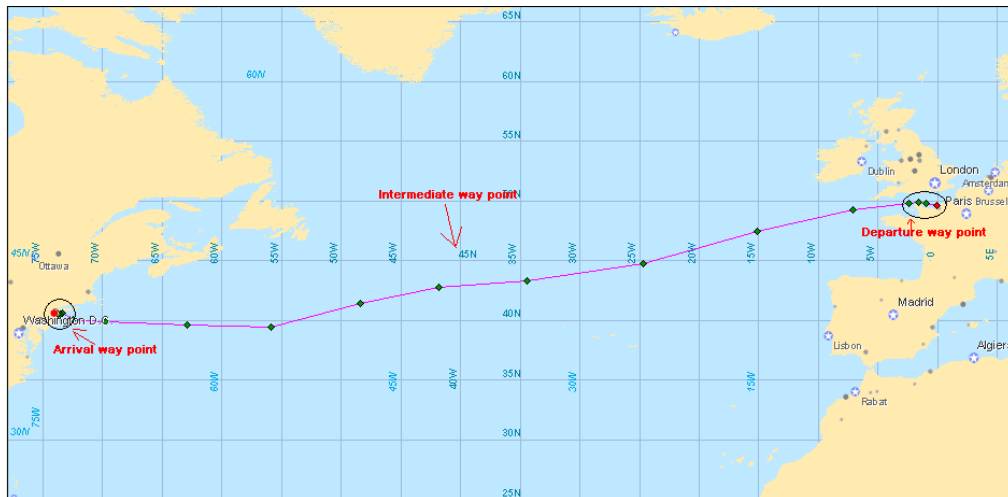
| | | |
|----------------------------------|----------------------------------|----------------------------------|
| Gen. | Pop. | Mut. |
| <input type="text" value="300"/> | <input type="text" value="300"/> | <input type="text" value="0.3"/> |
| Cro. | η_c | η_m |
| <input type="text" value="0.9"/> | <input type="text" value="20"/> | <input type="text" value="20"/> |

MOPSO_CD Method

| | |
|----------------------------------|----------------------------------|
| Gen. | Pop. |
| <input type="text" value="300"/> | <input type="text" value="300"/> |
| Mut. | Arch. |
| <input type="text" value="0.3"/> | <input type="text" value="500"/> |

SPEA Method

| | | |
|----------------------------------|----------------------------------|----------------------------------|
| Gen. | Pop. | Mut. |
| <input type="text" value="300"/> | <input type="text" value="300"/> | <input type="text" value="0.3"/> |
| Cro. | η_c | η_m |
| <input type="text" value="0.9"/> | <input type="text" value="20"/> | <input type="text" value="20"/> |



When use last four methods, the waypoints can be divided into three kinds: departure way point, intermediate way points and arrival way point. The departure and arrival way points are usually in the pilot time or estuary part of the route. The intermediate way points are usually in the open water area.

Specify the type of the way points:

- In “Route Design” module, select the type of way point by using the radio button in the “Waypoint Position” panel.



- Select the way points which the operator wants to specify the type on.
- Set the check box P (on the right side of “Current Route Table”) on, and then clicks the button. The type of the selected way point will be specified.


The default way point type is departure or arrival way point. The route certainly can just have the intermediate way points.

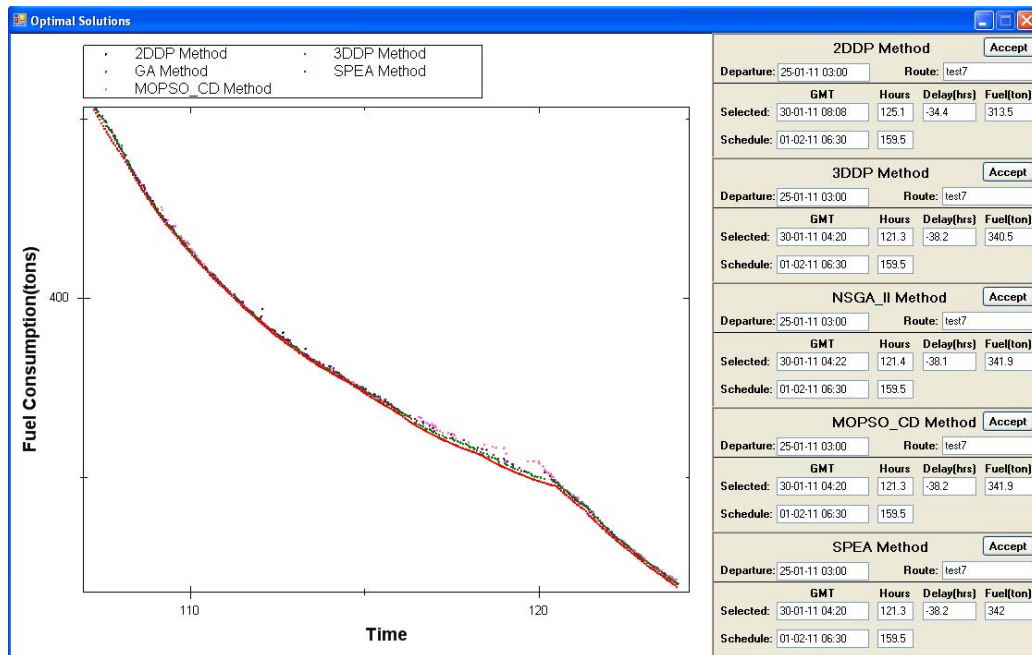
Set the parameters used in the optimisation algorithms:

When use the 2DDP method, no parameter is needed, but the accuracy are usually lower than other methods.

When use the 3DDP method, there two parameters need to be set: time interval and velocity interval. The maximum and minimum time interval are 2 and 0.1 hour respectively, and the maximum and minimum velocity interval are 1 and 0.1 knot respectively. The smaller parameter value is set, the better optimisation results can be got, certainly the more computing time it will used.

Like mentioned in “Simulate a Route”, before optimise a route the operator must ensure that propeller file, resistance file and weather forecast are already downloaded into ITEES; the route will be optimised must be in the scope of the loaded weather forecast; the departure time set in the “Input” module should be in the time range of the loaded weather forecast.

After set a route which needs to be optimised as the current route, and select an optimisation method, the operator can click the  button in “Optimise a Route” module, to run the optimisation process. The computing time depend on the total distance of the route, the waypoint numbers and the parameter settings. After the calculation is done, an “Optimal Solution” window will be shown as below.



The optimisation results are displayed in a diagram of this window. The horizontal axis presents the total en-route time and the vertical axis is the total fuel consumption of the route. Every point presents one optimisation solution and the colour of the point indicate which method is used to get this solution. All these solutions cover the time scope which has 12 hours before and after the schedule arrival time specified in the “Input” module. The operator can click the mouse and drag a rectangle on this diagram to change the display scope of the solution.

For 2DDP method, the maximum total solution number (using “maximum” because that there are maybe no solutions responding to certain ship speed which may violate the constraint conditions.) depends on the ship speed range specified in the “Input” module.

For 3DDP method, the difference between the arrival times of the solutions depends on the time interval set for this method.

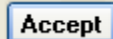

For NSGA II method, the total solution number is the population size set for this method.

For MOSP_CD method, the total solution number is the archive number set for this method.

For SPEA method, the total solution number is one fourth of the population size set for this method.

Generally speaking in a medium sea condition, the differences between the optimised results by each method are insignificant. But for a rough sea condition, the 3DDP method can show much more advantages in seeking the real global optimised.

Use the left button of the mouse to click on this diagram to select solutions. The information of these solutions will be displayed in the textboxes on the right side of this diagram. This information includes the departure time, the arrival time of the solution, schedule arrival time, fuel consumption and en-route time of the solution and so on.

Click  button, the “Route Information” window about the selected solution will display, and the route with the wind barbs is shown on the chart. This window displays the predicted performance on each 3 hour segment of the optimised solutions. The operator can do some operations for this route by using “Route Information” window as mentioned in last section. Once the “Route Solution” window is closed, the operator can use  button redisplay it.

B.8 Optimise grids

By using “Optimise Grids” function, the optimised course and ship engine power can be got. Under these optimised controls, the ship can arrive at the destination on time with minimum fuel consumption, and at the same time the constraint conditions can be satisfied for ship safety consideration.

The “OPTIMUM_G” module in the module tab is mainly used for optimise grids. Like “Optimise a Route”, the same methods and parameters setting can be used in this function.

Optimize The Current Ggrids

2D Method
 3D Method

Time interval

Velocity interval

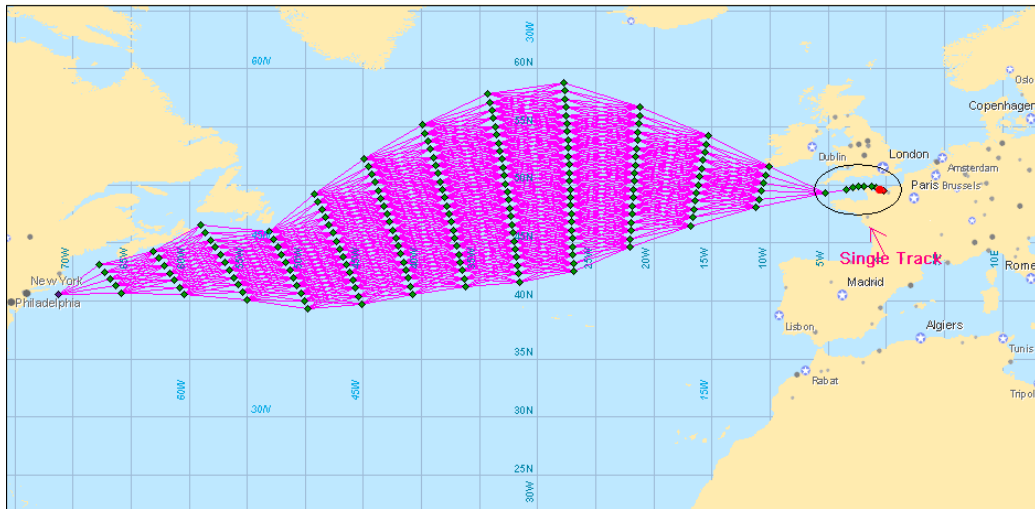
Using 2D Method as The Initial Population

NSGA II Method
 Gen. Pop. Mut.
 Cro. η_c η_m

MOPSO_CD Method
 Gen. Pop.
 Mut. Arch.

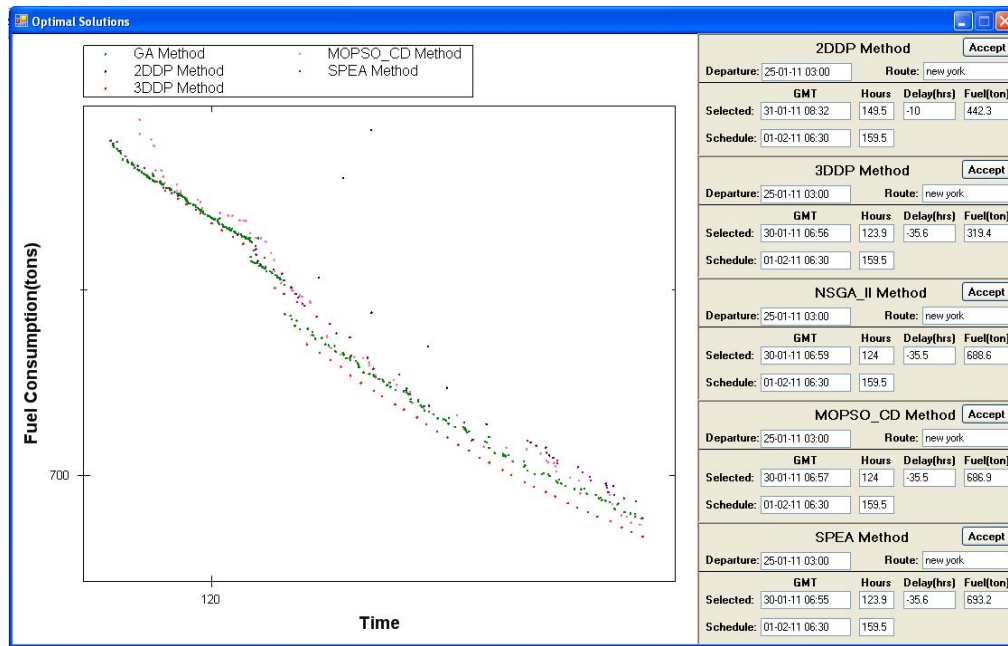
SPEA Method
 Gen. Pop. Mut.
 Cro. η_c η_m

When ship navigate during the pilot time or estuary part, the ship course are usually fixed, in this situation, the single track can be included when design a grids as shown below. During the optimisation process, the engine power of the ship in the single track part is treated as a constant value except for reducing the ship speed for ship safety consideration.



The operator first needs to set the grids which will be optimised as the current route, choose a method in the “OPTIMUM_G” module by using the radio button and set the corresponding parameters, then click button in this module to run the optimisation process. After finish the optimisation, an “Optimal Solution” window will be shown as below. The operations about this window are totally the same as it used in “Optimise a Route” function. The accuracy of the solution depends on the fineness of the grids system and the parameter setting in the “OPTIMUM_G” module.

Like mentioned in section B.7, in medium sea condition, 2DDP is recommended because of the shorter computing time and the tolerable results. But in rough sea condition, the 3DDP method offers the best results with a very uniform distribution but a longer computing time.

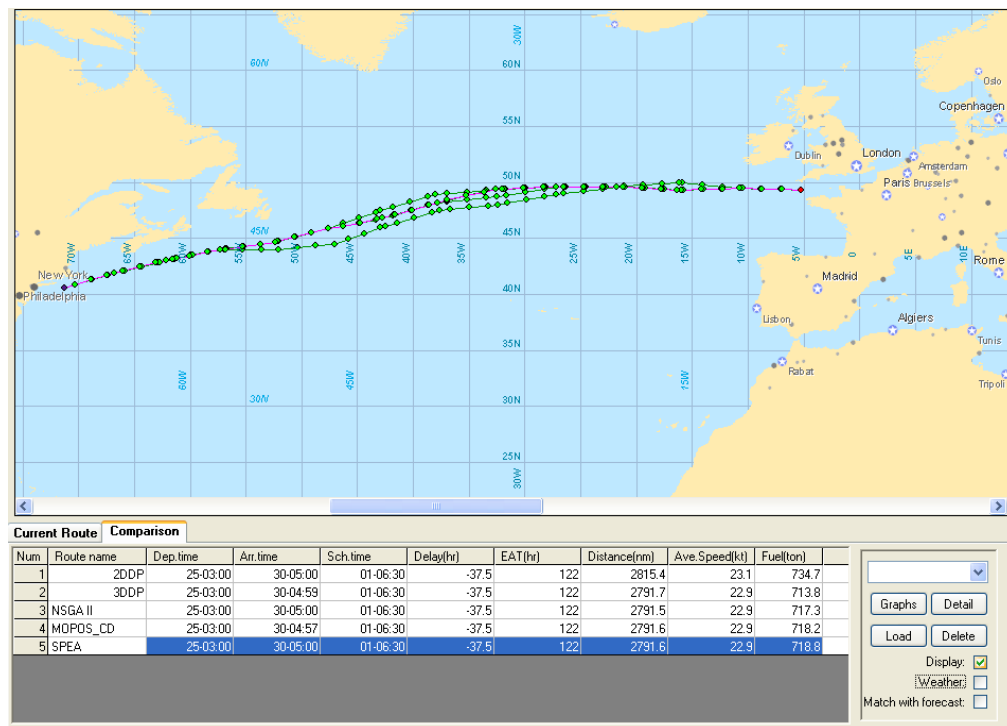


The operations about “Optimise Grids” are similar with “Optimise a Route”. The operator can treat section B.7 as a reference when using this function.

B.9 Compare routes

In “Route Information” window, the operator can use the **Add to compare** button to add a route (simulated or optimised solution) into “Comparison” table with the name specified in **Route name: SPEA** text box. “Comparison” table allows the operator to compared different simulated or optimised solutions against each other to assist the operator in determining the most efficient route for the planned passage in the expected weather forecast.

The route basic information will list in the table. The basic information includes departure and arrival time, en-route hours, total distance, average ship speed and so on.



Use the left mouse button can select a route in “Comparison” table. The selected route in the chart will be shown in red colour.

Select the items in the drop-down list button and then click **Graphs** button, some information about the selected route, which changes with time, like ship speed over ground, engine delivery power, propeller rotation speed, and weather and sea condition during the route, can be displayed by chart.

Click **Detail** button, a “Route Information” window will be shown to display the detail information of the selected route.

Click **Load** button can allow the operator to read an “.irou” file into “Comparison” table.


Click **Delete** button, the selected route will be delete in the table.

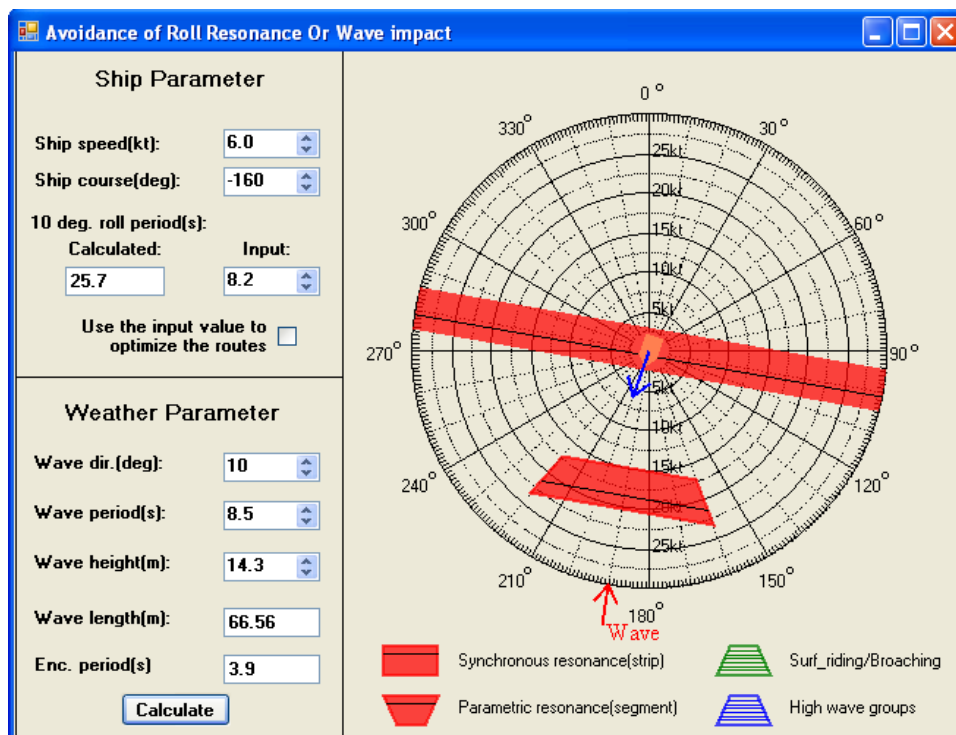
The check box **Display:** can decide display or hide the selected route.

The check box **Weather:** can decide display or hide the wind barbs on the route.

Set **Match with forecast:** is checked. When the operator selects a way point or a sub way point of one route in the "Comparison" table, the weather forecast whose time synchronize with the selected waypoint or sub way point will be displayed. When the operators display the weather forecast, the corresponding way point or sub way point of the selected route which indicated the ship planned position at the time of the displayed weather forecast will be shown in red.


B.10 Roll resonance module

Click the "Roll Resonance"  button on the toolbox, the "Avoidance of Roll Resonance or Wave impact" window with a polar diagram will be shown as below.



This window is a tactical tool for the operator to predict the severity of the responses to the specified ship speed, course and weather forecast or observed sea conditions.

The operator can see what effect the change of the ship operation would have by using a polar diagram. ITEES use the IMO guidelines to insure the ship safety during the voyage and the formula in the guideline will be transformed to facilitate the polar diagram drawing.

Set the parameters of the sip operation and the weather conditions (wave direction, wave period and wave height), and than click the  button, the wave encounter period, wave length, and the polar diagram will be update automatically according to these parameter setting.

In the polar diagram, the length and the direction of the blue arrow represent the ship speed and heading, respectively. Different colour zones are employed to represent different hazardous conditions of ship operation corresponding to a given weather condition.



indicates the dangerous situation caused by synchronous resonance.



indicates the dangerous situation caused by parametric resonance.



indicates the dangerous situation caused by Surf-riding and broaching-to.



indicates the dangerous situation caused by high wave groups.

If the arrow is fallen in a colour zone, it means the ship safety is at a risk. By using the polar diagram in ITEES, the assessment of situation or estimation of countermeasures can easily be done to find out suitable values of the ships' speed and course to avoid dangerous situation.

B 11 The formats of the file used by ITEES

The file “.pc” includes the propeller and engine characteristics. The content of the file are shown as

```

t      0.190 w      0.240 D      8.3  ETAR  1.009 ETAS  0.95  SFC   125
propeller open-water characteristics
J      KT      10KQ  ETAO  KT/J^2      10KQ/J^3
0.3    0.4003      0.5797      0.329703596  4.447777778  21.47037037
0.35   0.3729      0.5458      0.380580941  3.044081633  12.73002915
0.4    0.3453      0.5115      0.429765027  2.158125     7.9921875
0.45   0.3178      0.477 0.477164545  1.569382716  5.234567901
0.5    0.2907      0.4425      0.522783534  1.1628      3.54
0.55   0.2639      0.408 0.566189819  0.872396694  2.45229151
0.6    0.2375      0.3736      0.607055133  0.659722222  1.72962963
0.65   0.2114      0.3392      0.644737061  0.50035503   1.235138826
0.7    0.1855      0.3044      0.67891819   0.378571429  0.887463557
0.75   0.1594      0.2693      0.706534488  0.283377778  0.638340741
0.8    0.1327      0.2334      0.723902701  0.20734375   0.455859375
0.85   0.105 0.1963      0.723615839  0.14532872   0.319641767
0.9    0.0758      0.1577      0.688494001  0.093580247  0.216323731

```

Here t is thrust deduction factor, w is wake fraction, D is propeller disk diameter, $ETAR$ is relative rotative efficiency, $ETAS$ is shaft efficiency, SFC is the specific fuel consumption (g/PSh), J is advance ratio, KT is thrust coefficient, KQ is torque coefficient; $10KQ$ means 10 times of torque coefficient, $ETAO$ is open water efficiency.

The file “.hyd” gives the scope of the ship speed and the ship loading condition of the ship hydrodynamic database. The format is shown as:

| the number of velocity | vmin | vmax | interval of velocity | draft displacement | block coefficient |
|---------------------------|------|------|-------------------------|-----------------------|----------------------|
|---------------------------|------|------|-------------------------|-----------------------|----------------------|

V_{min} is the minimum ship speed and v_{max} corresponding to the maximum ship speed in the database. The unit of there parameters are knot.

The file “.DAT” is the ship hydrodynamic database corresponding to file “.hyd”.

```
vmin   vmax   amount
5      30 251
V(KTS)   Fn  RESISTANCE(N)   ENGINE POWER(PS)   PROPELLER REVOLUTIONS (RPM)
5.0      5.08e-002   92442.52331  451.44784   20.76831
5.1      5.19e-002   95964.79594  477.82963   21.17135
5.2      5.29e-002   99549.30477  505.19804   21.57419
5.3      5.39e-002   103195.93238   533.57006   21.97684
5.4      5.49e-002   106904.56401   562.96263   22.37929
```

Here F_n is Froude number associated with ship speed and ship length between perpendiculars.

Note that all the data in these three kind files are separate with Tab.

Appendix C.

PUBLICATIONS

The following papers have been published in journal or presented for international conference as a result of current research.

Wei Shao, Peilin Zhou and Sew Kait Thong (2012) ‘Development of a novel forward dynamic programming method for weather routing’. *Journal of Marine Science and Technology*, 17(2), pp. 239-251.

Wei Shao and Peilin Zhou (2011) ‘Development of 3D Dynamic Programming Method for Weather Routing’. *9th International Symposium on Marine Navigation and Safety of Sea Transportation*, Gdynia, Poland.

Wei Shao and Peilin Zhou (2011) ‘An Overview and Comparison of Different Methods for Ship Weather Routing’. *International Symposium on Marine Engineering*, Kobe, Japan.

Wei Shao and Peilin Zhou (2012) ‘Weather Routing Software Development and Case Study’. *International Conference on Maritime Technology*, Harbin, China.

Wei Shao and Peilin Zhou (2011) ‘Development of a Dynamic Programming Method for Low Fuel Consumption and Low Carbon emission from Shipping’. *Technologies, Operations, Logistics and Modelling for Low Carbon Shipping*, Glasgow, UK.